Examining signaling mechanisms by which colonic pro-inflammatory cytokines modulate obesity-promoted colonic carcinogenesis

A Dissertation Submitted By:

Anna C Pfalzer

A Dissertation Submitted to the Friedman School of Nutrition Science and Policy at Tufts University in Partial Fulfillment of the Requirements for the Degree of Doctor of Philosophy

February 2016

Thesis Committee:

Joel B Mason, MD (advisor, chair)
Xiang-Dong Wang, MD, PhD
Andrew Greenberg, MD
Rachel Buchsbaum, MD

Acknowledgements

First and foremost, I would like to thank my advisor, Joel Mason. Joel has been an excellent advisor, mentor, and life-coach. I could not have asked for a better mentor and certainly could not have done this without his support.

I would also like to thank the other members of my thesis committee, Andrew Greenberg, Rachel Buchsbaum and Xiang-Dong Wang. Their mentorship and thought-provoking questions have been invaluable and have played a central part in my development as a scientist. I am also very grateful to many other students, employees, and scientists of the Human Nutrition Research Center on Aging for their support and assistance along the way. There are too many to name.

Last but certainly not least, thank you to my husband, family and friends for unconditional love and support.

Abstract

Colorectal cancer (CRC) is the third most common cancer and third most common cause of cancer deaths in the United States. Amongst the many risk factors for this disease is obesity: those with a BMI of 25-29.9 have a relative risk of 1.2 and 1.5 for developing CRC, while those with a BMI of 30 have a relative risk of 1.5 and 2.0 for females and males, respectively. Recent evidence suggests that the low-grade chronic inflammatory state that accompanies obesity can have multiple promotional effects on pro-carcinogenic cell signaling cascades, and thus may be an important avenue by which excess adiposity promotes the risk of CRC.

The intent of the project described in this thesis was to define some of the mechanistic links between inflammation and colon carcinogenesis in obese rodent models as well as in humans. I aimed to: 1) elucidate the associations between pro-inflammatory cytokines in the colon and pro-carcinogenic signaling pathways in obese individuals; 2) delineate the mechanistic roles of colonic pro-inflammatory IL-1β on the activation of *Akt*, *NFkB* and *Wnt*; and 3) define differences in colonic pro-inflammatory cytokines and gene expression signatures in the colonic epithelium in diet-induced (DIO) and genetically-induced (GIO) obese mouse models.

To demonstrate the clinical relevance of these principles, and to begin understanding how obesity might generate biochemical inflammation in the human colon, we compared the concentrations of TNF-α, IL-1β, IL-6 and IFNγ in the colonic mucosa of 16 lean and 26 obese individuals. In a general linear model, colonic TNF-α ($r=0.41$; $p=0.01$) and IL-6 ($r=0.41$; $p=0.01$) concentrations increased incrementally with BMI. Among individuals with a BMI of ≥ 34 the mean colonic concentrations of TNF-α and IL-6 were two-fold greater than in lean subjects ($p<0.03$); those with milder obesity ($30 \leq BMI \leq 33.9$) had intermediate values. Regular use of NSAIDs diminished the concentration of colonic TNF-α and IL-6 by a constant amount ($p<.05$) at each BMI. RNA sequencing analysis identified 182 differentially expressed genes in the obese colons compared to lean. Pathway analysis indicated gene enrichment for biologic functions regulating cell cycle control, apoptosis and proliferation, as well as immune function. Further, the Wnt, NFκB, and ERK signaling cascades assumed central positions in the two gene expression networks that were most tightly linked to the altered gene signatures, and the direction of change in gene expression among the regulatory molecules surrounding these cascades was consistent with their activation.

To examine the role of IL-1β in mediating the early biochemical and molecular events leading up to CRC, male C57BL/6 (WT) mice were randomized to either low-fat or high-fat diets, as were two groups of male mice lacking a functional IL-1 receptor (IL1RKO) resulting in lean and obese mice. WT obese mice displayed significantly elevated levels of IL-1β and TNF-α in the colonic mucosa ($p<0.05$), an increase in active β-catenin in isolated colonocytes compared to lean WT mice ($p<0.05$), and a significant expansion of the proliferation zone in the colonic crypt ($p<0.05$); in contrast, in the absence of IL-1 signaling obesity had no effect on colonic IL-1β, TNF-α, proliferation or Wnt activation.

Lastly, to better understand whether obesity-induced inflammation and elevation in pro-carcinogenic signaling pathways is due to high-fat consumption or excess adiposity, we used a diet-induced (HF) mouse model of obesity in Apc^{1638} mice and compared them to Apc^{1638}Db/Db mice lacking the leptin receptor. Intestinal tumors were increased in both diet- and genetically-

induced obesity, but we found no difference in colonic or small intestinal cytokines in HF or DbDb mice. A transcriptome analysis identified 266 and 584 genes differentially expressed in the HF and DbDb compared to lean, respectively. Pathway analysis indicated that the genes altered in both obese models were related to immune function and cellular proliferation and cancer. Furthermore, the top-ranking networks of interacting genes identified in both gene sets centered around Protein kinase B (Akt).

In conclusion, observations from this thesis indicate that even moderate degrees of adiposity result in elevations in colonic cytokines and cytokinetic and molecular changes relevant for the development of colonic carcinogenesis. Furthermore, it is important to emphasize that obesity produces chronic exposure to this inflammatory environment, which over time would likely magnify its impact on the colonic epithelium. These findings suggest that strategies to attenuate the effects of cytokine signaling, in particular the impact of IL-1, may be an effective mechanism to alleviate the burden of obesity-promoted CRC.

Table of Contents

List of Figures

List of Tables

Manuscript I- Specific Aims 1

Manuscript III-Specific Aim 3

Manuscript IV-Specific Aim 3

Appendices

Manuscript III

Supplementary Table 1. Genes differentially expressed in the HF colonic epithelium compared to LF.

Supplementary Table 2. Genes differentially expressed in the DbDb colonic epithelium compared to LF.

I. Specific Aims

The objective of this thesis was to investigate the association between colonic pro-inflammatory cytokines and pro-carcinogenic signaling pathways in both pre-clinical and translational models of obesity, and to generate initial evidence that these obesity-induced elevations in cytokines are mechanistically responsible for the enhancement of colon cancer risk linked to obesity. Further, we postulated that IL-1β assumes a particularly central role and therefore hypothesized that obesity-induced increases in IL-1β are causally linked to downsteam events that promote carcinogenesis, including the upregulation of the pro-carcinogenic signaling pathways *Akt, NFkB,* and *Wnt*. I examined these central hypotheses by establishing, and then pursuing the following three specific aims:

Specific Aim 1: To examine the associations between obesity, colonic pro-inflammatory cytokines and the upregulation of pathways identified through the transcriptome analyses of obese human colonic epithelium. I examined this aim with colonic biopsies collected from obese and lean individuals. The primary outcomes for this aim were 1) changes in the protein expression of colonic inflammatory cytokines and 2) identification of signaling pathways by which obesity may promote colonic carcinogenesis.

Specific Aim 2: To delineate the mechanistic role(s) of colonic pro-inflammatory IL-1β on the activation of cellular events linked to the process of carcinogenesis, including upregulation of the *Akt*, *NFkB, Wnt* pathways. I examined this aim with a genetically-engineered mouse lacking the IL-1 receptor (IL1RKO) to study the effects of IL-1 signaling on obesity-induced alterations in the colonic mucosa. To induce obesity, male mice were fed a high-fat (HFD; 60% calories from fat) or low-fat (LFD; 10% calories from fat) diet for 16 weeks. The primary outcomes for this aim were 1) colonic inflammation, and 2) activation of cellular events relevant to carcinogenesis, including *Akt*, *Wnt*, and *NFkB* signaling.

Specific Aim 3: To define differences in colonic pro-inflammatory cytokines and gene expression signatures in the colonic epithelium in diet-induced (DIO) and genetically-induced (GIO) obese mouse models. I examined this aim with three genetically-engineered strains of mice, including DbDb mice, which become obese on low-fat diet, Apc^{1638N} mice, which develop spontaneous small intestinal tumors, and a genetic cross between these two to achieve an obese mouse with intestinal tumors. Mice were fed a high-fat (HFD; 60% calories from fat) or low-fat (LFD; 10% calories from fat) diet. The primary outcomes for this aim were: 1) colonic inflammation and 2) identification of pro-carcinogenic pathways upregulated in DIO and GIO mouse models. By comparing and contrasting DIO and GIO, we were able to speculate which pathways were upregulated by the obese state versus those that were upregulated by an obesogenic diet.

II. Background and Significance

Colorectal cancer and obesity

Colorectal cancer (CRC) remains a major public health issue in the US, with approximately 137,000 new cases and 50,000 deaths per year[1]. It is the third most common

cancer and third most common cause of cancer deaths[1]. Amongst the many risk factors for this disease is obesity: those with a BMI of 25-29.9 have a relative risk of 1.2 and 1.5 for developing CRC, while those with a BMI of 30 have a relative risk of 1.5 and 2.0, for females and males, respectively[2]. Mouse studies corroborate the epidemiological findings and prove causality, with both high fat-induced obesity[3] and genetically-induced obesity[3] significantly elevating tumor burden. Despite the consistent observations linking obesity and colon cancer, the molecular mechanism(s) responsible for this relationship remain a matter of debate. Furthermore, it is unclear whether it is the high-fat western style diet that elevates ones' cancer risk or whether it is the excess adiposity that disrupts physiologic homeostasis and elevates risk.

Obesity and colorectal cancer: mechanistic hypotheses

There are three prevailing hypotheses regarding the link between obesity and colon cancer: 1) inflammation[4], 2) excessive or aberrant insulin signaling[5] and 3) increased production/secretion of growth factors and adipokines such as leptin[6] and adiponectin[7]. These three avenues by which adiposity may promote cancer risk are by no means mutually exclusive and, in fact, it is likely that multiple avenues are at play.

The first hypothesis mentioned above purports that the causal link between obesity and colon cancer is due to the elevation of pro-inflammatory mediators that accompany obesity, the most commonly invoked of which are cytokines. It is well known that obesity results in a low-grade chronic inflammatory state[8]. Obese humans exhibit elevated concentrations of plasma pro-inflammatory cytokines, the most prominent being interleukin-6 (IL-6) and tumor necrosis factor-alpha (TNF-α)[9,10]. These elevated cytokines also appear in various adipose depots of obese individuals[10]. Studies have consistently demonstrated that C57BL/6 (wild-type) mice placed on

a high-fat diet (60% calories from fat) have elevated plasma and adipose TNF-α, IL-6 and IL-1β[4,11–13]. Genetically-induced models of obesity in rodents (which do not require high-fat diets to achieve the obese state) also display elevated adiposelevels of these cytokines[14] demonstrating that excess adiposity, regardless of dietary content, produces this inflammatory environment.

Despite the consistent findings regarding systemic and adipose inflammation, there is relatively little information regarding the inflammatory effects in the colon in response to obesity and the potential effects this might have on colon cancer risk. The significance of this low-grade inflammation as it pertains to carcinogenesis is that previous *in vivo* and *in vitro* studies have indicated that some of these pro-inflammatory cytokines such as TNF-α and IL-1β are capable of directly activating well-known pro-carcinogenic signaling pathways including protein kinase B (Akt), NFκB and Wnt[15,16]. Cytokine activation of phosphoinositide 3-K (PI3K) appears to be the common upstream event of all three signaling pathways[17]. A more detailed explanation of the mechanism(s) by which the cytokines TNF-α and IL-1β activate these signaling pathways is provided in the following section and depicted in figure 1.

As described in the following paragraphs, there are also hypotheses that invoke excessive insulin and leptin signaling as avenues by which obesity promotes carcinogenesis, and it is therefore relevant that cytokines have been observed to indirectly activate insulin[18] and leptin signaling[19]. The evidence that cytokines can both directly and indirectly activate pro-carcinogenic signaling pathways provides additional support for the critical role these pro-inflammatory mediators play in the development of obesity-promoted colonic carcinogenesis.

The second hypothesis posits that the link between obesity and colon cancer operates through aberrant insulin signaling through the PI3K/Akt pathway and subsequent hyperactivation of mitogenic components of the insulin signaling, such as the Ras-mitogen-activated protein

kinase (MAPK)[20]. For instance, insulin binding to the cell-surface insulin receptor leads to activation of insulin-receptor substrate proteins (IRS)[20]. IRS proteins phosphorylate and activate both the PI3K/Akt pathway and the MAPK pathway[20]. The proposed role of PI3K/Akt pathway activation in the development of colon cancer relates to its ability to activate NFκB – which has both oncogenic and pro-inflammatory consequences[21]. Insulin-promoted activation of the MAPK pathway has been linked to the development of colon cancer, primarily through regulation of cell proliferation, differentiation and survival[20].

The last theory postulates that altered secretion of the adipokines (increase in leptin and decrease in adiponectin) that occurs in obesity ultimately leads to an activation of Akt[7]. Similar to the cellular actions of insulin signaling, *in vitro* studies examining the impact of leptin on hepatocellular carcinoma cells found that stimulation with leptin leads to the phosphorylation of multiple substrates including Akt and enhances invasion and migration of these cells[22]. Furthermore, adiponectin has been demonstrated in similar studies to antagonize the effects of leptin – specifically by attenuating Akt activation[7]. In the setting of obesity, the reductions in adiponectin would further promote the leptin-induced activation of Akt[7]. The impact of these adipokines on Akt activation again emphasizes the interplay between these three pathways.

As described above, there is certainly much cross-talk between these three pathways, and therefore the effects of obesity on the risk of colon cancer likely involves each of these mechanisms. However, I have chosen to focus on the particular hypothesis addressing the role of obesity-induced inflammation because: 1) existing literature, combined with initial observations from our lab, indicate that obesity-induced inflammation plays a prominent role in the development of colonic tumorigenesis, and 2) defining and delineating one pathway of

several by which obesity promotes cancer risk may provide the opportunity to find means of blocking that pathway and diminishing the risk of cancer.

Inflammation: effects on cell signaling and colonic carcinogenesis

Epidemiologic studies support the link between inflammation and development of a variety of cancers, including colorectal cancer[23]. Among patients with chronic inflammatory bowel disease, the incidence of colorectal cancer increases progressively over time, reaching 19% after 30 years of disease[24]. Perhaps more convincing is that one of the most successful chemoprevention regimens ever demonstrated for colonic adenomas in human subjects utilized the non-steroidal anti-inflammatory drug (NSAID) sulindac[25]. Similarly, animal studies using pro-inflammatory agents or mice genetically-engineered to have heightened inflammatory responses acquire a greater burden of colonic carcinomas compared to control animals, while treatment with NSAIDs significantly reduces the development of these carcinomas[26].

A study from our lab in wild-type mice indicates that obesity induces elevations in colonic cytokines. Further, our observations concurred with two prior papers that similarly demonstrated that the colons of obese mice contain elevated concentrations of TNF-α[3,27]. Our group also provided evidence that elevations in select cytokines occur in concert with evidence of Wnt signaling activation[12]. Specifically, we examined several endpoints that were indirect measures of Wnt signaling[12]: a greater phosphorylation (i.e. inactivation) of GSK3β in conjunction with increased expression of total cellular β-catenin[12]. Further support for the activation of Wnt was obtained in a separate experiment in which Dr. Zhenhua Liu in our lab found that the Axin2 gene, whose expression is a specific downstream readout of *Wnt* signaling[28], had elevated

message levels in the colons of obese male mice compared to lean littermates (Liu, unpublished). However, we have yet to identify cellular mechanism(s) linking elevated colonic cytokines to an activation of Wnt signaling in the colon. Thus, based upon previous studies which show that select pro-inflammatory cytokines can activate well-known pro-carcinogenic signaling pathways such as PI3K, Akt and NFκB[29], I propose that elevations in specific colonic cytokines activate Wnt and NFκB signaling via phosphorylation (activation) of PI3K and Akt (Figure 1).

Akt, also known as Protein Kinase B, is a serine/threonine kinase which promotes cell survival through phosphorylation of various downstream mediators[30]. One of several connections between *Akt* and colon cancer relates to its' ability to inactivate GSK3β, the kinase responsible for targeting β-catenin for degradation via its N-terminal phosphorylation[31] as well as directly activating beta-catenin via phosphorylation of a C-terminal site[32]. Through these two avenues *Akt* upregulates *Wnt* signaling, causing cells to reacquire survival features[31] resulting in a loss of cell cycle regulation and the molecular onset of carcinogenesis. Akt also leads to the increased transcriptional activity of NFκB, a transcription factor known to promote the expression of pro-inflammatory cytokines[33] as well as genes whose protein products regulate cell cycle progression and apoptosis and are overexpressed in human colon tumors[34,35]. Specifically, phosphorylation of Akt leads to the degradation of IκBα – a negative regulator of the *NFκB,* which sequesters the transcriptionally active p65/p50 subunits of *NFκB* in the cytosol[30]. In fact, an *in vitro* study found that stimulation with exogenous TNF-α resulted in increased phosphorylation of Akt, degradation of IκBα, and increased phosphorylation and nuclear translocation of p65[36].

A basal level of Wnt signaling is critical for maintaining adequate colonocyte cell division in the base of the colonic crypt[37]. Wnt binds to its' cell surface receptor Frizzled, which inhibits the formation of the cytoplasmic Apc-Axin-GSK3β complex and allows β-catenin to

remain un-phosphorylated in the N-terminal region, avoid proteosomal degradation and translocate to the nucleus[38]. In contrast, phosphorylation of β-catenin at Serine 552 in the C-terminal domain by Akt also promotes nuclear translocation[32] (Figure 1). Upon translocation to the nucleus, β-catenin binds to the transcription factor complex TCF/LEF, which promotes the transcription of known oncogenes[38]. Hyperactivation of this signaling pathway has been shown to be a critical first step for the vast majority of colorectal cancers[39]. In fact, the most common genetically-engineered rodent models for colorectal cancer in mice utilize mutations in the Apc gene – a pivotal player in the *Wnt* signaling pathway[39]. Apc^{1638N} mice—one such model-- have a modification to exon 15 in the Apc gene leading to a chain-terminating truncation of the protein[40]. These mice develop 1-5 tumors in the small intestine, and rarely ones in the colon[40]. Despite the predominance of small, rather than large, intestinal tumors this animal model appears to have genuine value and relevance in examining issues attendant to the nutritional modulation of colorectal cancer since these tumors respond to dietary modifications (such as 1-carbon nutrients) in the same fashion as human colonic cancers[40,41]. Although the phenotype of this model is due to a mutation in the Apc gene, it has been shown that *Wnt* signaling can secondarily be activated through a number of additional molecular pathways, including *Akt* and *NFkB* signaling[42,43].

These data suggest that elevations in colonic IL-1β and TNF-α are associated with an increase in Wnt, Akt, and NFκB signaling in the colon, and subsequently, colonic carcinogenesis. Although our interests encompass all the inflammatory cytokines, we are particularly interested in the role of IL-1β for several reasons. First, elegant studies in mice showed that upregulated expression of IL-1β in the gastrointestinal epithelium is, by itself, sufficient to incite inflammation and cancer[44]. Additional studies indicate that IL-1β expression

is necessary for the acquisition of an invasive phenotype and for the stimulation of angiogenesis in several different types of tumors[45]. Moreover, several human studies have observed that polymorphisms in the IL-1β gene that increase its production or activity are associated with a higher risk of cancer or a shorter cancer survival[46–48] whereas associations with similarly functional polymorphisms in other pro-inflammatory cytokines have been inconsistent[49]. A prominent role for IL-1β signaling in carcinogenesis may relate to its multiplier effect, since it upregulates the expression of several other pro-inflammatory elements such as TNF-α, IL-6, and COX-2[49,50] and regulates insulin[51] and leptin secretion[19]. And lastly, IL-1β appears to be capable of activating well-known carcinogenic pathways such as *Akt* and NFκB in cells of colonic origin. Kaler et al found that with the addition of IL-1β to HCT116 colorectal carcinoma cells increased activation of Akt, NFκB and Wnt signaling[15,29]. This elevation in Wnt signaling was accompanied by increased proliferation and decreased apoptosis[15], cytokinetic aberrations that predispose to tumor development.

Figure 1

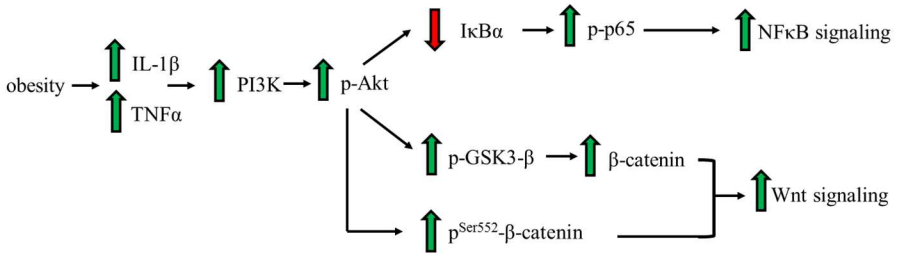

Figure 1. **Diagram illustrating the signaling mechanisms by which obesity-induced TNFα and IL-1β activate NFκB and Wnt.** Green 'up' arrows indicate an elevation and red 'down' arrows indicate a reduction. IL-1β, interleukin-1β; TNFα, tumor necrosis factor α; PI3K, phosphoinositide 3-kinase; p-Akt, phospho-Protein Kinase B; IκBα, nuclear factor of kappa light polypeptide gene enhancer in B-cells inhibitor, alpha; p-p65, phospho-p65 subunit of NFκB; p-GSK3-β, phospho-glycogen synthase kinase 3-β.

Collectively, the body of mechanistic work described in the previous few paragraphs indicates that pro-inflammatory cytokines such as TNF-α and IL-1β in particular can activate signaling pathways that will promote the process of carcinogenesis. I postulate that the low-grade inflammatory state associated with obesity mediates this effect, at least in part, by elevating Akt,

NFκB and Wnt signaling and that activation of these signaling cascades occur in concert with increases in cytokinetics and intestinal tumorigenesis.

References

1. Siegel R, Desantis C, Jemal A. Colorectal cancer statistics, 2014. *CA Cancer J Clin*. 2014;64(2):104-117. doi:10.3322/caac.21220.

2. Calle EE, Rodriguez C, Walker-Thurmond K, Thun MJ. Overweight, obesity, and mortality from cancer in a prospectively studied cohort of U.S. adults. *N Engl J Med*. 2003;348(17):1625-1638. doi:10.1056/NEJMoa021423.

3. Flores MB, Rocha GZ, Damas-Souza DM, et al. Obesity-induced increase in tumor necrosis factor-alpha leads to development of colon cancer in mice. *Gastroenterology*. 2012;143(3):741-744. doi:10.1053/j.gastro.2012.05.045.

4. Park EJ, Lee JH, Yu GY, et al. Dietary and genetic obesity promote liver inflammation and tumorigenesis by enhancing IL-6 and TNF expression. *Cell*. 2010;140(2):197-208. doi:10.1016/j.cell.2009.12.052.

5. Shoelson SE, Lee J, Goldfine AB. Inflammation and insulin resistance. *J Clin Invest*. 2006;116(7):1793-1801. doi:10.1172/JCI29069.

6. Lashinger LM, Rossi EL, Hursting SD. Obesity and resistance to cancer chemotherapy: interacting roles of inflammation and metabolic dysregulation. *Clin Pharmacol Ther*. 2014;96(4):458-463. doi:10.1038/clpt.2014.136.

7. Vansaun MN. Molecular pathways: adiponectin and leptin signaling in cancer. *Clin Cancer Res*. 2013;19(8):1926-1932. doi:10.1158/1078-0432.CCR-12-0930.

8. Hotamisligil GS. Inflammation and metabolic disorders. *Nature*. 2006;444(7121):860-867. doi:10.1038/nature05485.

9. Hotamisligil GS. Inflammatory pathways and insulin action. *Int J Obes Relat Metab Disord*. 2003;27 Suppl 3:S53-S55. doi:10.1038/sj.ijo.0802502.

10. Wellen KE, Hotamisligil GS. Obesity-induced inflammatory changes in adipose tissue. *J Clin Invest*. 2003;112(12):1785-1788. doi:10.1172/JCI20514.

11. Li H, Lelliott C, Hakansson P, et al. Intestinal, adipose, and liver inflammation in diet-induced obese mice. *Metabolism*. 2008;57(12):1704-1710. doi:10.1016/j.metabol.2008.07.029.

12. Liu Z, Brooks RS, Ciappio ED, et al. Diet-induced obesity elevates colonic TNF-alpha in mice and is accompanied by an activation of Wnt signaling: a mechanism for obesity-associated colorectal cancer. *J Nutr Biochem*. 2012;23(10):1207-1213. doi:10.1016/j.jnutbio.2011.07.002.

13. Day SD, Enos RT, McClellan JL, Steiner JL, Velazquez KT, Murphy EA. Linking

inflammation to tumorigenesis in a mouse model of high-fat-diet-enhanced colon cancer. *Cytokine*. 2013;64(1):454-462. doi:10.1016/j.cyto.2013.04.031.

14. Xu H, Barnes GT, Yang Q, et al. Chronic inflammation in fat plays a crucial role in the development of obesity-related insulin resistance. *J Clin Invest*. 2003;112(12):1821-1830. doi:10.1172/JCI19451.

15. Kaler P, Godasi BN, Augenlicht L, Klampfer L. The NF-kappaB/AKT-dependent Induction of Wnt Signaling in Colon Cancer Cells by Macrophages and IL-1beta. *Cancer Microenviron*. 2009. doi:10.1007/s12307-009-0030-y.

16. Hayden MS, Ghosh S. Regulation of NF-κB by TNF family cytokines. *Semin Immunol*. 2014;26(3):253-266. doi:10.1016/j.smim.2014.05.004.

17. Huang X-F, Chen J-Z. Obesity, the PI3K/Akt signal pathway and colon cancer. *Obes Rev*. 2009;10(6):610-616. doi:10.1111/j.1467-789X.2009.00607.x.

18. Tack CJ, Stienstra R, Joosten LA, Netea MG. Inflammation links excess fat to insulin resistance: the role of the interleukin-1 family. *Immunol Rev*. 2012;249(1):239-252. doi:10.1111/j.1600-065X.2012.01145.x.

19. Dinarello CA, Donath MY, Mandrup-Poulsen T. Role of IL-1beta in type 2 diabetes. *Curr Opin Endocrinol Diabetes Obes*. 2010;17(4):314-321. doi:10.1097/MED.0b013e32833bf6dc.

20. Jung UJ, Choi MS. Obesity and its metabolic complications: the role of adipokines and the relationship between obesity, inflammation, insulin resistance, dyslipidemia and nonalcoholic fatty liver disease. *Int J Mol Sci*. 2014;15(4):6184-6223. doi:10.3390/ijms15046184.

21. Hoesel B, Schmid J a. The complexity of NF-κB signaling in inflammation and cancer. *Mol Cancer*. 2013;12(1):86. doi:10.1101/cshperspect.a000141.

22. Saxena NK, Sharma D, Ding X, et al. Concomitant activation of the JAK/STAT, PI3K/AKT, and ERK signaling is involved in leptin-mediated promotion of invasion and migration of hepatocellular carcinoma cells. *Cancer Res*. 2007;67(6):2497-2507. doi:10.1158/0008-5472.CAN-06-3075.

23. Coussens LM, Werb Z. Inflammation and cancer. *Nature*. 2002;420(6917):860-867. doi:10.1038/nature01322.

24. Eaden JA, Abrams KR, Mayberry JF. The risk of colorectal cancer in ulcerative colitis: a meta-analysis. *Gut*. 2001;48(4):526-535. http://www.ncbi.nlm.nih.gov/pubmed/11247898.

25. Meyskens Jr. FL, McLaren CE, Pelot D, et al. Difluoromethylornithine plus sulindac for the prevention of sporadic colorectal adenomas: a randomized placebo-controlled, double-blind trial. *Cancer Prev Res*. 2008;1(1):32-38. doi:10.1158/1940-6207.CAPR-08-0042.

26. Itano O, Yang K, Fan K, et al. Sulindac effects on inflammation and tumorigenesis in the intestine of mice with Apc and Mlh1 mutations. *Carcinogenesis*. 2009;30(11):1923-1926.

doi:10.1093/carcin/bgp200.

27. Jain SS, Bird RP. Elevated expression of tumor necrosis factor-alpha signaling molecules in colonic tumors of Zucker obese (fa/fa) rats. *Int J Cancer*. 2010;127(9):2042-2050. doi:10.1002/ijc.25232.

28. Jho E, Zhang T, Domon C, Joo C-K, Freund J-N, Costantini F. Wnt/beta-catenin/Tcf signaling induces the transcription of Axin2, a negative regulator of the signaling pathway. *Mol Cell Biol*. 2002;22(4):1172-1183. http://www.pubmedcentral.nih.gov/articlerender.fcgi?artid=134648&tool=pmcentrez&rendertype=abstract. Accessed February 16, 2016.

29. Kaler P, Augenlicht L, Klampfer L. Macrophage-derived IL-1beta stimulates Wnt signaling and growth of colon cancer cells: a crosstalk interrupted by vitamin D3. *Oncogene*. 2009;28(44):3892-3902. doi:10.1038/onc.2009.247.

30. Chan CH, Jo U, Kohrman A, et al. Posttranslational regulation of Akt in human cancer. *Cell Biosci*. 2014;4(1):59. doi:10.1186/2045-3701-4-59.

31. Cross DA, Alessi DR, Cohen P, Andjelkovich M, Hemmings BA. Inhibition of glycogen synthase kinase-3 by insulin mediated by protein kinase B. *Nature*. 1995;378(6559):785-789. doi:10.1038/378785a0.

32. Fang D, Hawke D, Zheng Y, et al. Phosphorylation of beta-Catenin by AKT Promotes beta-Catenin Transcriptional Activity. *J Biol Chem*. 2007;282(15):11221-11229. doi:10.1074/jbc.M611871200.

33. Karin M. NF- B as a Critical Link Between Inflammation and Cancer. *Cold Spring Harb Perspect Biol*. 2009;1(5):a000141-a000141. doi:10.1101/cshperspect.a000141.

34. Temraz S, Mukherji D, Shamseddine A. Potential targets for colorectal cancer prevention. *Int J Mol Sci*. 2013;14(9):17279-17303. doi:10.3390/ijms140917279.

35. Lin Q, Lai R, Chirieac LR, et al. Constitutive activation of JAK3/STAT3 in colon carcinoma tumors and cell lines: inhibition of JAK3/STAT3 signaling induces apoptosis and cell cycle arrest of colon carcinoma cells. *Am J Pathol*. 2005;167(4):969-980. doi:10.1016/S0002-9440(10)61187-X.

36. Ozes ON, Mayo LD, Gustin J a, Pfeffer SR, Pfeffer LM, Donner DB. NF-kappaB activation by tumour necrosis factor requires the Akt serine-threonine kinase. *Nature*. 1999;401(6748):82-85. doi:10.1038/43466.

37. de Lau W, Barker N, Clevers H. WNT signaling in the normal intestine and colorectal cancer. *Front Biosci*. 2007;12:471-491. doi:2076 [pii].

38. Nusse R. Wnt signaling. *Cold Spring Harb Perspect Biol*. 2012;4(5). doi:10.1101/cshperspect.a011163.

39. Taketo MM. Shutting down Wnt signal-activated cancer. *Nat Genet*. 2004;36(4):320-322. doi:10.1038/ng0404-320.

40. Fodde R, Edelmann W, Yang K, et al. A targeted chain-termination mutation in the mouse Apc gene results in multiple intestinal tumors. *Proc Natl Acad Sci U S A*. 1994;91(19):8969-8973. http://www.ncbi.nlm.nih.gov/pubmed/8090754.

41. Basett JK, Severi G, Hodge AM, et al. Dietary intake of B vitamins and methionine and colorectal cancer risk. Nutr Cancer. 2013;65(5):659-67.doi: 10.1080/01635581.2013.789114.

42. Morin PJ, Sparks AB, Korinek V, et al. Activation of beta-catenin-Tcf signaling in colon cancer by mutations in beta-catenin or APC. *Science (80-)*. 1997;275(5307):1787-1790. http://www.ncbi.nlm.nih.gov/pubmed/9065402.

43. Suzuki H, Watkins DN, Jair KW, et al. Epigenetic inactivation of SFRP genes allows constitutive WNT signaling in colorectal cancer. *Nat Genet*. 2004;36(4):417-422. doi:10.1038/ng1330.

44. Dinarello CA. Interleukin 1 and interleukin 18 as mediators of inflammation and the aging process. *Am J Clin Nutr*. 2006;83(2):447S - 455. http://ajcn.nutrition.org/content/83/2/447S.full. Accessed December 18, 2014.

45. Voronov E, Shouval DS, Krelin Y, et al. IL-1 is required for tumor invasiveness and angiogenesis. *Proc Natl Acad Sci U S A*. 2003;100(5):2645-2650. doi:10.1073/pnas.0437939100.

46. Howell WM, Turner SJ, Theaker JM, Bateman AC. Cytokine gene single nucleotide polymorphisms and susceptibility to and prognosis in cutaneous malignant melanoma. *Eur J Immunogenet*. 2003. doi:425 [pii].

47. El-Omar EM, Carrington M, Chow WH, et al. Interleukin-1 polymorphisms associated with increased risk of gastric cancer. *Nature*. 2000;404(6776):398-402. doi:10.1038/35006081.

48. Barber MD, Powell JJ, Lynch SF, Fearon KC, Ross JA. A polymorphism of the interleukin-1 beta gene influences survival in pancreatic cancer. *Br J Cancer*. 2000;83(11):1443-1447. doi:10.1054/bjoc.2000.1479.

49. Tamura M, Sebastian S, Yang S, Gurates B, Fang Z, Bulun SE. Interleukin-1beta elevates cyclooxygenase-2 protein level and enzyme activity via increasing its mRNA stability in human endometrial stromal cells: an effect mediated by extracellularly regulated kinases 1 and 2. *J Clin Endocrinol Metab*. 2002;87(7):3263-3273. http://www.ncbi.nlm.nih.gov/pubmed/12107235.

50. Tu S, Bhagat G, Cui G, et al. Overexpression of Interleukin-1b Induces Gastric Inflammation and Cancer and Mobilizes Myeloid-Derived Suppressor Cells in Mice. *Cancer Cell*. 2008;14(5):408-419. doi:10.1016/j.ccr.2008.10.011.

51. Gao D, Madi M, Ding C, et al. Interleukin-1β mediates macrophage-induced impairment of insulin signaling in human primary adipocytes. *Am J Physiol Endocrinol Metab*. 2014;307(3):E289-E304. doi:10.1152/ajpendo.00430.2013.

III. Manuscript I- Specific Aim 1

Colonic concentrations of TNF-α and IL-6 increase incrementally with body mass index in conjunction with carcinogenesis-relevant alterations in the mucosal transcriptome

Authors: Anna C Pfalzer[1,6,8], Keith Leung[1,6], Jimmy W Crott[1,6,8], Susie J Kim[1,6], Albert K Tai[7], Laurence D Parnell[5], Frederick K Kamanu[2], Zhenhua Liu[11], Gail Rogers[3], M Kyla Shea[4], Paloma E Garcia[1,6], Joel B Mason[1,6,8-10*].

Affiliations:

[1]Vitamins & Carcinogenesis Laboratory, [2]Nutrition and Genomics Laboratory, [3]Nutritional Epidemiology Laboratory, [4]Vitamin K Laboratory, [5]Agricultural Research Service, USDA, [6]Jean Mayer-USDA Human Nutrition Research Center on Aging at Tufts University; [7]Genomics Core, Tufts University School of Medicine; [8]Friedman School of Nutrition Science and Policy, Tufts University; Divisions of [9]Gastroenterology, and [10]Clinical Nutrition, Tufts Medical Center; and [11]School of Public Health and Health Sciences, University of Massachusetts, Amherst, MA

* Joel B Mason, MD
USDA HNRCA at Tufts University
711 Washington St, Boston, MA 02111.
Joel.Mason@tufts.edu

One Sentence Summary: Incremental increases in colonic TNF-α and IL-6 accompany increasing BMI in conjunction with pro-cancerous alterations in the colonic transcriptome.

Abstract: Obesity is an important risk factor for colorectal cancer. Although it has been postulated that elevations in pro-inflammatory mediators accompanying obesity act mechanistically, objective evidence of inflammation in the colons of obese humans has not been demonstrated. We therefore compared concentrations of TNF-α, IL-1β, IL-6 and IFNγ in the blood and colonic mucosa of 16 lean and 26 obese individuals. Plasma TNF-α and IL-6 were elevated 1.3 and 2.5-fold, respectively, in the obese ($p<0.01$) and increased incrementally with BMI ($p<0.01$). In a general linear model, colonic TNF-α ($r=0.41$; $p=0.01$) and IL-6 ($r=0.41$; $p=0.01$) concentrations increased incrementally over the range of BMIs examined (18.1-45.7). Regular use of NSAIDs significantly reduced colonic TNF-α and IL-6 levels to a uniform extent

over this entire range. Among individuals with BMI ≥34 kg/m^2 mean colonic concentrations of TNF-α and IL-6 were two-fold greater than in lean subjects ($p<0.03$). RNA-sequencing analysis of the colonic transcriptomes identified 182 differentially expressed genes in obese colons compared to lean. Pathway analysis indicates gene enrichment for biologic functions regulating cell cycle control, apoptosis and proliferation, as well as immune function. The two biologic networks most strongly linked to the observed changes in expression were 'cell-cell signaling and interaction' and 'cancer, organismal injury and abnormalities'. These two networks included several differentially expressed genes known to regulate the pro-carcinogenic signaling pathways, including Wnt and NFκB.

Introduction

Colorectal cancer (CRC) remains a major public health issue in the U.S., with approximately 140,000 new cases and 50,000 deaths per year *(1)*. Across ethnic groups, one of the highly prevalent risk factors for the disease is excess adiposity: those with a BMI of 25-29.9 (overweight) have a relative risk of 1.2-1.5 for developing CRC compared to lean controls, while those with a BMI of ≥ 30 (obesity) have a relative risk of 1.5-2.0 *(2)*. The magnitude of increased risk is generally observed to be greater among men than women *(2)*.

Despite the consistent observations linking overweight, obesity and colon cancer, the molecular mechanisms responsible for this relationship continue to be debated. It has been known for over two decades that obesity produces a chronic, low-grade state of inflammation that is evident in the bloodstream and adipose tissue *(3)* and, although other concurrent cellular pathways might also be contributory *(4–6)*, this inflammatory state has been postulated to be an important factor in mediating the pro-carcinogenic effects of obesity *(6)*. Further, some evidence

indicates that it is the visceral pattern of obesity (so-called 'android-type') that is most prone to create inflammation *(7)* and increase cancer risk *(8)*.

Epidemiologic studies support the link between inflammation and development of a variety of cancers, including colorectal cancer *(9)*. Among patients with ulcerative colitis the incidence of colorectal cancer increases progressively over time, reaching 19% after 30 years of disease *(10)*. Further, prospective studies have shown that long-term use of aspirin—a prototypical non-steroidal anti-inflammatory agent—reduces the risk of both colorectal adenomas and cancers *(11, 12)*.

Nevertheless, the idea that obesity-associated inflammation might promote colorectal carcinogenesis rests on the assumption that an inflammatory milieu also exists within the colonic mucosa. Recent studies--including our own--have demonstrated that biochemical and molecular mediators of inflammation are elevated in the colons of obese laboratory rodents compared to lean controls *(13–15)*. Comparable evidence is lacking in humans, although it has been reported that weight loss in obese women can diminish colonic cytokines *(16)*. Two of the major goals of the present study, therefore, were to establish whether elevated concentrations of pro-inflammatory cytokines exist in the colons of obese humans and to determine whether a measure of overall (BMI), or visceral (waist-hip ratio, WHR), obesity is the stronger determinant of colonic cytokines.

Further, several lines of experimental evidence indicate that certain pro-inflammatory cytokines such as TNF-α, IL-6, and IL-1β are potent activators of oncogenic cell signaling pathways that are highly relevant to colonic carcinogenesis, such as NFκB, Akt and Wnt *(17–19)*. These cellular cascades are of particular interest because observations in colonocyte cell culture *(19, 20)* and in the gastrointestinal epithelia of intact animals *(14, 21)* demonstrate that

inflammatory cytokines activate them. Thus, we also postulated that a low-grade inflammatory state present in the colonic mucosa of obese subjects would be accompanied by changes in the colonic transcriptome that are pro-carcinogenic in nature, including changes in the abovementioned signaling pathways.

Results

Study Participants

Exclusion criteria and other details regarding these subjects can be found in the 'Materials and Methods' section. Seventeen lean (BMI range: 18.1-24.9) and twenty-six obese (range: 30.0-45.7) subjects between the ages of 45-70 years old were enrolled in the study. One lean enrolled subject did not complete the colonoscopy and data from this individual are not included in the analysis. Features of the 42 subjects who completed the study are displayed in Table 1.

Elevated plasma cytokines in obese subjects

Plasma IL-6 and TNF-α concentrations were elevated 2.5-fold and 1.3-fold in the obese group compared to the lean, respectively ($p<0.01$, Figure 1). In contrast, no significant differences were observed between the two groups for IL-1β and IFNγ. Plasma IL-6 and TNF-α concentrations increased incrementally with BMI ($r=0.52$, $p<0.001$; $r=0.43$, $p<0.01$, respectively) whereas no significant relationship was observed between TNF-α and IL-6 and WHR. Regular use of Nonsteroidal anti-inflammatory drugs (NSAID), defined as habitual intake of $\geq$1 dose/week, did not significantly alter the relationship between plasma cytokines and excess adiposity expressed either as a categorical variable (i.e.: obesity) or as a continuous variable (i.e.: BMI).

Elevated colonic cytokines in obese subjects

A general linear model demonstrated that gender, age, presence of a colonic polyp, and 'current' or 'ever' tobacco use were not significantly correlated with colonic cytokine concentrations. Colonic concentrations of TNF-α and IL-6 each increased incrementally with BMI ($r=0.41$, $p=0.01$; $r=0.41$, $p=0.01$). In contrast, no significant correlations existed between the concentrations of these two colonic cytokines and WHR. No significant changes in colonic IFNγ and IL-1β were observed with increases in either BMI or WHR.

Colonic cytokine concentrations were then examined categorically by dividing the 42 subjects into the following three BMI categories: 18-25, 30-33.9, and ≥34 (n=16,14,12, respectively). Those subjects with a BMI≥34 had significantly greater IL-6 and TNF-α concentrations—by approximately 2-fold--than those in the 18-25 category ($p<0.03$), and in the instance of both cytokines those in the 30-33.9 category had intermediate values (Figure 2A, B). The general linear model demonstrated that regular NSAID use significantly altered the relationship between colonic concentrations of IL-6 and TNF-α and BMI (Figure 3A, B). In the instance of each of these two cytokines, the predicted value of the cytokine diminished by a constant value at any given BMI with regular NSAID use. For each of these two cytokines the predicted colonic concentration decreased by 1-2 pg/mg of protein with the use of a NSAID. Interestingly, there were no significant correlations between plasma cytokine concentrations and the concentration of the corresponding colonic cytokine ($p>0.30$ for all four cytokines).

Alterations in the transcriptional profile of colonic mucosa

In order to eliminate the confounding effects of NSAIDs on gene expression, regular users of these drugs were not included in the RNA-Seq analysis. RNA sequencing of colonic mucosa from obese and lean subjects identified 182 genes whose differential expression was significant ($q<0.10$): these genes are presented in Supplementary Table 1. Ingenuity Pathway Analysis

(IPA®; Qiagen, Redwood City, CA) was used to identify functional categories and biologic networks that were enriched in the differentially expressed genes obtained from the DESeq2 analysis. Top diseases and functions were identified based upon a network score. The network score is a measure of the probability of finding a greater number of differentially expressed genes than a set threshold within a set of n genes randomly selected from IPA's Global Molecular Network. Within a network composed of 35 molecules, for example, a network score of 6 reflects the fact that there is a 1 in one million (i.e.: $-\log(10^{-6}) = 6$) chance of obtaining a network containing the same number of molecules when randomly picking 35 molecules (http://ingenuity.force.com/ipa/IPATutorials?id=kA250000000TNBZCA4). Among the top diseases and functions represented were 'cancer'; 'lipid metabolism'; 'cell to cell signaling', 'tissue development', 'cellular growth and proliferation', and 'cell death and survival' (Table 2). The top two biological networks that emerged (network score for each=25) regulate 'Cell-to-Cell Signaling and Interaction, Hair and Skin Development and Function, Embryonic Development' and 'Cancer, Organismal Injury and Abnormalities, Gene Expression' (Table 2).

These two networks are of particular interest because they include several differentially expressed genes that either directly or indirectly regulate cell signaling cascades pivotal in colonic carcinogenesis, including the NFκB, *Wnt*, p53, and MAPK-ERK pathways. It is notable that within the network identified as a regulator of 'Cell-to-Cell Signaling' (Figure 4A) 'NFκB complex' and 'ERK1/2' assume central positions. Several differentially expressed genes involved in regulation of NFκB signaling surround the complex: Fibrillarin (FBL), Myeloid differentiation primary response 88 (MYD88), Desmin (DES) and Cellular Inhibitor of Apoptosis Protein 1(BIRC2). Genes that encode intrinsic proteins of the NFκB complex (i.e.: *NFκB1, NFκB2, RELA, RELB,* and *REL*) did not appear in this network, presumably because the

extent to which this complex drives NFκB signaling is largely controlled by post-translational phosphorylation of these proteins and their immediate upstream IκB regulators rather than by up- and down-regulation of gene expression *(22)*. The same network identifies differential expression of the Regulatory-associated Protein of mTOR (RPTOR), Telomerase Reverse Transcriptase (TERT), and Interleukin-6 receptor (IL6R) as regulators of ERK.

The other network ranking highest in the IPA analysis ('Cancer, Organismal Injury and Abnormalities, Gene Expression', figure 4B) is also highly relevant to colorectal carcinogenesis. This network contains β-catenin (gene name: *CTNNB1*)—the proximate activator of canonical Wnt signaling in colonic carcinogenesis--as a central component along with other molecules such as GSK3-β, which assists in regulating the degradation of β–catenin *(45)*, and p53, which plays important tumor suppressor functions in determining whether colonocytes undergo malignant degeneration.

Discussion

The epidemiologic link between obesity and colorectal cancer has been well documented and causality has been convincingly proven by animal studies, yet the molecular mechanisms responsible for this effect of obesity remain a matter of debate. The focus of our study was to provide explicit evidence that inflammation on a biochemical level exists within the colonic mucosa of the obese human and to define associated changes in gene expression, thereby providing support to the hypothesis that inflammation contained within the colonic mucosa contributes to the elevated risk of CRC observed among obese individuals. Our observations establish, for the first time, that the colonic concentrations of two major pro-inflammatory cytokines in humans increase in concert with increasing BMI. When examined categorically, colonic TNF-α and IL-6 levels were approximately twice as great among those with a BMI ≥34

than in lean individuals. Regular use of NSAIDs reduced colonic concentrations of IL-6 and TNF-α by a constant amount over the entire range of BMIs examined. The fact that colonic concentrations of interferon-gamma did not display relationships to obesity similar to those observed with IL-6 and TNF-α is not surprising since its function appears to be primarily related to immune responses to viral, bacterial and protozoan infections *(23)* rather than as a more generalized mediator of inflammation, which is the role played by IL-6 and TNF-α. It is less evident why a relationship between colonic IL-1β and BMI was not observed, although one of the features that distinguishes IL-1β from TNF-α and IL-6 is that it is synthesized as a precursor molecule and must be cleaved by IL-1β-converting enzyme (ICE; caspase-1) in order to achieve its final, active form *(24)*. It is therefore feasible that either caspase-1 or its inflammasome platform were not sufficiently activated by obesity to observe increases in the fully processed cytokine.

Elevations in plasma TNF-α and IL-6 in obese subjects—as demonstrated in this study--are known features of the systemic inflammation that accompanies obesity *(25, 26)*. In this study, colonic TNF-α and IL-6 were also shown to each increase incrementally with BMI, and this was true even though over 60% of our obese subjects fell into the classification of mild or 'Class I' obesity (BMI 30-34.9). Thus, even a modest degree of obesity is accompanied by a state of biochemical inflammation in the colon. To the extent that inflammation plays a role in mediating the pro-cancerous effects of obesity, this is consistent with the observation that even modest degrees of adiposity in the 'overweight' range (BMI 25-29.9) produce a demonstrable rise in the risk of colorectal cancer *(2)*. Indeed, some have argued that the incremental increase in the risk of colon cancer begins with BMIs exceeding 22.5 *(27)*.

A metric of visceral adiposity, waist-hip ratio, did not correlate with either plasma or colonic cytokine concentrations in this study. This lack of an association between a measure of visceral adiposity (WHR) and colonic cytokines suggests that obesity can produce a state of biochemical inflammation in the colon regardless of the state of visceral adiposity. Some have argued that visceral adiposity--as opposed to a peripheral pattern of obesity--is more likely to incite systemic inflammation *(28)* and therefore is more predictive of obesity-associated cytokinemia than overall measures of obesity, and that the WHR is an independent predictor of systemic inflammation *(29)*. *In vitro* observations demonstrating that visceral adipose tissue secretes more IL-6 than subcutaneous adipose tissue support this concept *(7)*. Nevertheless, it is also clear that WHR is far from a perfect measure of visceral adiposity *(30)* and in a study such as ours containing a modest number of subjects, this measure of visceral adiposity may simply not have been accurate enough to detect its relationship with plasma or colonic cytokines.

Our results also indicate that concentrations of IL-6 and TNF-α in the colonic mucosa are lower among regular users of NSAIDs along the entire spectrum of BMIs that were studied, and that the absolute magnitude to which a NSAID lowers colonic levels of these cytokines is rather constant, regardless of whether an individual resides at the low or high end of BMI values. Our data are cross-sectional rather than interventional and thus cannot prove causality, but nevertheless they strongly implicate NSAIDs as an effective means of diminishing levels of pro-inflammatory cytokines in the colonic mucosa. Further, if colon cancer risk does begin to rise at BMI levels above 22.5, as has been suggested *(27)*, then our data would imply that protection against malignant transformation could be affected by NSAIDs even among those with relatively low BMIs.

An interesting difference between plasma and colonic cytokine concentrations was that regular NSAID use was associated with diminished cytokines in the colonic mucosa whereas NSAIDs did not seem to affect circulating concentrations. Other investigators have similarly observed no decrease, or even an increase, in plasma cytokines with NSAID use: in a recent study a variety of NSAIDs were shown to increase, rather than diminish, secretion of TNF-α and IL-1β by human blood monocytes as well as raise whole blood levels of TNF-α *(31)*; further, in another study administration of aspirin to healthy volunteers had no anti-inflammatory effect on the plasma *(32)*. It is also of considerable interest that no significant correlations were observed between plasma and colonic cytokine concentrations. Thus, plasma and colonic cytokine concentrations not only differ in regard to their response to NSAIDs, but other factors determining the levels of these molecules in the two tissues appear to be somewhat distinct.

To begin understanding the changes in the transcriptional signature associated with these elevations in pro-inflammatory cytokines in the colon, we compared the transcriptome of obese versus lean humans, and identified 182 differentially expressed genes. Pathway analysis of our transcriptional data identified enriched signaling pathways which have previously been shown to participate in the evolution of colorectal neoplasia. The analysis suggests that two of the primary biologic systems altered by obesity which may contribute to the elevation in CRC risk relates to cell cycle control; specifically, cell proliferation, apoptosis and transcriptional regulation. The two highest scoring biologic networks identified from IPA related to: 1) cell-to-cell signaling, cell proliferation and apoptosis and 2) cancer and gene regulation. The first network includes well-known regulators of pro-carcinogenic molecular cascades including nuclear-factor kappa B (NFκB) and extracellular signal-related kinases (ERK). Genes whose protein products constitute the central signaling molecules of these pathways were not found to be differentially expressed;

however, this is not surprising as activation of these two signaling pathways occurs post-translationally. We did identify, however, altered expression in several genes that either directly or indirectly regulate each of these two central mediators. For instance, Desmin (DES) was downregulated in obese subjects–a molecular event previously demonstrated to increase NFκB signaling*(33)*. Prior work in human cells has found that siRNA directed against DES leads to an increase in phosphorylation and nuclear translocation of NFκB*(33)*. Conversely, we observed that MYD88 and BIRC2 are significantly upregulated in obese individuals and these proteins are known to activate NFκB signaling *(34, 35)*. The changes in DES, MYD88 and BIRC2 are all consistent with our primary hypothesis that obesity induces pro-carcinogenic transcriptional changes in the colonic mucosa.

Thus, the first of the two top networks that were identified suggests that these pro-carcinogenic changes are predominantly mediated through NFκB and the ERK-MAPK pathway. The former acts as a pro-carcinogenic signaling molecule in many settings, promoting cellular proliferation and the activation of several proto-oncogenes *(36)*. A seminal role played by over-activation of NFκB signaling was first demonstrated to promote carcinogenesis in colitis-associated colon cancers but is now recognized to be instrumental in >50% of all human colon cancers *(37, 38)*. However, NFκB signaling also up-regulates, to varying degrees, pro-inflammatory genes such as IL-1β and TNF-α *(39)*. Thus, the activation of NFκB signaling through the upregulation of genes such as MYD88 and BIRC2 has both carcinogenic and inflammatory consequences, and may thereby create a positive feedback loop that magnifies its own effects.

Another central component of the first of the two top scoring biologic networks is the ERK family. ERK is a component of a family of serine/threonine kinases which are involved in

cell migration, adhesion, progression, proliferation and survival, and it is a major regulator of the oncogenic Ras pathway *(40)*. Our transcriptional analysis identified 2 differentially expressed genes that modulate ERK activity: RPTOR and IL6R. RPTOR is a negative regulator of ERK activity through its regulatory role in mTOR activity *(41)*. As such, a reduction in RPTOR expression, such as what we observed in the obese colon, would be expected to lead to increased oncogenicity due to ERK activation. Conversely, we observed an increase in the expression of the interleukin-6 receptor (IL6R) in the obese, an alteration in expression that incites an increase in ERK activity *(42)*. Thus, the alterations in colonic RPTOR and IL6R expression that we observed to accompany obesity are also consistent with pro-carcinogenic molecular changes in the human colon.

The other top-ranking biologic network also related to cancer and gene regulation, and contained two critical components of Wnt signaling: CTNNB1 (gene product: β-catenin) and GSK3β. In normal colonic epithelium *Wnt* signaling is critical for sustaining adequate colonocyte turnover; however, when inappropriately overactivated it is generally regarded as one of the earliest steps in the molecular carcinogenesis of 80-95% of spontaneous colorectal cancers *(43)*. The CTNNB1 and GSK3β genes assume central positions in network #2 but were not found to be differentially expressed. This is not surprising since the degree to which each of these proteins alters Wnt signaling is primarily determined by post-translational phosphorylation, as was the case for NFκB and ERK. Even though we were unable to directly demonstrate activation of Wnt signaling through our transcriptional data such an effect would be consistent with observations in laboratory rodents that have indicated that obesity promotes activation of colonic Wnt signaling *(13, 44)*. Moreover, indirect evidence of activation of colonic Wnt signaling from the Ref-seq analysis is apparent in biologic network #2: the gene for Ephrin type-

B receptor 3 (EphB3), a target gene suppressed by β–catenin/Tcf4-mediated signaling and held to be a tumor suppressor gene in human colorectal carcinogenesis *(45)*, was significantly downregulated in our obese subjects. In human colorectal neoplasms EphB protein expression decreases incrementally in parallel with stepwise increases in the stage of carcinogenesis, from aberrant crypt foci to adenomas to carcinomas *(45)*; further, its functional role as a suppressor of tumorigenesis is evidenced by the fact that mice whose expression of EphB3 has been knocked out experience greatly enhanced colonic tumorigenesis *(45)*. Thus IPA network #2 not only provides indirect evidence of Wnt activation but offers one avenue through which obesity-induced activation of Wnt might enhance the risk of neoplastic transformation, EphB3.

This translational study does have certain limitations. The size of the study population is modest, and therefore results should be confirmed within the context of a larger study. Inter-racial differences in cytokine levels are known to exist *(46)*, so in order to minimize the confounding effect of this variable the present study was confined to Caucasian subjects. Thus, it is unclear at this point whether the observed principles would apply to non-caucasian populations. A larger study would therefore allow for stratification of the subject population, and thereby determine whether gender- and/or race-specific effects exist.

In sum, this study demonstrates that the concentrations of two important pro-inflammatory cytokines in the colon rise incrementally over a wide range of BMI values and that regular use of NSAIDs diminish these levels to a fairly constant extent over the entire range. Although the extent to which obesity increases colonic cytokine levels is modest, the chronicity of exposure produced by obesity and the auto-amplifying nature of inflammation produced by inflammatory cytokines *(47, 48)* underscores the potential impact that such changes may have. In addition, the transcriptome analysis provides evidence that pro-transformational transcriptional

changes in the colonic mucosa accompany obesity that are highly relevant to colonic carcinogenesis. Given the cross-sectional nature of this study, the results cannot prove that the observed changes in the colonic transcriptome that accompany obesity are due to the rise in cytokines. Indeed, other metabolic alterations that accompany obesity, such as hyperinsulinemia and changes in adipokine secretion, have been shown to stimulate some of the same pathways observed in this study *(49, 50)*, so it is likely that multiple factors are contributing to the altered colonic transcriptome. Observations from this study nevertheless underscore the potential contribution that the establishment of an inflammatory milieu in the colonic mucosa may play in explaining the enhanced risk of colon cancer due to obesity.

Materials and Methods

Experimental Design

Prospective subjects were identified through the weekly list of individuals scheduled to undergo routine screening colonoscopy in the endoscopy suite at Tufts Medical Center. Obese (BMI: 30-50) and lean (BMI: 18-25) subjects were recruited to participate in the study. Exclusion criteria included: a past medical history of cancer (except non-melanoma skin cancer), polyposis syndromes, and any current or chronic inflammatory disease or infection. Use of non-steroidal anti-inflammatory drugs (NSAIDs) was documented, and regular users were defined as those using NSAIDs ≥1X/week. The subject population was confined to Caucasian subjects in order to minimize confounding by race since it is known that this factor modifies the relationship between obesity and inflammation *(48)*. On the day of the colonoscopy, subjects had height, weight, hip and waist circumference measured with shoes removed, and fasting blood samples were collected. Eight colonic biopsies were obtained during the colonoscopy from normal-

appearing mucosa at the rectosigmoid junction, at least 10 cm from any polyp. Biopsies were immediately placed on an aluminum foil square suspended on ice, then snap frozen in liquid nitrogen and stored at -80˚C for later analysis. Blood samples were spun at 1000g for 15 minutes at 4˚C, and plasma was divided into aliquots and stored at -80˚C for later analysis. All procedures for this study were approved by the Tufts University Health Sciences Institutional Review Board and informed consent was obtained from all subjects.

Cytokines

TNF-α, IL-1β, IFNγ and IL-6 protein levels were measured in duplicate in plasma and colon using a chemiluminescence system (MesoScale Discovery (MSD), Sector 2400, Rockville, MD). The inter-assay coefficients of variation were ≤8% for each cytokine. Colonic cytokine and total protein concentrations were measured in lysate preparations isolated from 2-3 colonic biopsies. Lysates were generated using a cell lysate kit (MSD), to which protease (Roche Diagnostics Corp., Indianapolis, IN) and phosphatase inhibitors (Sigma Aldrich, St Louis, MO) were added. Colonic cytokine concentrations were adjusted for protein concentration using the Bradford assay (Bio-Rad Laboratories, Hercules, CA) and reported as pg/mg of protein.

RNA extraction

Since we sought to compare differences in colonic expression due solely to obesity, without the confounding effects of NSAIDs (see Results) subjects who were regular users of NSAIDs were excluded from the RefSeq analysis. Nine subjects were randomly selected from each group, matched for age and gender, by an individual blinded to all characteristics of the subjects except for their group assignment, age and gender. RNA was isolated from one biopsy from each of these 18 individuals using the Ambion® RiboPure™ Kit (Life Technologies, Grand Island, NY). Total RNA was re-suspended in 200 µl of RNase/DNase-free water. RNA quality was assessed

using the 2100 Bioanalyzer system (Agilent Technologies, Santa Clara, CA) to verify that the RNA Integrity Number (RIN) was greater than 8.

RNA sequencing analysis

Preparation of the RNA sequence libraries was done using the TruSeq RNA Sample Preparation Kit v2 (Illumina, San Diego, CA), with 1 µg of input RNA per sample. Quality was assessed using the Fragment Analyzer (Advanced Analytical, Ames, IA). Single-end sequencing was performed on the HiSeq 2500 (Illumina, San Diego, CA). The analysis was run at a multiplexing level sufficient to generate 10-25 million reads per sample. Reads were aligned to the human genome version hg19 using the Tuxedo suite software package, which includes Bowtie, TopHat and Cufflinks *(51)*. The demultiplexed FASTQ files were generated using CASAVA 1.8.2 (Illumina), and the QC reports were generated with FastQC. Samples were considered of acceptable quality if the mean quality score was at least 30 and the percentage of bases with a quality score of ≥ 30 was at least 90%. One sample did not meet this threshold and was excluded from further analysis, leaving 9 samples from one group and 8 from the other. An average of 15,744,767 ± 2,745,633 (SEM) reads were generated per sample. Differential expression analysis was conducted using DESeq2, an open-source Bioconductor package (https://bioconductor.org/biocLite.R). Prior to this analysis it was necessary to convert BAM files generated from the TopHat output to SAM files using Samtools available from http://www.htslib.org/. HTSeq-count, an open-source tool available from http://www-huber.embl.de/HTSeq, utilizes SAM files to count the number of reads which map to an individual gene. DESeq2 then utilizes these counts to identify differential expressed genes. Only genes with counts in at least 80% of the samples were considered for differential expression analysis. Genes were identified as significantly differentially expressed with q-values (false

discovery rates) ≤ 0.10. The fold change in gene expression is indicated by a *regularized transformation* which mimics a $\log_2$ transformation *(52)*.

Statistical analysis

Plasma and colonic cytokine values were each log transformed to reduce skewness and data are reported as geometric means. An ANCOVA was used to evaluate differences in plasma cytokines between obese and lean subjects. Our initial analyses incorporated gender, age, presence of colonic polyp, 'ever' and 'current' tobacco use, and regular NSAID use as potential confounders, however these variables did not significantly alter the relationship between obesity and plasma cytokines. A general linear model was also constructed to look at the relationship between plasma cytokines and BMI and WHR including the same potential confounding variables.

Differences in colonic cytokines among the three BMI categories were also evaluated using an ANCOVA adjusted for the following variables: gender, regular NSAID use, age, presence of colonic polyp, and 'ever' and 'current' tobacco use. Colonic cytokines were also analyzed using a general linear model with BMI and WHR. Loess curves were drawn to confirm that localized regressions within lean and obese subjects were representative of an overall linear model. Regular NSAID use was the only significant confounding variable in each colonic analysis. All statistical analyses were performed using SAS version 9.2.

Supplementary Materials

Table S1. Genes differentially expressed in the obese versus lean human colonic mucosa.

References

1. R. Siegel, C. Desantis, A. Jemal, Colorectal cancer statistics, 2014, *CA Cancer J Clin* **64**, 104–117 (2014).

2. E. E. Calle, C. Rodriguez, K. Walker-Thurmond, M. J. Thun, Overweight, obesity, and mortality from cancer in a prospectively studied cohort of U.S. adults, *N Engl J Med* **348**, 1625–1638 (2003).

3. G. S. Hotamisligil, P. Arner, J. F. Caro, R. L. Atkinson, B. M. Spiegelman, Increased adipose tissue expression of tumor necrosis factor-alpha in human obesity and insulin resistance., *J. Clin. Invest.* **95**, 2409–15 (1995).

4. S. E. Shoelson, J. Lee, A. B. Goldfine, Inflammation and insulin resistance, *J Clin Invest* **116**, 1793–1801 (2006).

5. L. M. Lashinger, E. L. Rossi, S. D. Hursting, Obesity and resistance to cancer chemotherapy: interacting roles of inflammation and metabolic dysregulation, *Clin Pharmacol Ther* **96**, 458–463 (2014).

6. S. D. Hursting, J. Digiovanni, A. J. Dannenberg, M. Azrad, D. Leroith, W. Demark-Wahnefried, M. Kakarala, A. Brodie, N. A. Berger, Obesity, energy balance, and cancer: new opportunities for prevention., *Cancer Prev. Res. (Phila).* **5**, 1260–72 (2012).

7. S. K. Fried, D. a. Bunkin, A. S. Greenberg, Omental and subcutaneous adipose tissues of obese subjects release interleukin-6: Depot difference and regulation by glucocorticoid, *J. Clin. Endocrinol. Metab.* **83**, 847–850 (1998).

8. M. Song, F. B. Hu, D. Spiegelman, A. T. Chan, K. Wu, S. Ogino, C. S. Fuchs, W. C. Willett, E. L. Giovannucci, Long-term status and change of body fat distribution, and risk of colorectal cancer: a prospective cohort study., *Int. J. Epidemiol.* (2015), doi:10.1093/ije/dyv177.

9. L. M. Coussens, Z. Werb, Inflammation and cancer, *Nature* **420**, 860–867 (2002).

10. J. A. Eaden, K. R. Abrams, J. F. Mayberry, The risk of colorectal cancer in ulcerative colitis: a meta-analysis, *Gut* **48**, 526–535 (2001).

11. P. M. Rothwell, M. Wilson, C.-E. Elwin, B. Norrving, A. Algra, C. P. Warlow, T. W. Meade, Long-term effect of aspirin on colorectal cancer incidence and mortality: 20-year follow-up of five randomised trials., *Lancet (London, England)* **376**, 1741–50 (2010).

12. B. F. Cole, R. F. Logan, S. Halabi, R. Benamouzig, R. S. Sandler, M. J. Grainge, S. Chaussade, J. A. Baron, Aspirin for the chemoprevention of colorectal adenomas: meta-analysis of the randomized trials., *J. Natl. Cancer Inst.* **101**, 256–66 (2009).

13. Z. Liu, R. S. Brooks, E. D. Ciappio, S. J. Kim, J. W. Crott, G. Bennett, A. S. Greenberg, J. B. Mason, Diet-induced obesity elevates colonic TNF-alpha in mice and is accompanied by an activation of Wnt signaling: a mechanism for obesity-associated colorectal cancer, *J Nutr Biochem* **23**, 1207–1213 (2012).

14. M. B. Flores, G. Z. Rocha, D. M. Damas-Souza, F. Osorio-Costa, M. M. Dias, E. R. Ropelle, J. A. Camargo, R. B. de Carvalho, H. F. Carvalho, M. J. Saad, J. B. Carvalheira, Obesity-induced increase in tumor necrosis factor-alpha leads to development of colon cancer in mice,

Gastroenterology **143**, 741–744 (2012).

15. S. S. Jain, R. P. Bird, Elevated expression of tumor necrosis factor-alpha signaling molecules in colonic tumors of Zucker obese (fa/fa) rats., *Int. J. Cancer* **127**, 2042–50 (2010).

16. S. Pendyala, L. M. Neff, M. Suárez-Fariñas, P. R. Holt, Diet-induced weight loss reduces colorectal inflammation: Implications for colorectal carcinogenesis, *Am. J. Clin. Nutr.* **93**, 234–242 (2011).

17. E. J. Park, J. H. Lee, G. Y. Yu, G. He, S. R. Ali, R. G. Holzer, C. H. Osterreicher, H. Takahashi, M. Karin, Dietary and genetic obesity promote liver inflammation and tumorigenesis by enhancing IL-6 and TNF expression, *Cell* **140**, 197–208 (2010).

18. S. Teshima, H. Nakanishi, M. Nishizawa, K. Kitagawa, M. Kaibori, M. Yamada, K. Habara, A. H. Kwon, Y. Kamiyama, S. Ito, T. Okumura, Up-regulation of IL-1 receptor through PI3K/Akt is essential for the induction of iNOS gene expression in hepatocytes, *J. Hepatol.* **40**, 616–623 (2004).

19. P. Kaler, B. N. Godasi, L. Augenlicht, L. Klampfer, The NF-kappaB/AKT-dependent Induction of Wnt Signaling in Colon Cancer Cells by Macrophages and IL-1beta, *Cancer Microenviron* (2009), doi:10.1007/s12307-009-0030-y.

20. P. Kaler, L. Augenlicht, L. Klampfer, Macrophage-derived IL-1beta stimulates Wnt signaling and growth of colon cancer cells: a crosstalk interrupted by vitamin D3, *Oncogene* **28**, 3892–3902 (2009).

21. K. Oguma, H. Oshima, M. Aoki, R. Uchio, K. Naka, S. Nakamura, A. Hirao, H. Saya, M. M. Taketo, M. Oshima, Activated macrophages promote Wnt signalling through tumour necrosis factor-alpha in gastric tumour cells., *EMBO J.* **27**, 1671–81 (2008).

22. T. D. Gilmore, Introduction to NF-kappaB: players, pathways, perspectives., *Oncogene* **25**, 6680–4 (2006).

23. J. R. Schoenborn, C. B. Wilson, Regulation of interferon-gamma during innate and adaptive immune responses., *Adv. Immunol.* **96**, 41–101 (2007).

24. B. Siegmund, H. A. Lehr, G. Fantuzzi, C. A. Dinarello, IL-1 beta -converting enzyme (caspase-1) in intestinal inflammation, *Proc Natl Acad Sci U S A* **98**, 13249–13254 (2001).

25. B. Zahorska-Markiewicz, J. Janowska, M. Olszanecka-Glinianowicz, A. Zurakowski, Serum concentrations of TNF-alpha and soluble TNF-alpha receptors in obesity., *Int. J. Obes. Relat. Metab. Disord.* **24**, 1392–1395 (2000).

26. P. Ziccardi, F. Nappo, G. Giugliano, K. Esposito, R. Marfella, M. Cioffi, F. D'Andrea, A. M. Molinari, D. Giugliano, Reduction of inflammatory cytokine concentrations and improvement of endothelial functions in obese women after weight loss over one year., *Circulation* **105**, 804–9 (2002).

27. L. C. Thygesen, M. Grønbaek, C. Johansen, C. S. Fuchs, W. C. Willett, E. Giovannucci, Prospective weight change and colon cancer risk in male US health professionals., *Int. J. Cancer* **123**, 1160–5 (2008).

28. C. Tsigos, I. Kyrou, E. Chala, P. Tsapogas, J. C. Stavridis, S. a Raptis, N. Katsilambros, Circulating tumor necrosis factor alpha concentrations are higher in abdominal versus peripheral

obesity., *Metabolism.* **48**, 1332–5 (1999).

29. M. Visser, L. M. Bouter, G. M. McQuillan, M. H. Wener, T. B. Harris, Elevated C-reactive protein levels in overweight and obese adults., *JAMA* **282**, 2131–5 (1999).

30. H. Yamakage, R. Ito, M. Tochiya, K. Muranaka, M. Tanaka, Y. Matsuo, S. Odori, S. Kono, A. Shimatsu, N. Satoh-Asahara, The utility of dual bioelectrical impedance analysis in detecting intra-abdominal fat area in obese patients during weight reduction therapy in comparison with waist circumference and abdominal CT., *Endocr. J.* **61**, 807–19 (2014).

31. T. H. Page, J. J. O. Turner, A. C. Brown, E. M. Timms, J. J. Inglis, F. M. Brennan, B. M. J. Foxwell, K. P. Ray, M. Feldmann, Nonsteroidal anti-inflammatory drugs increase TNF production in rheumatoid synovial membrane cultures and whole blood., *J. Immunol.* **185**, 3694–3701 (2010).

32. A. Barden, E. Mas, K. D. Croft, M. Phillips, T. a Mori, Short-term n-3 fatty acid supplementation but not aspirin increases plasma proresolving mediators of inflammation., *J. Lipid Res.* **55**, 2401–7 (2014).

33. J. S. Mohamed, A. M. Boriek, Loss of desmin triggers mechanosensitivity and up-regulation of Ankrd1 expression through Akt-NF-κB signaling pathway in smooth muscle cells., *FASEB J.* **26**, 757–65 (2012).

34. D. J. Mahoney, H. H. Cheung, R. L. Mrad, S. Plenchette, C. Simard, E. Enwere, V. Arora, T. W. Mak, E. C. Lacasse, J. Waring, R. G. Korneluk, Both cIAP1 and cIAP2 regulate TNFalpha-mediated NF-kappaB activation., *Proc. Natl. Acad. Sci. U. S. A.* **105**, 11778–83 (2008).

35. P. Viatour, M. P. Merville, V. Bours, A. Chariot, Phosphorylation of NF-kappaB and IkappaB proteins: implications in cancer and inflammation, *Trends Biochem Sci* **30**, 43–52 (2005).

36. H. L. Pahl, Activators and target genes of Rel/NF-kappaB transcription factors., *Oncogene* **18**, 6853–6866 (1999).

37. M. Kojima, T. Morisaki, N. Sasaki, K. Nakano, R. Mibu, M. Tanaka, M. Katano, Increased nuclear factor-kB activation in human colorectal carcinoma and its correlation with tumor progression., *Anticancer Res.* **24**, 675–81.

38. M. Karin, F. R. Greten, NF-kappaB: linking inflammation and immunity to cancer development and progression., *Nat. Rev. Immunol.* **5**, 749–59 (2005).

39. J. Hiscott, J. Marois, J. Garoufalis, M. D'Addario, A. Roulston, I. Kwan, N. Pepin, J. Lacoste, H. Nguyen, G. Bensi, Characterization of a functional NF-kappa B site in the human interleukin 1 beta promoter: evidence for a positive autoregulatory loop., *Mol. Cell. Biol.* **13**, 6231–40 (1993).

40. R. Roskoski, ERK1/2 MAP kinases: structure, function, and regulation., *Pharmacol. Res.* **66**, 105–43 (2012).

41. M. C. Mendoza, E. E. Er, J. Blenis, The Ras-ERK and PI3K-mTOR pathways: Cross-talk and compensation*Trends Biochem. Sci.* **36**, 320–328 (2011).

42. A. Dreuw, H. M. Hermanns, R. Heise, S. Joussen, F. Rodríguez, Y. Marquardt, F. Jugert, H. F. Merk, P. C. Heinrich, J. M. Baron, Interleukin-6-type cytokines upregulate expression of

multidrug resistance-associated proteins in NHEK and dermal fibroblasts, *J. Invest. Dermatol.* **124**, 28–37 (2005).

43. H. Clevers, R. Nusse, Wnt/beta-catenin signaling and disease, *Cell* **149**, 1192–1205 (2012).

44. J. Mao, X. Hu, Y. Xiao, C. Yang, Y. Ding, N. Hou, J. Wang, H. Cheng, X. Zhang, Overnutrition stimulates intestinal epithelium proliferation through beta-catenin signaling in obese mice, *Diabetes* **62**, 3736–3746 (2013).

45. E. Batlle, J. Bacani, H. Begthel, S. Jonkeer, A. Gregorieff, M. van de Born, N. Malats, E. Sancho, E. Boon, T. Pawson, S. Gallinger, S. Pals, H. Clevers, EphB receptor activity suppresses colorectal cancer progression, *Nature* **435**, 1126–1130 (2005).

46. J. F. Carroll, K. G. Fulda, A. L. Chiapa, M. Rodriquez, D. R. Phelps, K. M. Cardarelli, J. K. Vishwanatha, R. Cardarelli, Impact of race/ethnicity on the relationship between visceral fat and inflammatory biomarkers., *Obesity (Silver Spring).* **17**, 1420–1427 (2009).

47. B. Heinhuis, M. I. Koenders, P. L. van Riel, F. A. van de Loo, C. A. Dinarello, M. G. Netea, W. B. van den Berg, L. A. B. Joosten, Tumour necrosis factor alpha-driven IL-32 expression in rheumatoid arthritis synovial tissue amplifies an inflammatory cascade., *Ann. Rheum. Dis.* **70**, 660–7 (2011).

48. Y. Liu, M. Biarnés Costa, C. Gerhardinger, IL-1β is upregulated in the diabetic retina and retinal vessels: cell-specific effect of high glucose and IL-1β autostimulation., *PLoS One* **7**, e36949 (2012).

49. M. N. Vansaun, Molecular pathways: adiponectin and leptin signaling in cancer., *Clin. Cancer Res.* **19**, 1926–32 (2013).

50. P. G. Vigneri, E. Tirrò, M. S. Pennisi, M. Massimino, S. Stella, C. Romano, L. Manzella, The Insulin/IGF System in Colorectal Cancer Development and Resistance to Therapy., *Front. Oncol.* **5**, 230 (2015).

51. C. Trapnell, A. Roberts, L. Goff, G. Pertea, D. Kim, D. R. Kelley, H. Pimentel, S. L. Salzberg, J. L. Rinn, L. Pachter, Differential gene and transcript expression analysis of RNA-seq experiments with TopHat and Cufflinks, *Nat Protoc* **7**, 562–578 (2012).

52. L. MI, W. Huber, S. Anders, Moderated estimation of fold change and dispersion for RNA-Seq data with DESeq2, *bioRxiv* (2014), doi:http://dx.doi.org/10.1101/002832,http://dx.doi.org/10.1101/002832.

Acknowledgments: We thank Albert Tai and staff of the Tufts University Core Facility Genomics Core for the performance of RNA-Sequencing and the physician and nursing staff of the colonoscopy suite at Tufts Medical Center for their generous cooperation.

Funding: Funded in part by the Agricultural Research Service of the United States Department of Agriculture, Cooperative Agreement #58-1950-0-014. Any opinions, findings, conclusions, or recommendations expressed in this publication are those of the authors and do not necessarily reflect the view of the U.S Dept. of Agriculture; and the U.S.D.A. Human Nutrition Research Center on Aging Pilot Project Program. We would especially like to thank Drs. Peter and Joan Cohn and the HNRCA Directors Student Innovation Fund for providing partial support for this study. **Author contributions**: SK, ZL, JC, JBM conceived the study design; KL and PG performed subject recruitment and sample collection; KL and ACP measured cytokine levels; ACP and AT performed RNAseq and analysis; GR, MKS, JC and ACP performed statistical analyses; ACP and JBM wrote initial drafts of the manuscript; all authors commented on these drafts.

Competing interests: The authors report no conflict of interest

Figures:

Figure 1.

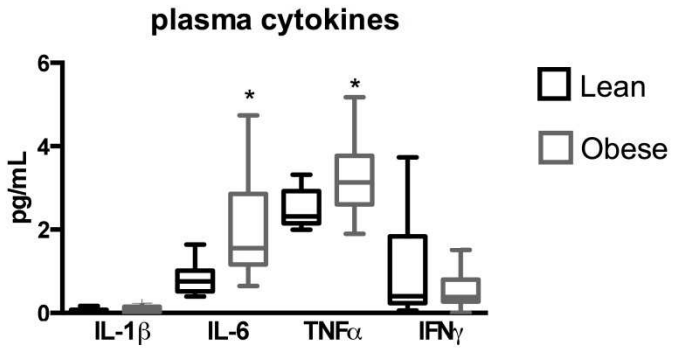

Figure 2

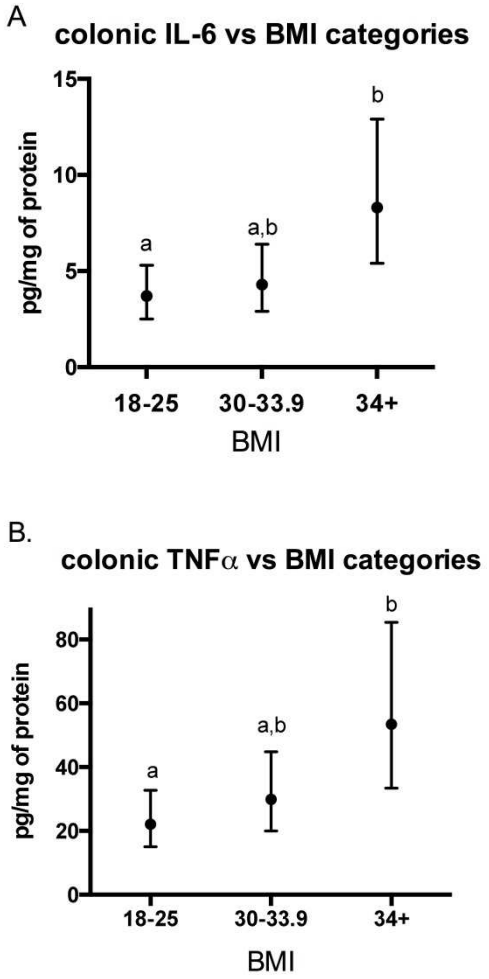

Figure 3

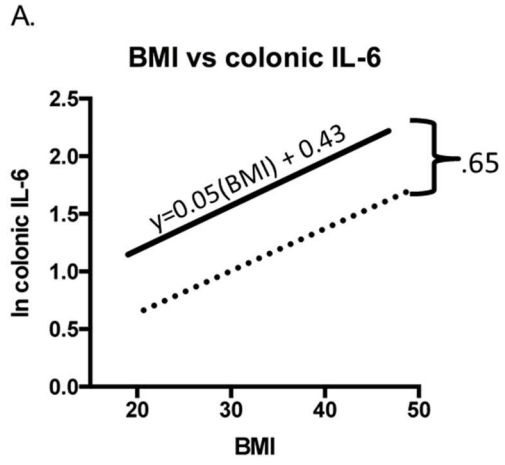

B.

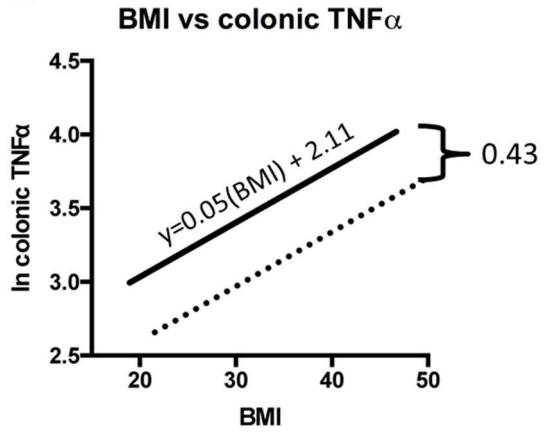
BMI vs colonic TNFα
ln colonic TNFα
4.5
4.0
3.5
3.0
2.5
y=0.05(BMI) + 2.11
0.43
20
30
40
50
BMI

Figure 4

A

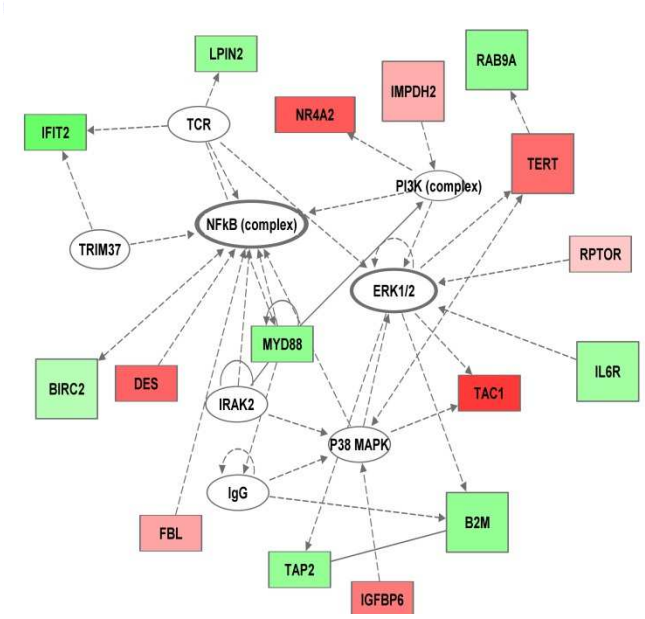
LPIN2
RAB9A
IMPDH2
NR4A2
IFIT2
TCR
TERT
PI3K (complex)
NFkB (complex)
TRIM37
RPTOR
ERK1/2
MYD88
IL6R
BIRC2
DES
IRAK2
TAC1
P38 MAPK
IgG
B2M
FBL
TAP2
IGFBP6

B

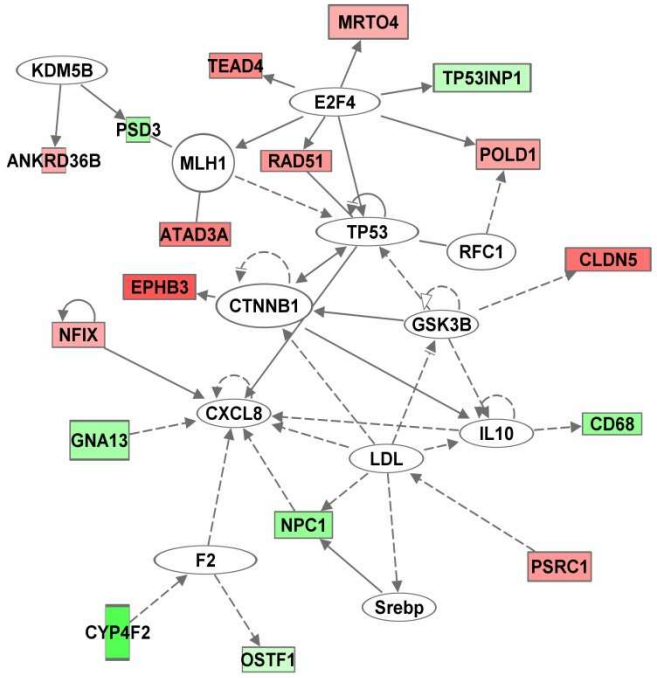
MRTO4
KDM5B
TEAD4
TP53INP1
E2F4
PSD3
ANKRD36B
MLH1
RAD51
POLD1
ATAD3A
TP53
RFC1
CLDN5
EPHB3
CTNNB1
GSK3B
NFIX
CXCL8
IL10
CD68
GNA13
LDL
NPC1
F2
PSRC1
Srebp
CYP4F2
OSTF1

Table 1

Endpoint	Lean	Obese	p-value
Gender (M,F)	9,7	14,12	p=0.99*
Age	56.1±1.70	58.6±1.3	p=.69
BMI	22.0±0.50	34.7±0.85	p<0.01
Waist(cm)	31.6±0.72	44.8±0.91	p<0.01
Hip(cm)	36.2±0.72	46.5±0.87	p<0.05
WHR	0.87±0.02	0.97±0.02	p<0.05

Table 2

Diseases and Disorders	**p value**	**# molecules**
Cancer	3.17E-04	120
Hematological disease	3.17E-04	43
Organismal injury and abnormalities	3.17E-04	125
Reproductive injury disease	7.25E-04	75
Immunological disease	8.27E-04	36
Molecular and Cellular Functions	**p value**	**# molecules**
Lipid metabolism	7.25E-07	16
Molecular transport	7.25E-07	20
Small molecule biochemistry	7.25E-07	22
Cell Death and Survival	1.19E-03	25
Cellular Development	1.19E-03	18
Top Networks		
Network ID	**Network Functions**	**Score**
1	Cell-To-Cell Signaling and Interaction, Hair and Skin Development and Function, Embryonic Development	25
2	Cancer, Organismal Injury and Abnormalities, Gene Expression	25
3	Tissue Development, Cellular Growth and Proliferation, Cancer	21
4	DNA Replication, Recombination, and Repair, Cellular Assembly and Organization, Cell Death and Survival	17
5	Cellular Movement, Cell-To-Cell Signaling and Interaction, Hematological System Development and Function	13

Figure Legends

Figure 1. Plasma cytokines in lean and obese subjects. Tumor necrosis factor-α (TNF-α), Interleukin-1β (IL-1β), Interleukin-6 (IL-6), Interferon γ (IFNγ); Data represented as the median with 95% confidence intervals. Asterisks indicate a p-value < 0.05, lean versus obese subjects.

Figure 2. Colonic cytokine concentrations by BMI category. A) Interleukin-6 (IL-6) and B) Tumor necrosis factor-α (TNF-α) concentrations in pg/mg protein; Median values displayed, with 25% and 75% quartiles generated from a general linear model between cytokines and BMI category, adjusted for NSAID use.

Figure 3. Regressions between BMI and colonic cytokines. The solid line in each figure was generated by performing a linear regression (equation shown) between BMI and the natural log values for colonic A) IL-6 and B) TNF-α. The dotted line represents the regression among those individuals regularly using NSAIDs. The value adjacent to these lines represents the decrease (as a natural log) in colonic cytokine concentration ascribable to the use of NSAIDs.

Fig. 4. Top-scoring Biologic networks identified by Ingenuity Pathway Analysis. The top-scoring networks in the Pathway Analysis were most closely associated with A) *Cell-to-Cell Signaling* and B) *Cancer and Gene Expression*. Genes differentially expressed in the colon of obese subjects compared to lean subjects (q-value≤0.10) are enclosed in a rectangle; genes enclosed in ovals are not differentially expressed but are part of the biologic network. Shades of

red indicate the magnitude of down-regulation in obese individuals and shades of green indicate the magnitude of up-regulation in obese subjects. Solid lines indicate a direct molecular relationship and dotted lines indicate an indirect molecular relationship.

Table Legends

Table 1. Study enrollment characteristics in the 42 lean and obese subjects. Data represents the mean ± standard error. M, male; F, female; WHR, waist:hip ratio. An asterisk indicates that the proportion of each gender in obese and lean groups is not significantly different.

Table 2. Top IPA categories enriched amongst the genes differentially expressed in the colonic epithelium of obese compared to lean individuals. IPA, Ingenuity Pathway Analysis®; # molecules indicates the number of differentially expressed genes associated with the particular disease or cellular function; Score is generated from a hypergeometric distribution and calculated with a right-tailed Fishers Exact Test. For instance, a network score of 25 indicates a 1 in 1 X 10^{25} chance of getting the same network by chance when randomly selecting the same number of molecules.

IV. Manuscript II- Specific Aim 2

Interleukin-1 signaling mediates obesity-promoted elevations in inflammatory cytokines, epithelial proliferation, and Wnt activation in the mouse colon.

Authors
Anna C Pfalzer[1,2], Jimmy W Crott[1,2], Donald E Smith[3], Paloma E Garcia[1], and Joel B Mason[1,2].

[1]Vitamins and Carcinogenesis Laboratory, USDA Jean Mayer Human Nutrition Research Center on Aging at Tufts University, Boston, Massachusetts, United States of America, [2]Friedman School of Nutrition Science and Policy, Tufts University, Boston, Massachusetts, United States of America, [3]Comparative Biology Unit, USDA Jean Mayer Human Nutrition Research Center on Aging at Tufts University, Boston, Massachusetts, United States of America

*Correspondence:
Joel B Mason, MD
USDA HNRCA at Tufts University
711 Washington St, Boston, MA 02111.
joel.mason@tufts.edu

Abstract

Obesity is an important risk factor for colorectal cancer (CRC). One mechanism by which obesity may promote the development of CRC is by generating a chronic, low-grade state of inflammation in the colon. Interleukin-1β is a pro-inflammatory cytokine that is often elevated in obesity and it is known to activate several pro-carcinogenic signaling pathways that are relevant to colonic carcinogenesis. We therefore sought to define the role of IL-1β in mediating the early biochemical and molecular events leading up to CRC in two experiments. In one experiment male C57BL/6 (WT) mice were randomized to either low-fat or high-fat diets resulting in lean and obese mice, and in a second experiment lean and obese groups of WT mice were compared to two analogous groups of male mice lacking a functional IL-1 receptor (IL1RKO). WT obese mice displayed significantly elevated levels of IL-1β and TNF-α in the colonic mucosa ($p<0.05$)

compared to WT lean controls, a significant expansion of the proliferation zone of the colonic crypt ($p<0.05$), and indications of activation of the Wnt signaling cascade, as evidenced by a 2-fold increase in the active form of β-catenin in isolated colonocytes ($p<0.05$). The latter was corroborated by a 2-fold increase in intranuclear β-catenin of marginal statistical significance ($p=0.10$). These obesity-induced alterations were absent in the obese IL1RKO mice. Measures of Akt and NFκB activation were not evident in either the WT or IL1RKO obese mice. In the absence of interleukin-1 signaling, obesity-induced elevations of colonic IL-1β, TNFα, enhanced epithelial proliferation and Wnt activation no longer occur. These observations underscore the important mechanistic roles that IL-1 signaling appears to play in mediating the pro-cancerous effects of obesity in the colon, thereby identifying a potential target for future strategies aimed at chemoprevention.

One sentence summary: Obesity-induced elevations of colonic IL-1β, TNFα, epithelial proliferation and Wnt signaling in WT mice are mediated by IL-1 signaling.

Acknowledgements

We thank the staff of the Comparative Biology Unit at the HNRCA for their assistance with animal care, the Boston Nutrition Obesity Research Center for use of their rodent EchoMRI, and Dr. Andrew Greenberg for his technical advice and comments on the study design. We would especially like to thank Drs. Peter and Joan Cohn and the Jean Mayer HNRCA Directors Student Innovation Fund for their support for this study. This study was funded by the Agricultural Research Service of the United States Department of Agriculture, Cooperative Agreement #58-

1950-0-014. Opinions and ideas expressed in this publication are not necessarily those of the U.S. Department of Agriculture.

Introduction

There is increasing epidemiologic and experimental evidence that obesity is a robust risk factor for several common cancers. In fact, a prospective cohort of ~1 million Americans recently estimated that 15-20% of all cancer deaths in the United States are attributable to overweightness and obesity*(2)*. Colorectal cancer (CRC) is clearly one of those cancers whose risk is increased by obesity: studies indicate that obesity causes a 50-100% increase in the risk of colorectal cancer in men and a 20-50% increase in women*(34)*. Even overweightness (BMI 25.1-29.9) produces a discernible (and statistically significant) 20% increase in relative risk*(2)*, underscoring how sensitive the development of this cancer is to excess adiposity. A genuine causal link between obesity and an increased risk of CRC has been demonstrated by animal studies*(35)*. Although it has been known for over two decades that obesity produces a chronic, low-grade inflammatory state that is evident in the blood and adipose tissue, it is only recently that observations have demonstrated that this inflammatory milieu also resides in the colons of obese animals and humans*(3, 36–38)*. The evidence to date suggests that this obesity-induced inflammation in the colon plays an important (although not necessarily an exclusive) role in mediating the increased risk of colonic carcinogenesis.

Although some studies have suggested that TNF-α may play a role in mediating the pro-cancerous effects of obesity in the colon*(3)*,*(36, 37)*, there are several reasons to believe that IL-1β plays an independent prominent role in mediating this effect. Elegant studies in mice by Tu *et al* showed that upregulated expression of IL-1β in the gastrointestinal epithelium is, by itself,

sufficient to incite inflammation and cancer*(39)*. In another mouse study, IL-1β expression was found to be necessary for the acquisition of an invasive phenotype and for the stimulation of angiogenesis in several different types of tumors*(40)*. Moreover, several human studies have observed that polymorphisms in the IL-1β gene that increase its production or activity are associated with a higher risk of cancer or a shorter cancer survival*(41)*,*(42)*,*(43)* whereas associations with analogous polymorphisms in other pro-inflammatory cytokines have not been nearly as consistent*(41)*. Also, a prominent role played by IL-1β signaling in carcinogenesis may relate to its multiplier effect, since it upregulates the expression of several other pro-inflammatory elements such as TNF-α, IL-6, and COX-2*(44)*,*(45)* and regulates insulin*(46)* and leptin secretion in humans and mice*(14)*.

IL-1β is also a potent promoter of several pro-carcinogenic signaling pathways, including the Wnt cascade. Basal activity of the Wnt signaling pathway is critical for maintenance of stem cell properties of the colonic crypt*(25)*. However, over-activation of this pathway is a pivotal step in the early development of the vast majority of colon cancers*(25)*. Further, IL-1β has been observed to activate other pro-cancerous pathways in addition to Wnt: colon cancer cells exposed to exogenous IL-1β also activates the Akt and NFκB pathways*(33)*. Thus, we hypothesized that the absence of IL-1 signaling would lead to a reduction in pro-inflammatory cytokine secretion in the colons of obese mice, coupled with a decrease in epithelial proliferation and attenuation in the pro-cancerous signaling pathways mentioned above. To examine this hypothesis we utilized a transgenic mouse lacking a functional IL-1 receptor.

Materials and Methods

Animal Studies

Study #1: All animal procedures were approved by the institutional review board of the Jean Mayer USDA Human Nutrition Research Center on Aging at Tufts University. Two strains of male mice were used for this study; wildtype C57BL6/J and IL1R1^{tm1lmx} (stock #664 and #3245, respectively, Jackson Laboratories, Bar Harbor, ME). The latter animals lack a response to both IL-1α and IL-1β although, *in vivo*, IL-1β appears to be, by far, the principal form of IL-1 acting upon non-neoplastic colonocytes*(47)*. At 8 weeks of age, animals were randomized to a 10% low-fat diet (LFD) or 60% high-fat diet (HFD, Research Diets, D12450BM, D12492M, respectively) for 16 weeks; 10 animals were allocated to each group. At diet week 15, body composition was measured by MRI (EchoMRI, 100H, Houston, TX). After 16 weeks on diet, mice were euthanized by CO_2 asphyxiation followed by cervical dislocation and exsanguination by cardiac puncture.

Study #2: Due to insufficient quantities of colonocytes remaining from the first study, a small accessory study was conducted, utilizing only wildtype C57BL6/J (stock# 664) male mice. At 6 weeks of age, animals were randomized to the same LFD or HFD for 14 weeks (n= 10 animals in each group). After 14 weeks on diet, animals were sacrificed with the same protocol described above. The abdomen was then opened and the large intestine removed and placed onto an ice-cold glass plate. The proximal half of the colon was used to isolate colonocytes. Colonocytes were isolated at 0°C to arrest their metabolism, as previously described*(48)*. Blood was spun at 1000g and plasma stored at -80°C.

Insulin and Leptin

Plasma insulin and leptin values for each animal were determined from study #1 plasma. Samples were measured using an electro-chemiluminescent assay, according to the manufacturer's guidelines (K15124C-1, MesoScale S600, Rockville, MD).

Colonic cytokines

Whole cell lysates were generated from isolated colonocytes and colonic mucosa from study #1 using RIPA buffer (ThermoFisher, cat# 89900) with protease and phosphatase inhibitors (Roche, Indianapolis, IN). Protein was quantified using the Bradford Assay (BioRad, Hercules, CA). Interleukin-1β (IL-1β), interleukin-6(IL-6), tumor necrosis factor-α(TNFα), and interferon-γ (IFNγ) protein levels were then measured in colonocytes and colonic mucosa with an electro-chemiluminescence assay (MesoScale, S600, Rockville, MD). Cytokine levels were adjusted for total protein and reported as picograms per milligram of protein.

Epithelial proliferation

Proliferation was assessed by immunohistochemistry (IHC). For IHC, the paraffin embedded slides were deparaffinized in xylene, followed by rehydration in ethanol. Slides were incubated with ki-67 antibody in PBS and 1% bovine serum albumin (Sigma-Aldrich, cat # 4501880). The antibody was diluted 1:500 in the antibody solution. Following incubation with the biotinylated anti-mouse secondary antibody (Vector Laboratories, Burlingame, CA, USA), the slides were treated with Vectastain Elite ABC reagent (Vector Laboratories) and hematoxylin counterstain. Five or more mid-longitudinal sections of crypts from each animal were assessed. Crypts were

only quantified if the entire crypt from the luminal surface to the base of the crypt were visible under magnification. Quantification was done by a blinded investigator under 400-fold magnification. Labelling index was assessed by quantifying the total number of ki-67 positive cells in each crypt divided by the total number of cells in the crypt. The extent of the proliferation zone was assessed by first visually dividing the crypt into upper, middle and lower thirds. Normally, ki-67 cells reside almost exclusively in the bottom third*(49)*; the metric used to measure expansion of the proliferation zone was the mean number of ki-67 positive cells located in the middle and top thirds of the crypt.

Akt, NFκB and Wnt Activation

Whole cell lysates from isolated colonocytes and scraped mucosa from study #1 were used for all the following analytes except for the western blot of non-phosphorylated β-catenin, which used colonocytes from study #2.

In cell culture Akt and NFκB activation is typically assessed by measuring the degree of phosophorylation of each of these proteins*(50, 51)*. However we, like others, had difficulty quantifying these phosphoproteins in samples from intact animals. Therefore, as other investigators have done for *in vivo* studies*(52, 53)*, we assessed activation of these two pathways by quantifying proteins that are known to negatively regulate the activity of these Akt and NFκB proteins. Akt activation was measured using a Western blot for carboxy terminal modulator protein (CTMP, #4612; Cell Signaling, Danvers, MA). CTMP is a direct inhibitor of Akt phosphorylation at both Ser473 and Thr308*(54)* and the degree of its expression is generally found to be inversely proportional to the extent of Akt activation*(55, 56)*. NFκB activation was measured using a Western blot for its negative regulator, inhibitor of kappa B α (IκBα) protein

(#9242, Cell Signaling, Danvers, MA). IκBα binds to the nuclear localization signal of NFκB, inhibiting its nuclear translocation*(57)*. Its expression is acknowledged to be inversely proportional to NFκB activation*(58)*. GAPDH was used as a loading control (#2118 Cell Signaling, Danvers,MA). Wnt activation was measured using quantitative immunohistochemistry for intranuclear β-catenin (data not shown; BD Biosciences, San Jose, CA). Quantification was conducted by an investigator blinded to group assignment of the samples. In study #2 protein levels for un-phosphorylated (active) β-catenin were measured in isolated colonocytes with a western blot (BD Biosciences, San Jose, CA) with GAPDH as a loading control (Cell Signaling, Danvers, MA).

Statistics

All data is reported as mean ± SEM. Statistical calculations were performed in GraphPad Prism (La Jolla,CA) with Tukey's post-hoc test for multiple comparisons when appropriate. Significance was accepted at a p-value of <0.05.

Results

Physiology

By the end of the study #1, both IL1RKO and WT mice on the HFD had approximately 25% greater body weight and 35% greater fat mass compared to their LFD controls ($p<0.01$ for both measures; Figure 1A, 1B). Slight, but significant differences in weight existed between the IL1RKO and WT mice on the LFD at weeks 15 and 16; IL1RKO and WT on the HFD differed slightly at week 5 (Figure 1A). Both HFD groups had significantly elevated plasma insulin ($p<0.05$; Figure 1C) and leptin ($p<0.01$; Figure 1D) levels compared to mice on the LFD.

Similarly, in study #2, HFD animals had approximately 30% greater body weight ($p<0.01$) and 50% greater fat mass ($p<0.01$) compared to their LFD controls (data not shown).

Colonic cytokines

In study #1, analysis of the colonic mucosa revealed that there was an approximate 60% increase in colonic IL-1β and 20% increase in TNF-α in WT HFD compared to WT LFD mice ($p<0.05$; Figure 2A, 2B). In contrast, no significant increase in these two cytokines was observed in the obese IL1RKO mice compared to either the lean WT or IL1RKO controls. There were no significant differences in colonic IL-6 or IFNγ among the four groups (data not shown).

When cytokine concentrations were similarly compared in isolated colonocytes from study #1, no differences between the four groups were present (data not shown).

Epithelial Proliferation

In study #1, WT HFD-fed mice had approximately 25% more ki-67 positive cells in the upper two-thirds of the colonic crypts (i.e.: expansion of the proliferation zone) than their lean counterparts ($p<0.05$; Figure 3). This increase was not present in the HFD IL1RKO animals.

When proliferation was instead measured by the mean percentage of crypt cells that were ki-67 positive (i.e.: the labeling index) there were no significant differences among the groups. However, it is recognized in both rodent[43] and human studies[31,32] that expansion of the proliferation zone is a more robust predictor of subsequent tumor development than the labeling index.

CTMP, IκBα, and Wnt Signaling

In study #1 there was a numerical 2-fold increase in crypt cells positive for intranuclear β-catenin in the WT HFD mice compared to the lean WT mice that fell slightly short of statistical significance (p=0.10; data not shown). In contrast, the mean difference in cells positive for intra-nuclear β–catenin between the obese and lean IL1RKO mice did not approach significance (p=0.37; data not shown).

Since the apparent increase in nuclear β-catenin via quantitative immunohistochemistry did not reach statistical significance, we sought to confirm that observation using an alternative methodology, which prompted an accessory study of similar design, study #2. In that study, in which we only compared WT LFD and HFD mice, we found a significant 2-fold increase in the non-phosphorylated form of β-catenin in isolated colonocytes of obese WT mice compared to lean ($p<0.05$; Figure 4). This is the form of β–catenin that can translocate into the nucleus and affect Wnt signaling*(59)*.

In study #1 CTMP and IκBα protein expression were assessed in isolated colonocytes. Colonocytes were first assessed since the primary concern is whether activation of pro-cancerous signaling pathways is occurring in those cells specifically that have the potential of undergoing malignant transformation. No differences could be discerned in the four groups of mice (Figures 5A and B). These two proteins were then probed in the samples of colonic scrapings, and the results were similarly null.

Discussion

The link between obesity and colorectal cancer (CRC) has been well-documented in epidemiologic studies*(34, 60)* and causality has been proven in animal models*(61)*. Furthermore, there is growing evidence that the inflammatory environment created in the colon by obesity is

an important mechanistic factor in this relationship*(3, 18)*. The focus of our study was to provide explicit evidence that the pro-inflammatory cytokine interleukin-1β (IL-1β) mediates, at least in part, obesity-promoted elevations in colonic cytokines, proliferation and alterations in pro-carcinogenic signaling pathways. Our observations confirm that diet-induced obesity results in an elevation in colonic TNFα and IL-1β and like the observed alterations in proliferation and Wnt signaling, these changes depended on the presence of an intact IL-1 signaling system. These effects of IL-1 signaling are entirely consistent with an extensive literature that indicates that IL-1β produces a positive feedback that both magnifies inflammation*(44)* and stimulates Wnt signaling*(12)*. It is not surprising that elevations in both IL-1β and TNF-α occurred when intact IL-1 signaling was present since there is a considerable degree of cross-talk among the downstream signaling events incited by these two cytokines*(62)*. Further, the addition of exogenous IL-1β is able to increase the transcription and translation of TNF*(32)* and the production of other pro-inflammatory molecules*(44)*. The ability of IL-1β to regulate the production and downstream signaling of a host of other pro-inflammatory cytokines underscores the potential importance of this particular cytokine in inciting events leading to the development of obesity-promoted colon cancer.

It is notable that the rise in colonic cytokines was only observed in the colonic mucosa rather than isolated colonocytes. The inflammatory state produced by obesity is thought to be largely due the secretion of pro-inflammatory molecules by macrophages*(63, 64)*. Thus, colonocytes themselves might not be the source of the excess colonic cytokines observed in obesity. Rather, it may be that macrophages or other immune cells located in the lamina propria that underlies the epithelium are the source of the mediators. Macrophage recruitment, and the

cytokine secretion that ensues, has consistently been observed in the adipose tissue of obese mice*(65)*; however, future studies will be necessary to identify the particular cell type(s) in the colonic mucosa that are responsible for these elevations in colonic cytokines.

Rodent studies have demonstrated a significant positive correlation between expansion of the proliferation zone and the development of colonic carcinomas*(66)*, and in addition, a significant body of literature indicates that expansion of the proliferation zone is more closely linked to the development of human colonic neoplasms than an increase in the labeling index alone*(67, 68)*. It is therefore of considerable import that we detected a significant expansion of the proliferation zone in the colons of obese mice even though no change in the labeling index was observed. The expansion of the proliferation zone in the obese WT mice was another observation which was absent in the IL1RKO obese mice (Figure 3), indicating that IL-1 signaling is an important factor in producing the abnormal pattern of epithelial proliferation that accompanies obesity. The expansion of the proliferation zone that accompanied obesity in this study would be expected since IL-1β also activated Wnt signaling: one downstream effect of activated Wnt signaling is enhanced proliferation*(12)*. The link between IL-1 signaling and proliferation has been identified previously*(69)* in various *in vitro* models, but the observation that IL1RKO mice are resistant to the proliferative effect of obesity provides further evidence for the particularly pivotal role of this cytokine in the development of CRC.

Collectively, our observations suggest that obesity elevates Wnt signaling in colonocytes and that this effect is lost when IL-1 signaling is ablated. In normal colonic epithelium, Wnt signaling is critical for sustaining adequate colonocyte turnover but when inappropriately

activated it is generally regarded as one of the earliest, and most consistent, steps in the molecular carcinogenesis of spontaneous colorectal cancers*(59)*. Activated β-catenin is the final common mediator of canonical Wnt signaling and the nuclear availability of this molecule concurs with the magnitude of signaling activation. Since the apparent increase in Wnt activity accompanying obesity that was measured by quantitative immunohistochemistry was not, by itself, convincing we sought further evidence of Wnt activation in the follow-up study, which did demonstrate a significant increase in the active form of β-catenin in the colonocytes of obese WT mice (Figure 4). Numerous investigators have found that increases in the cellular levels of non-phosphorylated β-catenin concur with increased signaling through the Wnt pathway and its downstream sequalae*(70, 71)*.

IL-1β signaling has also been shown to activate the Akt and NFκB pathways in certain settings*(12, 72)*, but our observations do not support such activation under the conditions of these experiments. Additional *in vivo* studies are indicated that utilize alternative means of detecting Akt and NFκB activation, since many investigators have found it difficult to assess direct activation of these pathways by quantifying phosphorylation of the effector molecules. Although our indirect methods of detecting Akt and NFκB activation suggest no changes with obesity, ultimately they may have lacked the sensitivity necessary to detect slight differences due to obesity.

This study possesses certain limitations. First, the engineered mice we used lack a response to both IL-1α and IL-1β and therefore we cannot definitively distinguish between the effects produced by these two forms of IL-1. Nevertheless, IL-1β appears to be, by far, the

principal form of IL-1 acting upon non-neoplastic colonocytes in the intact human*(47)*, so the assumption in this study is that most of the IL-1 mediated effects are due to IL-1β. Obesity can be reliably induced in male mice but for reasons that remain unclear, a significant proportion of female mice are resistant to the induction of obesity by a high fat diet, as described by prior investigators*(73)*. It was for this reason that we chose to confine these studies to male mice. This represents a limitation of our conclusions since we cannot exclude the possibility that our observations are not generalizable to females. Another limitation of this study is the potential roles played by the observed elevations in plasma insulin and leptin. Obesity-induced alterations in the insulin axis, as well as in the adipocytokines (leptin and adiponectin) are implicated as additional mechanistic factors that may assist in mediating the pro-carcinogenic effects of obesity*(74)*,[34]. Nevertheless, the reversal of most of the important endpoints in this study that occurred with the ablation of IL-1 signaling indicate that, regardless of what downstream events might be effected by the insulin axis and adipocytokines, IL-1 mediated effects are important.

This study contributes several novel pieces of information about the relationship between IL-1 signaling and early events in obesity-promoted colonic carcinogenesis. First, IL-1 signaling appears to be an important effector of several of the pro-cancerous biochemical, cell signaling, and cytokinetic anomalies that obesity produces in the colon. Secondly, the discrepancies we observed by comparing results from isolated colonocytes versus those from scraped colonic mucosa suggest that the origin of the excess cytokines is not the colonocytes themselves. These observations underscore the importance of IL-1 signaling in regulating physiologic and molecular mechanisms relevant to the development of obesity-promoted colonic carcinogenesis

and, by doing so, offer a signaling pathway that can be targeted in order to mitigate the increased risk of cancer due to obesity.

References

1. R. Siegel, C. Desantis, A. Jemal, Colorectal cancer statistics, 2014, *CA Cancer J Clin* **64**, 104–117 (2014).
2. E. E. Calle, C. Rodriguez, K. Walker-Thurmond, M. J. Thun, Overweight, obesity, and mortality from cancer in a prospectively studied cohort of U.S. adults, *N Engl J Med* **348**, 1625–1638 (2003).
3. M. B. Flores, G. Z. Rocha, D. M. Damas-Souza, F. Osorio-Costa, M. M. Dias, E. R. Ropelle, J. A. Camargo, R. B. de Carvalho, H. F. Carvalho, M. J. Saad, J. B. Carvalheira, Obesity-induced increase in tumor necrosis factor-alpha leads to development of colon cancer in mice, *Gastroenterology* **143**, 741–744 (2012).
4. S. E. Shoelson, J. Lee, A. B. Goldfine, Inflammation and insulin resistance, *J Clin Invest* **116**, 1793–1801 (2006).
5. L. M. Lashinger, E. L. Rossi, S. D. Hursting, Obesity and resistance to cancer chemotherapy: interacting roles of inflammation and metabolic dysregulation, *Clin Pharmacol Ther* **96**, 458–463 (2014).
6. E. J. Park, J. H. Lee, G. Y. Yu, G. He, S. R. Ali, R. G. Holzer, C. H. Osterreicher, H. Takahashi, M. Karin, Dietary and genetic obesity promote liver inflammation and tumorigenesis by enhancing IL-6 and TNF expression, *Cell* **140**, 197–208 (2010).
7. U. J. Jung, M. S. Choi, Obesity and its metabolic complications: the role of adipokines and the relationship between obesity, inflammation, insulin resistance, dyslipidemia and nonalcoholic fatty liver disease, *Int J Mol Sci* **15**, 6184–6223 (2014).
8. F. M. Mendonca, F. R. de Sousa, A. L. Barbosa, S. C. Martins, R. L. Araujo, R. Soares, C. Abreu, Metabolic syndrome and risk of cancer: Which link?, *Metabolism* (2014), doi:10.1016/j.metabol.2014.10.008.
9. M. N. Vansaun, Molecular pathways: adiponectin and leptin signaling in cancer., *Clin. Cancer Res.* **19**, 1926–32 (2013).
10. R. Fodde, W. Edelmann, K. Yang, C. van Leeuwen, C. Carlson, B. Renault, C. Breukel, E. Alt, M. Lipkin, P. M. Khan, et al., A targeted chain-termination mutation in the mouse Apc gene results in multiple intestinal tumors, *Proc Natl Acad Sci U S A* **91**, 8969–8973 (1994).
11. S. Teshima, H. Nakanishi, M. Nishizawa, K. Kitagawa, M. Kaibori, M. Yamada, K. Habara, A. H. Kwon, Y. Kamiyama, S. Ito, T. Okumura, Up-regulation of IL-1 receptor through PI3K/Akt is essential for the induction of iNOS gene expression in hepatocytes, *J. Hepatol.* **40**, 616–623 (2004).
12. P. Kaler, L. Augenlicht, L. Klampfer, Macrophage-derived IL-1beta stimulates Wnt signaling and growth of colon cancer cells: a crosstalk interrupted by vitamin D3, *Oncogene* **28**, 3892–3902 (2009).
13. C. J. Tack, R. Stienstra, L. A. Joosten, M. G. Netea, Inflammation links excess fat to insulin resistance: the role of the interleukin-1 family, *Immunol Rev* **249**, 239–252 (2012).
14. C. A. Dinarello, M. Y. Donath, T. Mandrup-Poulsen, Role of IL-1beta in type 2 diabetes, *Curr Opin Endocrinol Diabetes Obes* **17**, 314–321 (2010).

15. G. S. Hotamisligil, Inflammatory pathways and insulin action, *Int J Obes Relat Metab Disord* **27 Suppl 3**, S53–5 (2003).
16. K. E. Wellen, G. S. Hotamisligil, Obesity-induced inflammatory changes in adipose tissue, *J Clin Invest* **112**, 1785–1788 (2003).
17. H. Li, C. Lelliott, P. Hakansson, K. Ploj, A. Tuneld, M. Verolin-Johansson, L. Benthem, B. Carlsson, L. Storlien, E. Michaelsson, Intestinal, adipose, and liver inflammation in diet-induced obese mice, *Metabolism* **57**, 1704–1710 (2008).
18. Z. Liu, R. S. Brooks, E. D. Ciappio, S. J. Kim, J. W. Crott, G. Bennett, A. S. Greenberg, J. B. Mason, Diet-induced obesity elevates colonic TNF-alpha in mice and is accompanied by an activation of Wnt signaling: a mechanism for obesity-associated colorectal cancer, *J Nutr Biochem* **23**, 1207–1213 (2012).
19. S. D. Day, R. T. Enos, J. L. McClellan, J. L. Steiner, K. T. Velazquez, E. A. Murphy, Linking inflammation to tumorigenesis in a mouse model of high-fat-diet-enhanced colon cancer, *Cytokine* **64**, 454–462 (2013).
20. H. Xu, G. T. Barnes, Q. Yang, G. Tan, D. Yang, C. J. Chou, J. Sole, A. Nichols, J. S. Ross, L. A. Tartaglia, H. Chen, Chronic inflammation in fat plays a crucial role in the development of obesity-related insulin resistance, *J Clin Invest* **112**, 1821–1830 (2003).
21. L. M. Coussens, Z. Werb, Inflammation and cancer, *Nature* **420**, 860–867 (2002).
22. J. A. Eaden, K. R. Abrams, J. F. Mayberry, The risk of colorectal cancer in ulcerative colitis: a meta-analysis, *Gut* **48**, 526–535 (2001).
23. F. L. Meyskens Jr., C. E. McLaren, D. Pelot, S. Fujikawa-Brooks, P. M. Carpenter, E. Hawk, G. Kelloff, M. J. Lawson, J. Kidao, J. McCracken, C. G. Albers, D. J. Ahnen, D. K. Turgeon, S. Goldschmid, P. Lance, C. H. Hagedorn, D. L. Gillen, E. W. Gerner, Difluoromethylornithine plus sulindac for the prevention of sporadic colorectal adenomas: a randomized placebo-controlled, double-blind trial, *Cancer Prev Res* **1**, 32–38 (2008).
24. O. Itano, K. Yang, K. Fan, N. Kurihara, H. Shinozaki, S. Abe, B. Jin, C. Gravaghi, W. Edelmann, L. Augenlicht, L. Kopelovich, R. Kucherlapati, S. Lamprecht, M. Lipkin, Sulindac effects on inflammation and tumorigenesis in the intestine of mice with Apc and Mlh1 mutations, *Carcinogenesis* **30**, 1923–1926 (2009).
25. M. M. Taketo, Shutting down Wnt signal-activated cancer, *Nat Genet* **36**, 320–322 (2004).
26. P. J. Morin, A. B. Sparks, V. Korinek, N. Barker, H. Clevers, B. Vogelstein, K. W. Kinzler, Activation of beta-catenin-Tcf signaling in colon cancer by mutations in beta-catenin or APC, *Science (80-.).* **275**, 1787–1790 (1997).
27. H. Suzuki, D. N. Watkins, K. W. Jair, K. E. Schuebel, S. D. Markowitz, W. D. Chen, T. P. Pretlow, B. Yang, Y. Akiyama, M. Van Engeland, M. Toyota, T. Tokino, Y. Hinoda, K. Imai, J. G. Herman, S. B. Baylin, Epigenetic inactivation of SFRP genes allows constitutive WNT signaling in colorectal cancer, *Nat Genet* **36**, 417–422 (2004).
28. C. H. Chan, U. Jo, A. Kohrman, A. H. Rezaeian, P. C. Chou, C. Logothetis, H. K. Lin, Posttranslational regulation of Akt in human cancer, *Cell Biosci* **4**, 59 (2014).
29. D. A. Cross, D. R. Alessi, P. Cohen, M. Andjelkovich, B. A. Hemmings, Inhibition of glycogen synthase kinase-3 by insulin mediated by protein kinase B, *Nature* **378**, 785–789 (1995).
30. G. Lee, T. Goretsky, E. Managlia, R. Dirisina, A. P. Singh, J. B. Brown, R. May, G. Y. Yang, J. W. Ragheb, B. M. Evers, C. R. Weber, J. R. Turner, X. C. He, R. B. Katzman, L. Li, T. A. Barrett, Phosphoinositide 3-kinase signaling mediates beta-catenin activation in intestinal epithelial stem and progenitor cells in colitis, *Gastroenterology* **139**, 869–81, 881 e1–9 (2010).

31. S. Temraz, D. Mukherji, A. Shamseddine, Potential targets for colorectal cancer prevention, *Int J Mol Sci* **14**, 17279–17303 (2013).
32. M. Knöfler, H. Kiss, B. Mösl, C. Egarter, P. Husslein, Interleukin-1 stimulates tumor necrosis factor-α (TNF-α) release from cytotrophoblastic BeWo cells independently of induction of the TNF-α mRNA, *FEBS Lett.* **405**, 213–218 (1997).
33. P. Kaler, B. N. Godasi, L. Augenlicht, L. Klampfer, The NF-kappaB/AKT-dependent Induction of Wnt Signaling in Colon Cancer Cells by Macrophages and IL-1beta, *Cancer Microenviron* (2009), doi:10.1007/s12307-009-0030-y.
34. E. E. Calle, R. Kaaks, Overweight, obesity and cancer: epidemiological evidence and proposed mechanisms., *Nat. Rev. Cancer* **4**, 579–591 (2004).
35. C. Gravaghi, J. Bo, K. M. Laperle, F. Quimby, R. Kucherlapati, W. Edelmann, S. A. Lamprecht, Obesity enhances gastrointestinal tumorigenesis in Apc-mutant mice, *Int J Obes* **32**, 1716–1719 (2008).
36. S. S. Jain, R. P. Bird, Elevated expression of tumor necrosis factor-alpha signaling molecules in colonic tumors of Zucker obese (fa/fa) rats., *Int. J. Cancer* **127**, 2042–50 (2010).
37. Z. Liu, R. S. Brooks, E. D. Ciappio, S. J. Kim, J. W. Crott, G. Bennett, A. S. Greenberg, J. B. Mason, Diet-induced obesity elevates colonic TNF-alpha in mice and is accompanied by an activation of Wnt signaling: a mechanism for obesity-associated colorectal cancer, *J Nutr Biochem* **23**, 1207–1213 (2012).
38. A. Pfalzer, K. Leung, P. Garcia, Z. Liu, S. Kim, J. Mason, in *Federal of American Societies for Experimental Biology: April 26-30; San Diego, CA.*, (2014).
39. C. A. Dinarello, Interleukin 1 and interleukin 18 as mediators of inflammation and the aging process, *Am J Clin Nutr* **83**, 447S–455 (2006).
40. E. Voronov, D. S. Shouval, Y. Krelin, E. Cagnano, D. Benharroch, Y. Iwakura, C. A. Dinarello, R. N. Apte, IL-1 is required for tumor invasiveness and angiogenesis., *Proc. Natl. Acad. Sci. U. S. A.* **100**, 2645–50 (2003).
41. W. M. Howell, S. J. Turner, J. M. Theaker, A. C. Bateman, Cytokine gene single nucleotide polymorphisms and susceptibility to and prognosis in cutaneous malignant melanoma., *Eur. J. Immunogenet.* (2003), doi:425 [pii].
42. E. M. El-Omar, M. Carrington, W. H. Chow, K. E. McColl, J. H. Bream, H. A. Young, J. Herrera, J. Lissowska, C. C. Yuan, N. Rothman, G. Lanyon, M. Martin, J. F. Fraumeni, C. S. Rabkin, Interleukin-1 polymorphisms associated with increased risk of gastric cancer., *Nature* **404**, 398–402 (2000).
43. M. D. Barber, J. J. Powell, S. F. Lynch, K. C. Fearon, J. A. Ross, A polymorphism of the interleukin-1 beta gene influences survival in pancreatic cancer., *Br. J. Cancer* **83**, 1443–7 (2000).
44. M. Tamura, S. Sebastian, S. Yang, B. Gurates, Z. Fang, S. E. Bulun, Interleukin-1beta elevates cyclooxygenase-2 protein level and enzyme activity via increasing its mRNA stability in human endometrial stromal cells: an effect mediated by extracellularly regulated kinases 1 and 2, *J Clin Endocrinol Metab* **87**, 3263–3273 (2002).
45. S. Tu, G. Bhagat, G. Cui, S. Takaishi, E. a. Kurt-Jones, B. Rickman, K. S. Betz, M. Penz, O. Bjorkdhl, J. G. Fox, T. C. Wang, M. Penz-Oesterreicher, O. Bjorkdahl, J. G. Fox, T. C. Wang, Overexpression of Interleukin-1b Induces Gastric Inflammation and Cancer and Mobilizes Myeloid-Derived Suppressor Cells in Mice, *Cancer Cell* **14**, 408–419 (2008).
46. D. Gao, M. Madi, C. Ding, M. Fok, T. Steele, C. Ford, L. Hunter, C. Bing, Interleukin-1β mediates macrophage-induced impairment of insulin signaling in human primary adipocytes.,

Am. J. Physiol. Endocrinol. Metab. **307**, E289–304 (2014).
47. a Jarry, G. Vallette, E. Cassagnau, a Moreau, C. Bou-Hanna, P. Lemarre, E. Letessier, J. C. Le Neel, J. P. Galmiche, C. L. Laboisse, Interleukin 1 and interleukin 1beta converting enzyme (caspase 1) expression in the human colonic epithelial barrier. Caspase 1 downregulation in colon cancer., *Gut* **45**, 246–251 (1999).
48. B. Schwartz, C. Avivi, S. A. Lamprecht, Isolation and characterization of normal and neoplastic colonic epithelial cell populations, *Gastroenterology* **100**, 692–702 (1991).
49. R. C. van der Wath, B. S. Gardiner, A. W. Burgess, D. W. Smith, Cell organisation in the colonic crypt: a theoretical comparison of the pedigree and niche concepts., *PLoS One* **8**, e73204 (2013).
50. G. Song, G. Ouyang, S. Bao, The activation of Akt/PKB signaling pathway and cell survival, *J. Cell. Mol. Med.* **9**, 59–71 (2005).
51. N. D. Perkins, Post-translational modifications regulating the activity and function of the nuclear factor kappa B pathway., *Oncogene* **25**, 6717–30 (2006).
52. M. Wehenkel, J.-O. Ban, Y.-K. Ho, K. C. Carmony, J. T. Hong, K. B. Kim, A selective inhibitor of the immunoproteasome subunit LMP2 induces apoptosis in PC-3 cells and suppresses tumour growth in nude mice., *Br. J. Cancer* **107**, 53–62 (2012).
53. S. Zhao, J. Fu, F. Liu, R. Rastogi, J. Zhang, Y. Zhao, Small interfering RNA directed against CTMP reduces acute traumatic brain injury in a mouse model by activating Akt., *Neurol. Res.* **36**, 483–90 (2014).
54. D. R. Alessi, M. Andjelkovic, B. Caudwell, P. Cron, N. Morrice, P. Cohen, B. A. Hemmings, Mechanism of activation of protein kinase B by insulin and IGF-1., *EMBO J.* **15**, 6541–51 (1996).
55. S. M. Maira, I. Galetic, D. P. Brazil, S. Kaech, E. Ingley, M. Thelen, B. A. Hemmings, Carboxyl-terminal modulator protein (CTMP), a negative regulator of PKB/Akt and v-Akt at the plasma membrane., *Science* **294**, 374–80 (2001).
56. T. Miyawaki, D. Ofengeim, K.-M. Noh, A. Latuszek-Barrantes, B. A. Hemmings, A. Follenzi, R. S. Zukin, The endogenous inhibitor of Akt, CTMP, is critical to ischemia-induced neuronal death., *Nat. Neurosci.* **12**, 618–26 (2009).
57. Z. J. Chen, L. Parent, T. Maniatis, Site-specific phosphorylation of IkappaBalpha by a novel ubiquitination-dependent protein kinase activity., *Cell* **84**, 853–62 (1996).
58. J. Hu, M. Haseebuddin, M. Young, N. H. Colburn, Suppression of p65 phosphorylation coincides with inhibition of I??B?? polyubiquitination and degradation, *Mol. Carcinog.* **44**, 274–284 (2005).
59. H. Clevers, R. Nusse, Wnt/beta-catenin signaling and disease, *Cell* **149**, 1192–1205 (2012).
60. M. J. Gunter, M. F. Leitzmann, Obesity and colorectal cancer: epidemiology, mechanisms and candidate genes, *J Nutr Biochem* **17**, 145–156 (2006).
61. B. O. Karim, D. L. Huso, Mouse models for colorectal cancer., *Am. J. Cancer Res.* **3**, 240–50 (2013).
62. S.-K. Yang, Y.-C. Wang, C.-C. Chao, Y.-J. Chuang, C.-Y. Lan, B.-S. Chen, Dynamic cross-talk analysis among TNF-R, TLR-4 and IL-1R signalings in TNFalpha-induced inflammatory responses., *BMC Med. Genomics* **3**, 19 (2010).
63. E. Cassol, T. Rossouw, S. Malfeld, P. Mahasha, T. Slavik, C. Seebregts, R. Bond, J. du Plessis, C. Janssen, T. Roskams, F. Nevens, M. Alfano, G. Poli, S. W. van der Merwe, CD14+ macrophages that accumulate in the colon of African AIDS patients express pro-inflammatory cytokines and are responsive to lipopolysaccharide, *BMC Infect. Dis.* **15**, 430 (2015).

64. C. C. Bain, C. L. Scott, H. Uronen-Hansson, S. Gudjonsson, O. Jansson, O. Grip, M. Guilliams, B. Malissen, W. W. Agace, A. M. Mowat, Resident and pro-inflammatory macrophages in the colon represent alternative context-dependent fates of the same Ly6Chi monocyte precursors., *Mucosal Immunol.* **6**, 498–510 (2013).
65. V. Dam, T. Sikder, S. Santosa, From neutrophils to macrophages: differences in regional adipose tissue depots, *Obes. Rev.* **17**, 1–17 (2016).
66. T. J. Koh, G. J. Dockray, A. Varro, R. J. Cahill, C. A. Dangler, J. G. Fox, T. C. Wang, Overexpression of glycine-extended gastrin in transgenic mice results in increased colonic proliferation., *J. Clin. Invest.* **103**, 1119–26 (1999).
67. G. M. Paganelli, G. Biasco, R. Santucci, G. Brandi, A. A. Lalli, M. Miglioli, L. Barbara, Rectal cell proliferation and colorectal cancer risk level in patients with nonfamilial adenomatous polyps of the large bowel., *Cancer* **68**, 2451–2454 (1991).
68. M. Risio, M. Lipkin, G. Candelaresi, A. Bertone, S. Coverlizza, F. P. Rossini, Correlations between rectal mucosa cell proliferation and the clinical and pathological features of nonfamilial neoplasia of the large intestine., *Cancer Res.* **51**, 1917–21 (1991).
69. J. M. Vela, E. Molina-Holgado, A. Arévalo-Martín, G. Almazán, C. Guaza, Interleukin-1 regulates proliferation and differentiation of oligodendrocyte progenitor cells., *Mol. Cell. Neurosci.* **20**, 489–502 (2002).
70. M. van de Wetering, E. Sancho, C. Verweij, W. de Lau, I. Oving, A. Hurlstone, K. van der Horn, E. Batlle, D. Coudreuse, A. P. Haramis, M. Tjon-Pon-Fong, P. Moerer, M. van den Born, G. Soete, S. Pals, M. Eilers, R. Medema, H. Clevers, The beta-catenin/TCF-4 complex imposes a crypt progenitor phenotype on colorectal cancer cells, *Cell* **111**, 241–250 (2002).
71. M. van Noort, J. Meeldijk, R. van der Zee, O. Destree, H. Clevers, Wnt signaling controls the phosphorylation status of beta-catenin., *J. Biol. Chem.* **277**, 17901–5 (2002).
72. B.-C. Chen, W.-T. Wu, F.-M. Ho, W.-W. Lin, Inhibition of interleukin-1beta -induced NF-kappa B activation by calcium/calmodulin-dependent protein kinase kinase occurs through Akt activation associated with interleukin-1 receptor-associated kinase phosphorylation and uncoupling of MyD88., *J. Biol. Chem.* **277**, 24169–79 (2002).
73. H. Shi, D. J. Clegg, Sex differences in the regulation of body weight., *Physiol. Behav.* **97**, 199–204 (2009).
74. E. H. Allott, S. D. Hursting, Obesity and cancer: mechanistic insights from transdisciplinary studies., *Endocr. Relat. Cancer* **22**, R365–86 (2015).
75. L. MI, W. Huber, S. Anders, Moderated estimation of fold change and dispersion for RNA-Seq data with DESeq2, *bioRxiv* (2014), doi:http://dx.doi.org/10.1101/002832,http://dx.doi.org/10.1101/002832.

Figures

Figure 1

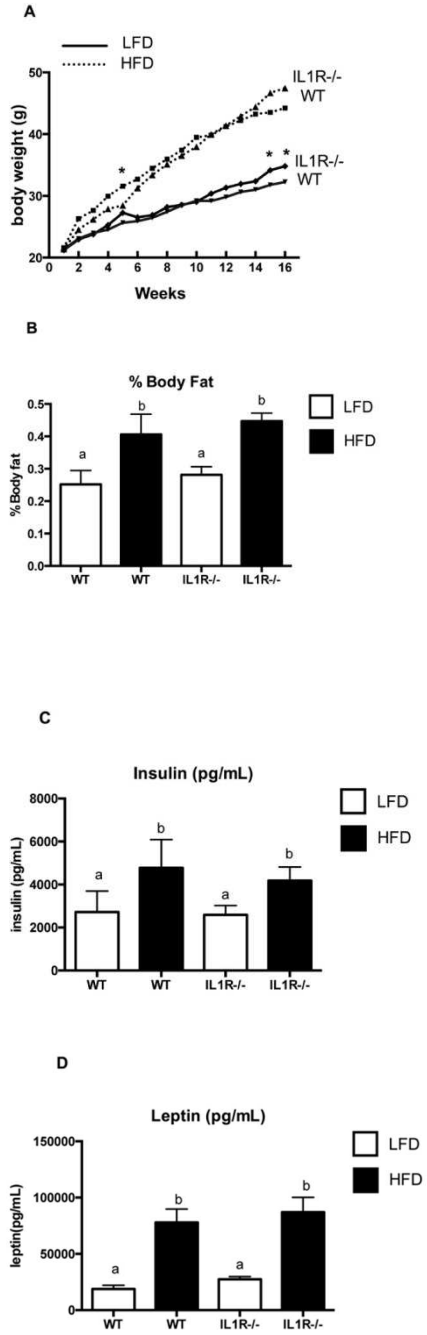

Figure 2

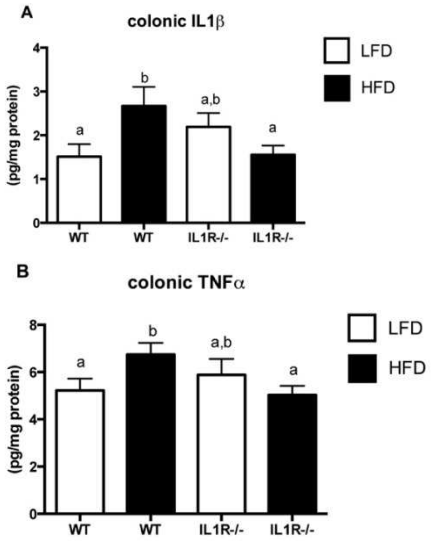

Figure 3

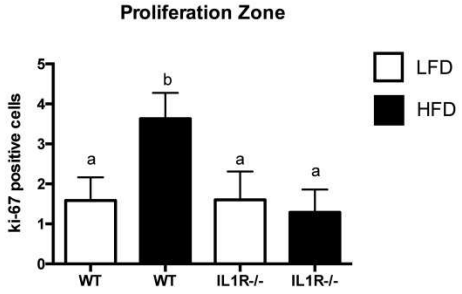

Figure 4

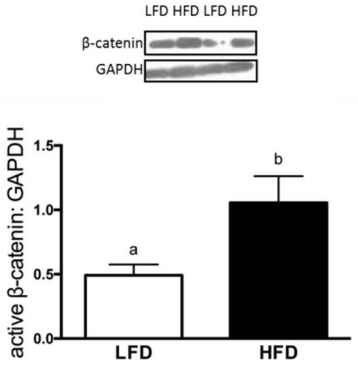

Figure 5

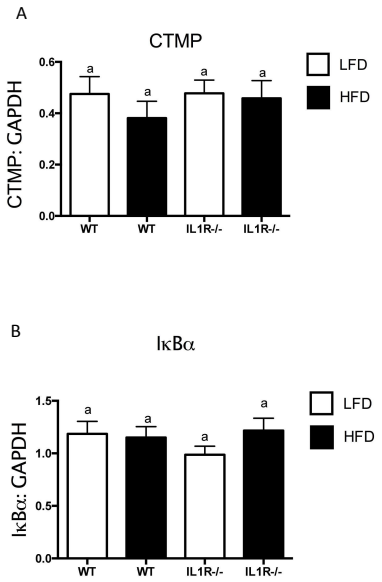

Figure Legends

1. **The high-fat diet increases metabolic markers of obesity in WT and IL1RKO mice**. A) weekly body weights, B) percent body fat, C) plasma insulin and D) leptin levels. The bars shown in each figure are mean ± SEM; n=12 animals per group. P-value <0.05 and determined by unpaired Student's t-test with Tukey's post-hoc test for multiple comparisons (P-value<0.01 for Figure 1B and 1D). Bars sharing a superscript are not significantly different and an asterisk indicates that body weights were significantly different for a single weekly weight.

2. **High fat-fed wild-type mice have an elevation in pro-inflammatory cytokines in the colonic mucosa**. Colonic A) IL-1β and B) TNF-α are presented in picograms per milligram of protein. P-value <0.05 and determined by unpaired Student's t-test with Tukey's post-hoc test for multiple comparisons. Bars sharing a superscript are not significantly different.

3. **Colonic proliferation in obese and lean mice**. A) WT mice on HFD had a significant expansion of the proliferation zone in the colonic crypt compared to lean WT mice while there was no difference between IL1RKO lean and obese mice. Values indicate mean number of ki-67 positive cells in the upper two-thirds of the colonic crypts. P-value <0.05 and determined by unpaired Student's t-test with Tukey's post-hoc test for multiple comparisons. Bars sharing a superscript are not significantly different.

4. Obesity elevates Wnt signaling in the colon of obese male mice. WT mice on a HFD exhibited increased levels of non-phosphorylated (i.e.: active) β-catenin protein in isolated colonocytes compared to lean WT mice. P-value <0.03 and determined by Student's t-test. n=8 for LFD and n=8 for HFD. The blot shows the protein expression for 2 LFD and 2 HFD mice. Bars with different superscript are significantly different.

5. **Obesity does not alter A) CTMP or B) IκBα expression in isolated colonocytes in WT or IL1RKO lean or obese male mice**. Protein levels were normalized with GAPDH as a control. Similar results were obtained with colonic scrapings (not shown). P-value <0.05 and determined by unpaired Student's t-test with Tukey's post-hoc test for multiple comparisons. n=7 for WT LFD, n=6 for WT HFD; n=7 for IL1RKO LFD, n=7 for IL1RKO HFD. Bars sharing a superscript are not significantly different.

V. Manuscript III-Specific Aim 3

****NOTE: The following manuscript is included in this dissertation because it includes the inflammatory (Figure S1) and tumorigenesis endpoints (Figure 1) of Specific Aim 3. The additional analyses comparing the colonic microbiome and metabolome was work largely done by my co-authors and is outside the scope of Specific Aim 3, and is therefore not addressed further in this thesis.**

Title

Diet- and genetically-induced obesity differentially affect the fecal microbiome and metabolome in Apc^{1638N} mice.

Authors

Anna C. Pfalzer[1,2,3,#], Paula-Dene C. Nesbeth[1,2,3,#], Laurence D. Parnell[1,4], Lakshmanan K. Iyer[5], Zhenhua Liu[1,2,6], Anne V. Kane [1,7,] C-Y. Oliver Chen[1,3,8], Albert K. Tai[9], Thomas A. Bowman[1,10], Martin S. Obin[1,3,4], Joel B. Mason[1,2,3], Andrew S. Greenberg[1,3,10], Sang-Woon Choi[11], Jacob Selhub[1,3,12], Ligi Paul[1,3,12] and Jimmy W. Crott[1,2,3].

[1] Cancer Cluster [a], [2] Vitamins and Carcinogenesis Laboratory [a], [3] Friedman School of Nutrition Science and Policy, Tufts University, [4] Nutrition and Genomics Laboratory [a], [5] Neuroscience Department, Tufts University School of Medicine, [6] Department of Nutrition, University of Massachusetts, Amherst. [7] Phoenix Laboratory, Tufts Medical Center, [8] Antioxidants Laboratory [a], [9] Genomics Core, Tufts University School of Medicine, [10] Obesity Metabolism Laboratory [a], [11] CHA University School of Medicine, Seoul, South Korea, [12] Vitamin Metabolism Laboratory [a]. [a] Jean Mayer USDA Human Nutrition Research center on Aging at Tufts University. [#] Authors contributed equally to this work

Running title

Obesity alters the gut microbiome and metabolome

Keywords

Obesity, colorectal cancer, adenosine, *Parabacteroides distasonis, inflammation*.

Correspondence

Jimmy W Crott PhD
USDA HNRCA at Tufts University
711 Washington St, Boston, MA 02111.

Jimmy.crott@tufts.edu
+1 617 556 3117

Abbreviations

LF, low fat. HF, high fat. Apc, Adenomatous Polyposis Coli (gene). DbDb, leptin receptor homozygous mutant mice. CRC, colorectal cancer. BMI, body mass index. OTU, operational taxonomic unit.

Abstract

Obesity is a risk factor for colorectal cancer (CRC), and alterations in the colonic microbiome and metabolome may be mechanistically involved in this relationship. The relative contribution of diet and obesity *per se* are unclear. We compared the effect of diet- and genetically-induced obesity on the intestinal microbiome and metabolome in a mouse model of CRC. Apc^{1638N} mice were made obese by either high fat (HF) feeding or the presence of the $Lepr^{db/db}$ (DbDb) mutation. Intestinal tumors were quantified and stool microbiome and metabolome were profiled.

Genetic obesity, and to a lesser extent HF feeding, promoted intestinal tumorigenesis. Each induced distinct microbial patterns: taxa enriched in HF were mostly Firmicutes (6 of 8) while those enriched in DbDb were split between Firmicutes (7 of 12) and Proteobacteria (5 of 12). *Parabecteroides distasonis* was lower in tumor-bearing mice and its abundance was inversely associated with colonic Il1b production ($p<0.05$). HF and genetic obesity altered the abundance of 49 and 40 fecal metabolites respectively, with 5 in common. Of these 5, adenosine was also lower in obese and in tumor-bearing mice ($p<0.05$) and its concentration was inversely associated with colonic Il1b and Tnf production ($p<0.05$). HF and genetic obesity differentially

alter the intestinal microbiome and metabolome. A depletion of adenosine and *P.distasonis* in tumor-bearing mice could play a mechanistic role in tumor formation. Adenosine and *P. distasonis* have previously been shown to be anti-inflammatory in the colon and we postulate their reduction could promote tumorigenesis by de-repressing inflammation.

Introduction

Colorectal cancer (CRC) remains a major public health issue in the US, with approximately 137,000 new cases and 50,000 deaths per year. It is the third most common cancer and third most common cause of cancer deaths [1]. Among the many risk factors for this disease is obesity. Females and males with a BMI of 25-29.9 have relative risks of 1.2 and 1.5 respectively, while those with a BMI of 30 have relative risks of 1.5 and 2.0 [2]. Studies in mice corroborate these epidemiological findings, with both high fat (HF)- [3] and genetically-induced obesity [4] elevating tumor burden. Compelling evidence indicates that elevated colonic inflammation constitutes a major mechanistic link between obesity and CRC [5,6].

A link between the gut microbiome and colorectal cancer is becoming increasingly apparent and observations that an altered microbiota is already present among individuals with adenomas [7,8] suggests an involvement at an early stage of carcinogenesis, preceding the appearance of cancer. In one comparison of CRC cases and controls 11 operational taxonomical units (OTUs) belonging to the genera *Enterococcus, Escherichia/Shigella, Klebsiella, Streptococcus and Peptostreptococcus* were significantly more abundant in CRC cases, while 5 OTUs belonging to the genus *Roseburia* and other butyrate-producing bacteria of the family *Lachnospiraceae* were

less abundant [9]. Others report a relative enrichment of phylum Bacteroidetes and depletion of Firmicutes was observed in CRC [10].

Studies in which germ-free mice inoculated with stool from tumor-bearing mice had more tumors than those inoculated with stool from tumor-free mice support a causal role for the gut microbiota in colorectal carcinogenesis [11]. Stool from tumor-bearing donor mice was enriched for OTUs of the genera *Bacteroides*, *Odoribacter* and *Turicibacter* as well as a member of the *Erysipelotrichaceae* family and relatively depleted for members of the genus *Prevotella.* Further demonstrating the importance of the colonic microbiota in tumorigenesis, antibiotic administration significantly attenuated tumorigenesis in conventional mice [11]. Interestingly, when repeated using stool from human CRC patients, differences in tumor burden in recipient mice were strongly related to community structure but not to the cancer status of the donor [12]. Genera within the order Bacteroidales (*Parabacteroides* and *Alistipes*), as well as the Verrucomicrobia genus *Akkermansia*, were associated with highest tumor burden while several genera within the order Clostridiales (*Clostridium* Groups XIVa, XI and XVIII, *Flavonifractor*, and unclassified *Lachnospiraceae*) were associated with the lowest tumor burden.

Diet and obesity are potent modulators of the gut microbiome. Mouse studies indicate that both genetically-induced (leptin knockout) [13] and diet-induced obesity promote an expansion of the phylum Firmicutes coincident with a reduction in Bacteroidetes [14]. Human studies comparing lean and obese twins similarly observed a lower abundance of Bacteroidetes but no differences in Firmicutes [15]. Cross-sectional analyses have also linked dietary components with microbial patterns or ‘enterotypes’; an enterotype characterized by high *Bacteroidetes* abundance was

highly associated with dietary animal protein, several amino acids and saturated fats while the '*Prevotella*' enterotype was associated with lower intakes for these components but high values for carbohydrates and simple sugars [16].

While these studies have implicated the microbiota as a causal factor in colonic tumorigenesis and have established its sensitivity to diet and obesity, it remains unclear whether dysbiosis explains, at least partly, the elevation in CRC risk associated with obesity. Fully understanding how obesity promotes CRC will require an understanding of not only how obesity affects the composition of the gut microbiota, but also its metabolic capacity and the metabolome of the colonic lumen. To further our understanding of the role of the gut microbiota in obesity-associated CRC and to identify the relative contributions of HF consumption and obesity *per se* to tumorigenesis we compared the effect of HF- and genetic ($Lepr^{db/db}$)-induced obesity on the gut microbiome and intestinal tumorigenesis in Apc^{1638N} mice. Because alterations in the stool metabolome likely play an important role in mediating these phenomena we also profiled the stool metabolome to identify elements that might contribute to the formation of a pro-tumorigeneic milieu in these two modes of obesity.

Materials and Methods

Animal Study

Animal procedures were approved by the Institutional Animal Care and Use Committee of the Jean Mayer USDA HNRCA at Tufts University. To study tumorigenesis we utilized Apc^{1638N} mice [17] (NCI Mouse Repository. Frederick, MD); heterozygosity for this *Apc* mutation (codon 1638) results in the formation of 1-5 small bowel adenomas or carcinomas by 8 months of age. Although the predilection for developing small, rather than large, intestinal tumors is a common

phenomenon in genetically-engineered models of CRC—such as the widely utilized Apc^{min} mouse--the small intestinal tumorigenesis in the Apc^{1638N} animal appears to be highly relevant to colonic carcinogenesis since it responds to dietary modifications like obesity and 1-carbon nutrient depletion in the same fashion as to what occurs in the colon [18,19].

To study genetically-induced obesity we utilized $Lepr^{db/db}$ mice, which lack a functional leptin receptor and become obese at 3-4 weeks of age [20] (Jackson Laboratory. Bar Harbor, Maine). Wildtype C57BL6/J (Charles River, Wilmington, MA) were also utilized. The following three genotypes were generated: $Apc^{+/+}$ $Lepr^{+/+}$ (wildtype, Wt), $Apc^{+/1638N}$ $Lepr^{+/+}$ (Apc) and $Apc^{+/1638N}$ $Lepr^{db/db}$ (DbDb). Starting at 8 weeks of age, Wt (n=12) and DbDb (n=10) mice were fed a low fat (LF) diet while Apc mice were randomized to receive LF (N=10) or HF (N=12) diet for 16 weeks. LF and HF diets provided 10 and 60% of calories from fat respectively (Table 1. BioServ, Frenchtown, NJ). Mice were individually housed on a 12 hr light-dark cycle at 23°C and provided *ad libitum* access to water.

Mice were weighed weekly. After 15 weeks on diet, body composition was measured by MRI (EchoMRI, Houston, TX). After 16 weeks on diet, mice were euthanized by CO_2 asphyxiation followed by cervical dislocation and exsanguination by cardiac puncture. The abdomen was then opened and the small intestine (SI) and large intestines removed onto ice-cold glass plates, opened longitudinally and contents removed. Colon and cecum contents were combined, aliquots frozen in liquid N_2 and then stored at -80°C. Small and large intestines were then rinsed thoroughly with ice-cold PBS with protease inhibitors (Roche, Indianapolis, IN). The SI and colon were inspected for tumors by a blinded investigator under a dissecting microscope. Tumors were measured before being excised and fixed in formalin for later grading by a rodent pathologist. The remaining normal-appearing SI mucosa was scraped with microscope slides and

frozen. Liver, mesenteric fat and gonadal fat depots were also excised, weighed and frozen. Blood was spun at 1000x g and plasma frozen. Plasma insulin and glucose concentrations were measured by ELISA and colorimetric assays respectively (Millipore, Billerica, MA).

To assess colonic inflammation we used a colon organ culture method as previously described [21]. Briefly, two 1 cm sections of the colon were cultured for 24 hr in Dulbecco's Modified Eagle's Medium media with protease inhibitors (Roche, Indianapolis, IN) at 37˚C with 5% CO_2. After 24 hr, supernatant was collected and Il1b, Tnf, Il6 and Il4 were measured by electrochemiluminescence array and Sector S600 imager according to manufacturer's protocols (Mesoscale Discovery, Rockville, MD). Protein concentration was determined by the Bradford assay (Bio-Rad, Hercules, CA).

Fecal metabolomics

Fecal samples (100 mg) were sent for non-targeted metabolic profiling (Metabolon, Durham, NC) as previously described [22,23]. Briefly, lyophilized samples were analyzed by three independent platforms; ultrahigh performance liquid chromatography/tandem mass spectrometry (UHPLC/MS/MS) optimized for basic species, UHPLC/MS/MS optimized for acidic species, and gas chromatography/mass spectrometry (GC/MS). Metabolites were identified by automated comparison of the ion features in the experimental samples to a reference library of chemical standard entries that included retention time, mass-to-charge ratio (m/z), preferred adducts, and in-source fragments as well as associated MS spectra, and were curated by visual inspection for quality control using software developed at Metabolon [24]. Missing values were imputed with the compound minimum. Following median scaling and imputation of missing values, statistical analysis of (log-transformed) data was performed.

Metabolomic data were analyzed with MetaboAnalyst 2.0 (http://www.metaboanalyst.ca) [25]. Data were normalized by sum and autoscaled. Heatmap visualization was performed based on Student's *t*-test results and reorganization of metabolites to show contrast between the groups. Correction for multiple testing was done by calculating false discovery rate (FDR). Principal component analysis (PCA) and partial least-squares discriminant analysis (PLS-DA) were used for classification analyses.

Fecal microbiome

DNA was extracted from frozen fecal samples using QiaAMP DNA Stool MiniKits (Qiagen, Valencia, CA). The V4 region of the 16S rRNA gene was amplified as previously described [26] and purified using the AMPure XP kit (Agencourt, Indianapolis, IN). Paired-end sequencing (250bp) was performed on an Illumina MiSeq (SanDiego, CA). After quality filtering using Qiime v1.8.0 (http://qiime.org)[27], paired-end sequences were concatenated and demultiplexed. Closed reference OTUs at 99% similarity were assigned using Greengenes [28] and an OTU table generated. The number of sequences were normalized to 41000 (minimum read depth returned) and phylotype-based alpha diversity measures including equitability, number of observed species, Shannon diversity index, Chao-1 and phylogenetic distance were determined. Differences in OTU abundance between groups were identified using LDA (Linear Discriminant Analysis) Effect Size (Lefse) and Multivariate Association with Linear Models (MaAsLin) tools [29](http://huttenhower.sph.harvard.edu/galaxy/).

Gene expression

We profiled the expression of genes encoding adenosine-metabolizing enzymes in the small intestinal mucosa: adenosine deaminase (*Ada*), adenosine kinase (*Adk*), ectonucleoside triphosphate diphosphohydrolases (*Entpd1, Entpd3, Entpd8*), purine nucleoside phosphoylases

(*Pnp, Pnp2*), S-adenosylhomocysteine hydrolase (*Ahcy*), deoxycytidine kinase (*Dck*) and 5' nucleotidases (*Nt5c, Nt5c1a, Nt5c1b, Nt5c2, Nt5c3, Nt5c3b, Nt5e, Nt5m*). Total RNA was isolated from small intestinal scrapings using Trizol reagent and cDNA synthesized using Superscript III reverse transcriptase. Real-time PCR was performed using SYBR green master mix (Life technologies, Grand Island, NY) and an ABI7300 thermocyler (Applied Biosystems, Foster City, CA). Primer sequences were obtained from qPrimerDepot (http://mouseprimerdepot.nci.nih.gov/) or NCBI Primer Blast [30] (Table S1). Relative expression was calculated using the $2^{-\square\square Ct}$ method and statistical analyses were performed on $\square$Ct values. *Gapdh* was used as the control gene.

Statistics

All data are reported as mean ± SEM. Statistical calculations were performed in Systat (San Jose, CA) and R [31]. Between groups comparisons were made with ANOVA, 2way ANOVA or t-test where appropriate. Associations between variables were assessed by linear regression. Significance was accepted when $p<0.05$ or, when multiple comparisons conducted, a False Discovery Rate cutoff of $q< 0.2$ or less was used. Cluster analysis and heatmaps were generated with CIMminer [32].

Results

Physiology

HF consumption significantly increased body weight (Figure 1A,B). Although the dietary interventions were begun when all animals were at the same age, DbDb mice initially were approximately double the body weight of all other mice and continued to gain weight thereafter. At week 15 fat mass was significantly higher in DbDb mice than LF mice. Although numerically

higher in females, HF feeding significantly elevated fat mass only in male mice. Liver weight, insulin and glucose were significantly elevated in DbDb mice but not in HF fed mice. Lean mass was not altered by HF fed or DbDb mice (Table 2).

Intestinal Tumors

No tumors were observed in the SI of Wt mice. Amongst Apc mice, the SI tumor incidence was 33%, 67% and 100% in LF, HF and DbDb mice respectively (□□□P=0.008). A similarly significant step-wise increase in tumor multiplicity and burden was also observed (Figure 1C). Sex-specific data are reported in Supplemental Table 2. No tumors were observed in the colon of any mouse. All tumors were confirmed to be adenomatous polyps.

Fecal Microbiome

Population diversity was assessed via several metrics. Significant between-group differences were found with Observed Species and PD whole tree metrics ($p<0.05$), and a trend was apparent for Chao index ($p=0.064$). For these analyses the HF group had the lowest numerical value of population diversity, which attained significance in comparison with the DbDb group. No significant differences were observed between groups for Shannon index or Equitability index ($p> 0.05$). When comparing between groups at a phylum level there were no significant differences in the four major phyla present (Actinobacteria, Bacteroidetes, Firmicutes, Proteobacteria) or in the ratio of Firmicutes to Bacteroidetes (ANOVA $p>0.05$).

LEfSe analysis was performed on data from Apcmice, identifying 26 significantly enriched taxa across three phyla; 6, 8 and 12 taxa enriched in LF, HF and DbDb mice respectively (Figure 2A,B). Firmicutes featured prominently amongst those enriched in both modes of obesity (6 of 8 and 7 of 12 for HF and DbDb respectively). For HF mice, the remainder of the defining taxa

were Bacteroidetes (2 of 8), while for DbDb the remainder were Proteobacteria (5 of 12). MaAsLin analysis facilitated the parsing out of associations with genotype, diet, sex and tumor number (Table 3). In agreement with the LEfSe analysis, the family *Clostridiacea* (phyla Firmicutes) was associated with the DbDb genotype; families *Ruminococcaceae* and *Lachnospiracea* (both phyla Firmicutes) were associated with HF diet and the family *Enterococcaceae* (phyla Firmicutes) was associated with the LF diet. In addition several OTUs from the phyla Firmicutes and Bacteroidetes were associated with each sex.

MaAsLin analysis also identified OTUs both positively (phyla Firmicutes and Actinobacteria) and negatively (phyla Bacteroidetes) associated with tumor number. Amongst these, *Parabacteroides distasonis* was also identified by LefSe analysis as being lower in tumor-bearing mice. Further, t-test ($p=0.02$) and regression analyses ($R= -0.31$, $p=0.04$) corroborate a depletion of *P.distasonis* in tumor-bearing mice and with increasing tumor number respectively. *P.distasonis* abundance was also inversely related to colonic production of Il1b ($R= -0.34$, $p=0.05$) but not Tnf, Il6 or Il4 ($p>0.05$) (Figure S1).

Fecal metabolome

415 metabolites were detected in fecal samples. Comparing (Apc) LF and HF fed Apc mice, 49 metabolites returned a p value of <0.05 and 14 with a $q<0.2$ (Figure 3A). Comparing LF and DbDb Apc mice 41 metabolites returned a p value of <0.05 but none attained a $q<0.2$ (Figure 3B). Using the relaxed cut-off of $p<0.05$, 5 metabolites were changed in both comparisons: adenosine, 2-oxindole-3-acetate, caproic acid, arachadic acid and tyrosyl glycine. Comparing mice with and without tumors, 29 metabolites returned a p value of <0.05 but none attained a $q<0.2$ (Figure 3C). Adenosine and 2-oxindole-3-acetate were altered in all three comparisons.

Because previous studies have demonstrated an anti-inflammatory role for adenosine in the colon we tested its association with inflammatory cytokines in the colon. Consistent with this role, fecal adenosine concentrations were inversely associated with the production of Tnf (R=-0.5, p=0.01) and Il1b (R=-0.73, $p=1.3x10^{-5}$) but not Il4 or Il6 (p>0.05) (Figure S1).

Adenosine participates in endogenous reactions that form AMP, adenine, inosine and S-Adenosyl homocysteine (SAM). To identify possible mechanisms for the observed depletion of adenosine, we assessed whether its concentration was related to that of any immediately related metabolites or to the expression of genes encoding adenosine-metabolizing enzymes. Although AMP and SAM were not detected in our samples, fecal adenosine levels were positively associated with inosine (R= 0.5, p=0.009) but not adenine (R= 0.05, p=0.8) concentrations. Interestingly, inosine and hypoxanthine were inversely related (R= -0.53, p=0.006), while hypoxanthine and adenine concentrations were positively related (R=0.44, p=0.03). Fecal adenosine concentration was not significantly associated with the expression of any adenosine-metabolizing gene in the small intestinal mucosa (p>0.05).

Using the relaxed cut-off for metabolites, PLS-DA could effectively separate HF and DbDb groups from the LF group (Figure 3 D,E). The metabolites that most heavily drove the separation were 2-oxindole-3-acetate, tyrosol and lactic acid for the HF vs. LF comparison and serinyl tyrosine, isoleucyl serine and arachidic acid for the DbDb vs LF comparison (Figure 3 G,H). Similarly mice with and without tumors could be distinguished in this analysis, with oleic acid,

adenosine and vaccenic acid being most influential (Figure 3 F,I). In contrast, PCA could not effectively distinguish groups in these two comparisons (data not shown).

Integrative analysis

Correlation analysis between all OTUs and metabolites identified 107 metabolites and 31 OTUs had at least one significant association ($q<0.05$). We performed a cluster analysis of the correlation R values and observed two clear clusters of bacteria, suggesting similarities in their metabolic capacities and/or requirements with regard to this subset of detectable metabolites (Figure S2). Cluster 1 was comprised mostly of members of the Firmicutes class Bacilli while Cluster 2 is made up of 3 classes of Proteobacteria (beta, delta and gamma), Firmicutes class Clostridia and Phyla TM7class TM7-3.

Although the concentration of adenosine was not significantly associated with the abundance of any OTU ($q>0.2$), its immediate precursor adenine was strongly associated with the genus *Lactobacillus* ($R= 0.75$, $q=0.002$) and 3 other higher order taxa associated with this genus (family *Lactobacillaceae*, order Lactobacillales and Class bacilli. $R=0.75$ - 0.65, $q= 0.002$ - 0.03).

Discussion

In the current study we show that obesity that is driven by either HF feeding or by genetic mutation promotes intestinal tumorigenesis. Although prior studies have demonstrated the pro-tumorigenic effects of these two means of producing obesity [3,4], the two modalities have not previously been compared side-by-side under parallel experimental conditions. Although the high dietary fat content in the HF group might, by itself, have driven tumorigenesis since dietary

fat activates pro-inflammatory TLR receptors in the colon [33], our observations underscore the fact that even in the absence of excess dietary fat, obesity *per se* enhances tumorigenesis.

At a phylum level we did not observe any between-group differences in the four major phyla present: Firmicutes, Bacteroidetes, Proteobacteria and Actinobacteria. Similarly, no phylum level differences were observed between mice with and without tumors. Unlike others [13,14], we did not observe an alteration in the ratio of Firmicutes: Bacteroidetes in either type of obesity: this absence in a shift in the Firmicutes: Bacteroidetes ratio agrees with recent studies of human stool, which also failed to detect such differences [34]. LDA effect size analysis identified 26 significantly discriminative features across three phyla. Interestingly, although we didn't detect differences in the total abundance of each phyla, species enriched in HF mice were mostly Firmicutes (class clostridia) while those enriched in DbDb mice were split between Firmicutes and Proteobacteria (class Gamma Proteobacteria)(Figure 2B). In contrast to recent studies showing a depletion of *Ruminococcaceae* in HF fed male mice [35], we observed an enrichment of this family in our study (Figure 2A).

A potentially important observation of ours was the significant depletion of the species *Parabacteroides distasonis* in those mice who harbored tumors. Although there are no reports linking this species to CRC, there is evidence that *P.distasonis* has anti-inflammatory effects in the colon. In patients with Crohn's disease, *P.distasonis* is more frequently absent than in those who are disease free, and, in those with Crohn's, it is more frequently absent in those with severe compared to mild inflammation [36]. A *bona fide* anti-inflammatory role for this species is supported by data showing that oral administration of a membrane fraction of *P.distasonis*

significantly attenuated dextran sodium sulfate-induced colitis in mice [37]. Moreover, these authors demonstrated that the membrane fraction of *P.distasonis* reduced the release of Tnf, Il6, Ccl2 (MCP-1) and Ccl12 (MCP-5) by RAW264.7 macrophages after LPS challenge. Consistent with this anti-inflammatory role, the relative abundance of *P.distasonis* was inversely associated with colonic production of the inflammatory cytokine Il1b (R= -0.34, p=0.05) in our own study. One of the prevailing theories as to how obesity promotes colorectal carcinogenesis is by producing a chronic, low-grade state of inflammation in the colon [5,6]; a reduced abundance of this organism mice may therefore play a mechanistic role in enhancing tumorigenesis. Because the anti-inflammatory properties of *P.distasonis* were demonstrated with a membrane fraction [37] and its abundance was not significantly related to any metabolites in the current study, we suggest that its putative protective effect is more likely related to an immune-modulatory capacity of specific membrane components rather than the production of chemoprotective metabolites.

While both modes of obesity appeared to cause a similar degree of impact, in terms of taxa with altered abundance, HF feeding was more perturbing to the metabolome than genetic obesity (Figure 3). For some of the differentially abundant metabolites it is likely that differences in stool may be directly related to amounts of those nutrients present in the diet consumed. For example, the higher abundance of alpha-tocopherol may be explained by a higher relative amount of vitamin mix added to the HF diet. However, other metabolite changes could result from diet-microbial interactions. For example, the HF fed mice have relatively less lactate (q= 0.03) and specific taxa belonging to the order Lactobacillales (Table 3), which as their name suggests, produce lactate from sugars. Their altered abundance, in turn, may be related to the fact that the

HF diet has substantially less sucrose than the LF diet (325 vs. 90 g/kg). To assess microbiome-metabolite interactions systematically, we correlated all metabolites against all OTUs and found that 107 metabolites correlated with at least one OTU and 31 OTUs correlated with at least one metabolite (Figure S2). This analysis clearly identified two major clusters of taxa with apparently opposite substrate requirements or metabolite production. Interestingly, these clusters segregated based on bacterial class; the first cluster is mostly Bacilli (phylum Firmicutes) while the second was a combination of alpha, beta and gamma proteobacteria (phylum Proteobacteria), clostridia (phylum Firmicutes) and TM7-3 (phylum TM7).

When considering all three comparisons i.e. LF vs. HF, LF vs. DbDb and Tumor No vs. Yes, only two metabolites were found to be altered in all three; 2-oxindole-3 acetate and adenosine. Very little information is available on the former; however there is an abundance of literature demonstrating an anti-inflammatory role of adenosine in the colon. Specifically, interventions to increase adenosine signaling, either by restoring endogenous adenosine by inhibiting its breakdown [38,39,40], or by agonizing adenosine receptors [41,42,43] have been shown to attenuate inflammation in rodent colitis models. Conversely, decreasing adenosine signaling by reducing endogenous adenosine [44] or knocking out [45] or antagonizing [45] adenosine receptors increases inflammation in these models. Consistent with this anti-inflammatory role, in our study fecal adenosine was inversely associated with mucosal production of pro-inflammatory cytokines Tnf ($R=-0.5$, $p=0.01$) and Il1b($R=-0.73$, $p=1.3x10^{-5}$).

There is a large body of evidence that existing cancers use adenosine to suppress anti-tumor immunity (reviewed in [46]). Specifically, tumors recruit and activate T_{reg}, myeloid-derived

suppressor cells and M2 macrophages which express CD39 and/or CD73 [47]. These ectonucleotidases convert AMP to adenosine on the cell surface which subsequently suppresses natural killer cells and effector T cells via the A2A receptor [48], thus suppressing the anti-tumor response. Adenosine also stimulates VEGF production by M2 macrophages, promoting angiogenesis [47]. Based on our data and the substantial body of evidence that adenosine is anti-inflammatory in the colon, we suggest that early in tumorigenesis this same immune suppression activity of adenosine may, paradoxically, have an anti-tumor effect by suppressing inflammation-induced initiation. Extrapolating from this, we suggest that a depletion of adenosine, such as that observed in our obese mice, may contribute to the formation of a pro-carcinogenic milieu by de-repressing inflammation.

In order to gain an understanding of the mechanism for the observed depletion of adenosine depletion we measured the expression of all endogenous genes encoding adenosine-metabolizing enzymes in the small intestinal mucosa. Others have previously reported that genetic-induced obesity reduces the expression of *Cd39* and *Cd73* and diet-induced obesity reduced *Cd73* in epididymal fat of mice [49]. These ectonucleotidases cleave ATP to adenosine and a reduced intestinal expression of these could account for the reduced fecal adenosine concentration observed. We found no association between intestinal *Cd39* or *Cd73* expression and adenosine concentrations, neither were any other adenosine-metabolizing genes related to its concentration. One possible metabolic fate for adenosine is its sequential metabolism to inosine, hypoxanthine and adenine. We noted a robust positive association of adenosine with inosine, negative association of inosine with hypoxanthine and positive association of hypoxanthine with adenine. Thus alterations in adenosine concentration could be due to flux through this pathway. While

fecal adenosine was not correlated with the abundance of any bacterial taxa ($q>0.2$), adenine concentrations were positively related to the class Bacilli, order Lactobacillales, family *Lactobacillaceae* and genus *Lactobacillus* (Figure S2. $q<0.05$ $R= 0.65 – 0.75$). Thus it is conceivable that fluctuations in the abundance of these taxa could alter adenosine concentrations through hypoxanthine and inosine.

Weir et al profiled the fecal metabolome of human subjects with and without CRC and identified 22 biochemicals with differing abundances [50]. Interestingly, there is little overlap in these changes with those we observed. Further, for three metabolites changes occurred in the opposite direction between the two studies (oleic acid, linoleic acid and monooleoglycerol). Such discrepancies are not surprising in a human versus mouse comparison and since dietary differences were equally distinct. One limitation of the current study is that tumors formed in the small intestine, while microbes and metabolites were profiled downstream in the cecum and colon. Thus, while some of the metabolites and taxa detected may have been present at the site of tumor formation, others may have been unique to the colon and cecum and as such are unlikely directly to affect tumorigenesis.

In summary, our studies have confirmed the tumor promoting effect of diet and genetic-induced obesity in a mouse model of CRC. Profiling the gut microbiome revealed distinct patterns for each model of obesity implying that the microbiome is sensitive to both diet and host physiology. The lack of consistency between studies profiling the effect of obesity on the microbiome highlights the high model and environment specificity. Nevertheless, in our model we observed a depletion of the species *P.distasonis* in tumor-bearing mice, and we postulate that this may have important functional implications given its known anti-inflammatory actions. We noted an

inverse association between the abundance of this species and colonic Il1b production, which is consistent with data from others demonstrating anti-inflammatory effects of this species in the colon. Metabolomic profiling also revealed relatively distinct patterns in response to these different models of obesity. Several metabolites were changed in both models and, amongst these; the nucleoside adenosine was also lower in tumor-bearing mice. Considerable data has established the anti-inflammatory role of adenosine in the colon, and its inverse association with colonic Il1b and Tnf production in our study is consistent with this. Based on these data we suggest that a depletion of adenosine and *P.distasonis* could be permissive to the development of intestinal inflammation, thereby promoting tumorigenesis. Further work is required to confirm this supposition, but if true, strategies to restore, replace or agonize the same signaling pathways could possess some utility in reducing colonic inflammation and thereby reducing the risk for CRC in those with elevated levels of inflammation including the obese.

Acknowledgements

We thank Donald Smith and the staff of the Comparative Biology Unit at the HNRCA for their assistance with and animal care. Dr Roderick T. Bronson (Dana-Farber/Harvard Cancer Center Rodent Histopathology Core) is acknowledged for his expert tumor classification and Larry Zhang for technical assistance. Dr Simin Meydani is especially thanked for her support of the Cancer Cluster and enthusiasm for this work.

Any opinions, findings, conclusion, or recommendations expressed in this publication are those of the author(s) and do not necessarily reflect the view of the U.S. Dept. of Agriculture.

Figures

Figure 1.

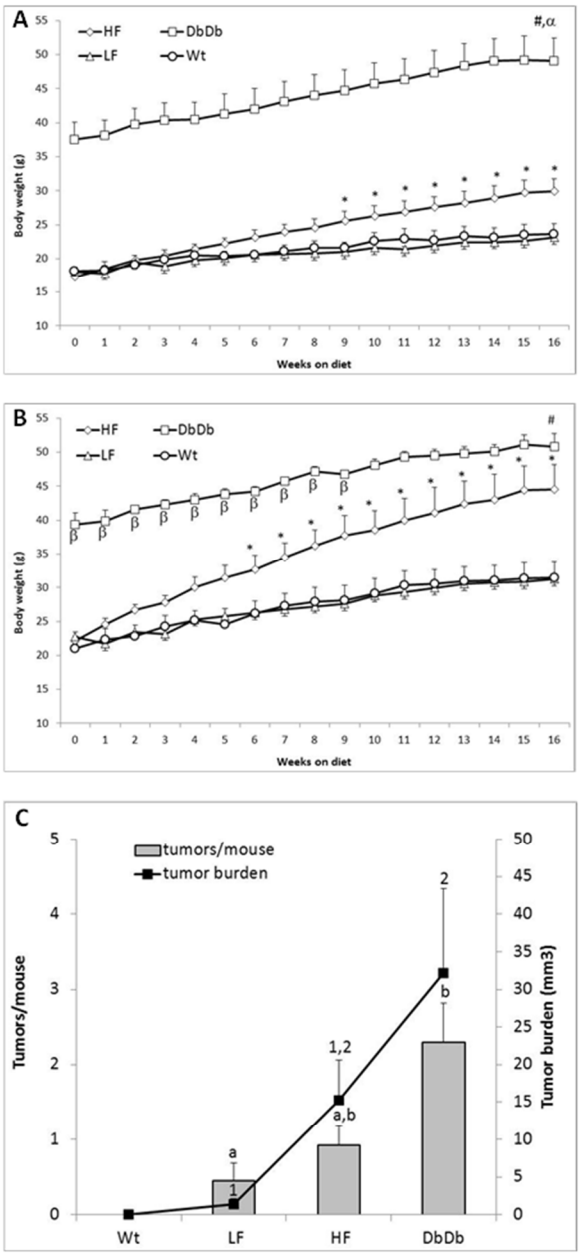

Figure 2.

A.

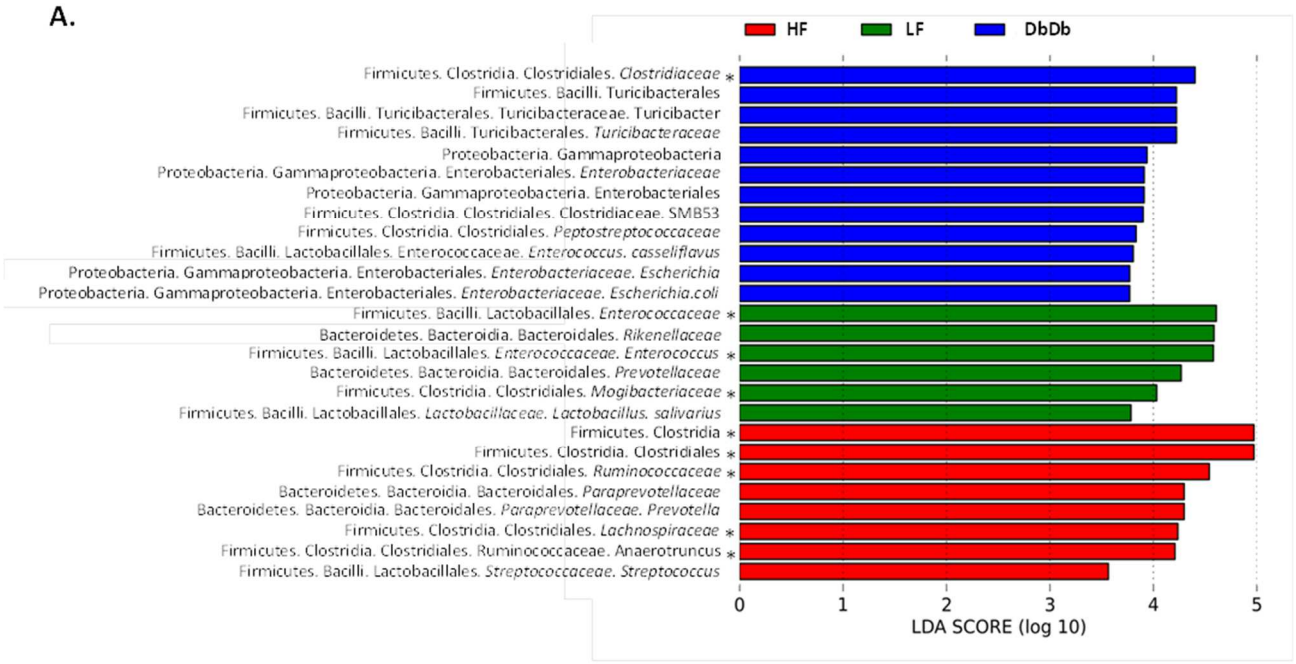
HF
LF
DbDb
Firmicutes. Clostridia. Clostridiales. Clostridiaceae *
Firmicutes. Bacilli. Turicibacterales
Firmicutes. Bacilli. Turicibacterales. Turicibacteraceae. Turicibacter
Firmicutes. Bacilli. Turicibacterales. Turicibacteraceae
Proteobacteria. Gammaproteobacteria
Proteobacteria. Gammaproteobacteria. Enterobacteriales. Enterobacteriaceae
Proteobacteria. Gammaproteobacteria. Enterobacteriales
Firmicutes. Clostridia. Clostridiales. Clostridiaceae. SMB53
Firmicutes. Clostridia. Clostridiales. Peptostreptococcaceae
Firmicutes. Bacilli. Lactobacillales. Enterococcaceae. Enterococcus. casseliflavus
Proteobacteria. Gammaproteobacteria. Enterobacteriales. Enterobacteriaceae. Escherichia
Proteobacteria. Gammaproteobacteria. Enterobacteriales. Enterobacteriaceae. Escherichia.coli
Firmicutes. Bacilli. Lactobacillales. Enterococcaceae *
Bacteroidetes. Bacteroidia. Bacteroidales. Rikenellaceae
Firmicutes. Bacilli. Lactobacillales. Enterococcaceae. Enterococcus *
Bacteroidetes. Bacteroidia. Bacteroidales. Prevotellaceae
Firmicutes. Clostridia. Clostridiales. Mogibacteriaceae *
Firmicutes. Bacilli. Lactobacillales. Lactobacillaceae. Lactobacillus. salivarius
Firmicutes. Clostridia *
Firmicutes. Clostridia. Clostridiales *
Firmicutes. Clostridia. Clostridiales. Ruminococcaceae *
Bacteroidetes. Bacteroidia. Bacteroidales. Paraprevotellaceae
Bacteroidetes. Bacteroidia. Bacteroidales. Paraprevotellaceae. Prevotella
Firmicutes. Clostridia. Clostridiales. Lachnospiraceae *
Firmicutes. Clostridia. Clostridiales. Ruminococcaceae. Anaerotruncus *
Firmicutes. Bacilli. Lactobacillales. Streptococcaceae. Streptococcus
0
1
2
3
4
5
LDA SCORE (log 10)

B.

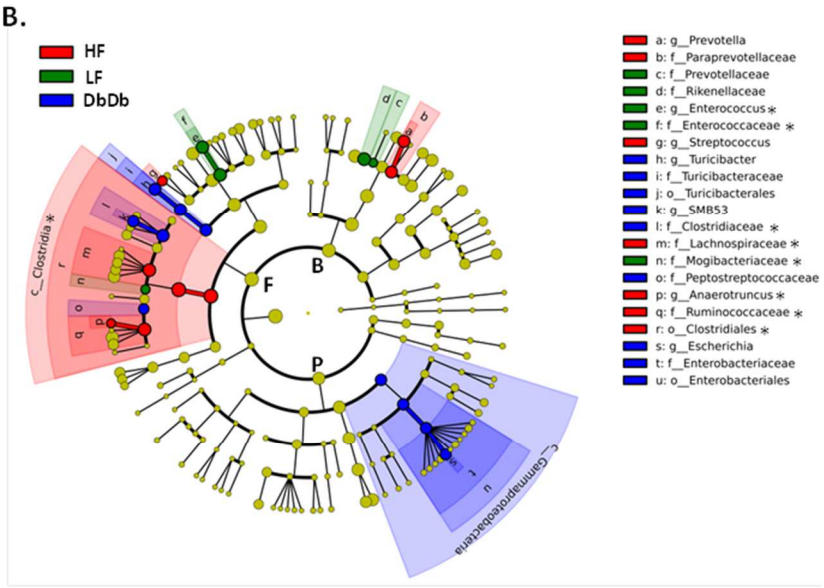
HF
LF
DbDb
B
F
P
c__Clostridia *
c__Gammaproteobacteria
a: g__Prevotella
b: f__Paraprevotellaceae
c: f__Prevotellaceae
d: f__Rikenellaceae
e: g__Enterococcus *
f: f__Enterococcaceae *
g: g__Streptococcus
h: g__Turicibacter
i: f__Turicibacteraceae
j: o__Turicibacterales
k: g__SMB53
l: f__Clostridiaceae *
m: f__Lachnospiraceae *
n: f__Mogibacteriaceae *
o: f__Peptostreptococcaceae
p: g__Anaerotruncus *
q: f__Ruminococcaceae *
r: o__Clostridiales *
s: g__Escherichia
t: f__Enterobacteriaceae
u: o__Enterobacteriales

Figure 3.

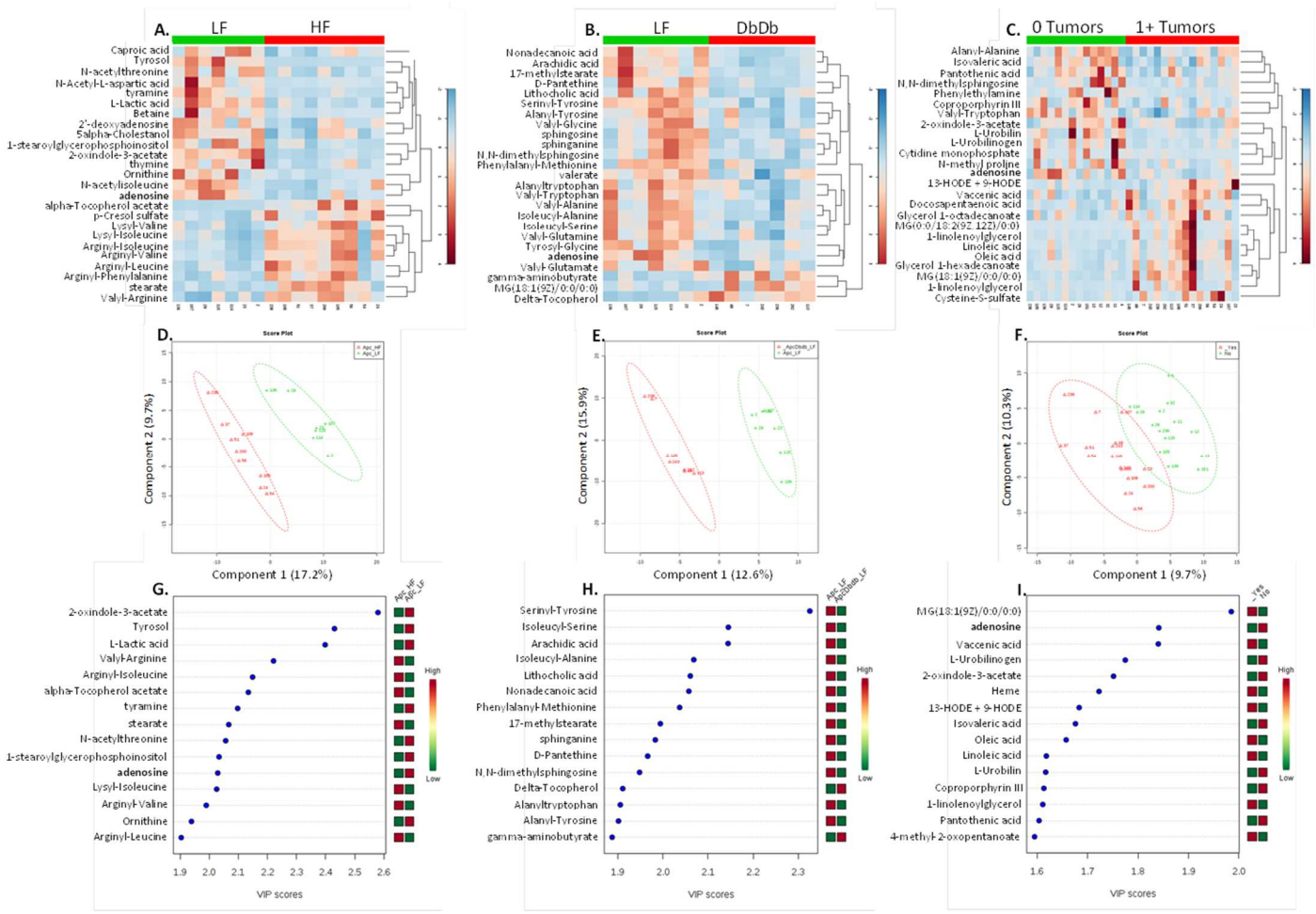
A.
LF
HF
Caproic acid
Tyrosol
N-acetylthreonine
N-Acetyl-L-aspartic acid
tyramine
L-Lactic acid
Betaine
2'-deoxyadenosine
5alpha-Cholestanol
1-stearoylglycerophosphoinositol
2-oxindole-3-acetate
thymine
Ornithine
N-acetylisoleucine
adenosine
alpha-Tocopherol acetate
p-Cresol sulfate
Lysyl-Valine
Lysyl-Isoleucine
Arginyl-Isoleucine
Arginyl-Valine
Arginyl-Leucine
Arginyl-Phenylalanine
stearate
Valyl-Arginine
B.
LF
DbDb
Nonadecanoic acid
Arachidic acid
17-methylstearate
D-Pantethine
Lithocholic acid
Serinyl-Tyrosine
Alanyl-Tyrosine
Valyl-Glycine
sphingosine
sphinganine
N,N-dimethylsphingosine
Phenylalanyl-Methionine
valerate
Alanyltryptophan
Valyl-Tryptophan
Valyl-Alanine
Isoleucyl-Alanine
Isoleucyl-Serine
Valyl-Glutamine
Tyrosyl-Glycine
adenosine
Valyl-Glutamate
gamma-aminobutyrate
MG(18:1(9Z)/0:0/0:0)
Delta-Tocopherol
C.
0 Tumors
1+ Tumors
Alanyl-Alanine
Isovaleric acid
Pantothenic acid
N,N-dimethylsphingosine
Phenylethylamine
Coproporphyrin III
Valyl-Tryptophan
2-oxindole-3-acetate
L-Urobilin
L-Urobilinogen
Cytidine monophosphate
N-methyl proline
adenosine
13-HODE + 9-HODE
Vaccenic acid
Docosapentaenoic acid
Glycerol 1-octadecanoate
MG(0:0/18:2(9Z,12Z)/0:0)
1-linolenoylglycerol
Linoleic acid
Oleic acid
Glycerol 1-hexadecanoate
MG(18:1(9Z)/0:0/0:0)
1-linolenoylglycerol
Cysteine-S-sulfate
D.
Score Plot
Apc_HF
Apc_LF
Component 2 (9.7%)
Component 1 (17.2%)
E.
Score Plot
ApcDbDb_LF
Apc_LF
Component 2 (15.9%)
Component 1 (12.6%)
F.
Score Plot
Yes
No
Component 2 (10.3%)
Component 1 (9.7%)
G.
Apc_HF
Apc_LF
2-oxindole-3-acetate
Tyrosol
L-Lactic acid
Valyl-Arginine
Arginyl-Isoleucine
alpha-Tocopherol acetate
tyramine
stearate
N-acetylthreonine
1-stearoylglycerophosphoinositol
adenosine
Lysyl-Isoleucine
Arginyl-Valine
Ornithine
Arginyl-Leucine
1.9
2.0
2.1
2.2
2.3
2.4
2.5
2.6
VIP scores
High
Low
H.
Apc_LF
ApcDbDb_LF
Serinyl-Tyrosine
Isoleucyl-Serine
Arachidic acid
Isoleucyl-Alanine
Lithocholic acid
Nonadecanoic acid
Phenylalanyl-Methionine
17-methylstearate
sphinganine
D-Pantethine
N,N-dimethylsphingosine
Delta-Tocopherol
Alanyltryptophan
Alanyl-Tyrosine
gamma-aminobutyrate
1.9
2.0
2.1
2.2
2.3
VIP scores
High
Low
I.
Yes
No
MG(18:1(9Z)/0:0/0:0)
adenosine
Vaccenic acid
L-Urobilinogen
2-oxindole-3-acetate
Heme
13-HODE + 9-HODE
Isovaleric acid
Oleic acid
Linoleic acid
L-Urobilin
Coproporphyrin III
1-linolenoylglycerol
Pantothenic acid
4-methyl-2-oxopentanoate
1.6
1.7
1.8
1.9
2.0
VIP scores
High
Low

Tables

Table 1. Diet composition.

Ingredient (g/kg)	LF	HF
Casein	210	265
L-Cystine	3	4
Corn Starch	280	0
Maltodextrin	50	160
Sucrose	325	90
Lard	20	310
Soybean Oil	20	30
Cellulose	37.2	65.5
Mineral Mix AIN-93G	35	48
Calcium Phosphate Dibasic	2	3.4
Vitamin Mix AIN-93	15	21
Choline Bitartrate	2.8	3
Total	1000	1000
Energy (%kcal)	**LFD**	**HFD**
Carbohydrate	70	21
Protein	20	19
Fat	10	60
Total	100	100

Diets: LF, Low fat . HF, High fat . BioServ (custom) catalog numbers F6654, and F6653 respectively.

Table 2. Physiological characteristics of mice by group.

	Wt		LF		HF		DbDb		2Way ANOVA P	
Endpoint	M (7)	F (5)	M (4)	F (5)	M (4)	F (8)	M (3)	F (7)	Group	Sex
Body weight (g)	31.31 ± 2.33	23.58 ± 1.42	30.83 ± 1.80	22.60 ± 0.46	44.41 ± 3.66 *	29.73 ± 1.83	51.13 ± 1.38 *	49.17 ± 3.51 *	<0.0001	<0.0001
Total fat mass (g)	8.05 ± 1.70	5.07 ± 0.89	7.60 ± 1.41	4.85 ± 1.04	19.13 ± 3.08 *	9.94 ± 1.96	28.22 ± 1.04 *	26.51 ± 1.93 *	<0.0001	0.006
Total lean mass (g)	18.95 ± 0.85	15.24 ± 0.86	18.66 ± 0.32	14.27 ± 1.14	21.06 ± 1.17	16.75 ± 0.37	18.89 ± 0.62	17.39 ± 1.56	0.1	<0.0001
Mesenteric fat (g)	0.55 ± 0.11	0.28 ± 0.07	0.41 ± 0.07	0.28 ± 0.04	1.23 ± 0.28 *	0.39 ± 0.09	1.04 ± 0.16	1.00 ± 0.13 *	<0.0001	0.002
Gonadal fat (g)	1.01 ± 0.24	0.58 ± 0.15	0.97 ± 0.18	0.52 ± 0.09	2.48 ± 0.26 *	1.53 ± 0.35	1.57 ± 0.18	1.84 ± 0.26 *	<0.0001	0.063
Liver (g)	1.29 ± 0.17	0.94 ± 0.10	1.19 ± 0.06	1.04 ± 0.07	1.33 ± 0.15	0.96 ± 0.04	4.93 ± 0.30 *	3.63 ± 0.29 *	<0.0001	<0.0001
Plasma insulin (ng/ml)	3.10 ± 1.26	0.94 ± 0.16	1.70 ± 0.23	1.20 ± 0.20	4.09 ± 1.91	1.09 ± 0.18	11.44 ± 0.82	16.03 ± 2.43 *	<0.0001	0.8
Plasma glucose (μM)	8.09 ± 0.87	5.08 ± 2.56	8.21 ± 0.42	7.78 ± 0.47	11.19 ± 1.07	10.05 ± 0.92	20.81 ± 1.73 *	18.26 ± 2.51 *	<0.0001	0.1

Total lean and fat mass measured by MRI. M, male; F , female. Samples size in parentheses. * $p<0.05$ vs LF (of same sex).

Table 3. Multivariate Association with Linear Models (MaAsLin) output.

Variable	Feature (OTU)	Coefficient	P-value	Q-value
Apc WT	p__ Actinobacteria|c__Actinobacteria	0.00	0.004	0.097
Apc WT	p__Proteobacteria|c__Gammaproteobacteria|o__Pseudomonadales	0.00	0.010	0.163
Apc WT	p__Bacteroidetes|c__Bacteroidia|o__Bacteroidales|f__Paraprevotellaceae	-0.08	0.012	0.163
Apc WT	p__Bacteroidetes|c__Bacteroidia|o__Bacteroidales|f__Paraprevotellaceae|g__Prevotella	-0.08	0.012	0.163
Apc WT	p__Actinoc__Actinoo__Bifidobacteriales|f__Bifidobacteriaceae	0.00	0.013	0.163
Apc WT	p__Actinoc__Actinoo__Bifidobacteriales|f__Bifidobacteriaceae|g__Bifidobacterium	0.00	0.013	0.163
Apc WT	p__Firmicutes|c__Clostridia|o__Clostridiales|f__Peptococcaceae	-0.02	0.018	0.197
DbDb WT	p__Firmicutes|c__Clostridia|o__Clostridiales|f__Clostridiaceae| g__Sarcina	0.00	0.002	0.055
DbDb WT	p__Bacteroidetes|c__Bacteroidia|o__Bacteroidales|f__Paraprevotellaceae	0.09	0.007	0.128
DbDb WT	p__Bacteroidetes|c__Bacteroidia|o__Bacteroidales|f__Paraprevotellaceae|g__Prevotella	0.09	0.007	0.128
DbDb WT	p__Bacteroidetes|c__Bacteroidia|o__Bacteroidales|f__Rikenellaceae	0.12	0.014	0.170
DbDb WT	p__Bacteroidetes|c__Bacteroidia|o__Bacteroidales|f__Prevotellaceae	0.01	0.014	0.170
DbDb WT	**p__Firmicutes|c__Clostridia|o__Clostridiales|f__Clostridiaceae**	-0.10	0.017	0.192
DbDb WT	p__Firmicutes|c__Bacilli|o__Lactobacillales|f__Carnobacteriaceae	0.00	0.018	0.197

LF Diet	**p__Firmicutes|c__Clostridia|o__Clostridiales|f__Ruminococcaceae**	-0.11	4.03E-05	0.024
LF Diet	**p__Firmicutes|c__Clostridia|o__Clostridiales|f__Ruminococcaceae|g__Anaerotruncus**	-0.01	0.000	0.040
LF Diet	**p__Firmicutes|c__Bacilli|o__Lactobacillales|f__Enterococcaceae|g__Enterococcus**	0.17	0.000	0.040
LF Diet	**p__Firmicutes|c__Bacilli|o__Lactobacillales|f__Enterococcaceae**	0.17	0.001	0.040
LF Diet	p__Firmicutes|c__Bacilli|o__Lactobacillales|f__Enterococcaceae|g__Enterococcus|s__casseliflavus	0.01	0.001	0.040
LF Diet	p__Firmicutes|c__Clostridia|o__Clostridiales|f__Lachnospiraceae|g__Roseburia	-0.03	0.001	0.040
LF Diet	p__Firmicutes|c__Clostridia|o__Clostridiales|f__Peptostreptococcaceae	0.03	0.001	0.040
LF Diet	**p__Firmicutes|c__Clostridia|o__Clostridiales|f__Mogibacteriaceae**	0.01	0.002	0.062
LF Diet	p__Bacteroidetes|c__Bacteroidia|o__Bacteroidales|f__S24-7	0.11	0.005	0.114
LF Diet	p__Firmicutes|c__Bacilli|o__Turicibacterales	0.05	0.011	0.163
LF Diet	p__Firmicutes|c__Bacilli|o__Turicibacterales|f__Turicibacteraceae	0.05	0.011	0.163
LF Diet	p__Firmicutes|c__Bacilli|o__Turicibacterales|f__Turicibacteraceae| g__Turicibacter	0.05	0.011	0.163
LF Diet	p__Firmicutes|c__Clostridia|o__Clostridiales|f__Clostridiaceae|g__SMB53	0.06	0.012	0.163
LF Diet	**p__Firmicutes|c__Clostridia|o__Clostridiales|f__Lachnospiraceae**	-0.06	0.012	0.163
LF Diet	p__Firmicutes|c__Clostridia|o__Clostridiales|f__Lachnospiraceae| g__Coprococcus	-0.02	0.012	0.163
LF Diet	p__Firmicutes|c__Bacilli	0.17	0.014	0.170
LF Diet	**p__Firmicutes|c__Clostridia**	-0.15	0.017	0.192

LF Diet	**p__Firmicutes|c__Clostridia|o__Clostridiales**	-0.15	0.017	0.192
Male Sex	p__Firmicutes	0.15	0.000	0.040
Male Sex	p__Firmicutes|c__Clostridia|o__Clostridiales|f__Lachnospiraceae|g__Dorea	-0.01	0.001	0.040
Male Sex	p__Bacteroidetes|c__Bacteroidia|o__Bacteroidales|f__Porphyromonadaceae	-0.08	0.001	0.040
Male Sex	p__Bacteroidetes|c__Bacteroidia|o__Bacteroidales|f__Porphyromonadaceae|g__Parabacteroides	-0.08	0.001	0.040
Male Sex	p__Bacteroidetes	-0.16	0.001	0.040
Male Sex	p__Bacteroidetes|c__Bacteroidia	-0.16	0.001	0.040
Male Sex	p__Bacteroidetes|c__Bacteroidia|o__Bacteroidales	-0.16	0.001	0.040
Male Sex	p__Bacteroidetes|c__Bacteroidia|o__Bacteroidales| f__Porphyromonadaceae|g__Parabacteroides|s__distasonis	-0.07	0.003	0.083
Male Sex	p__Firmicutes|c__Clostridia|o__Clostridiales|f__Dehalobacteriaceae	-0.01	0.008	0.150
Male Sex	p__Firmicutes|c__Clostridia|o__Clostridiales|f__Dehalobacteriaceae|g__Dehalobacterium	-0.01	0.009	0.163
Male Sex	p__Firmicutes|c__Clostridia|o__Clostridiales|f__Lachnospiraceae|g__Coprococcus	-0.02	0.013	0.163
Male Sex	p__Firmicutes|c__Bacilli	0.14	0.014	0.170
Tumor #	p__Bacteroidetes|c__Bacteroidia|o__Bacteroidales|f__Porphyromonadaceae	-0.05	0.001	0.040
Tumor #	p__Bacteroidetes|c__Bacteroidia|o__Bacteroidales|f__Porphyromonadaceae|g__Parabacteroides	-0.05	0.001	0.040
Tumor #	**p__Bacteroidetes|c__Bacteroidia|o__Bacteroidales|f__Porphyromonadaceae|g__Parabacteroides|s__distasonis**	-0.04	0.001	0.051
Tumor #	p__Actinobacteria|c__Actinobacteria|o__Actinomycetales|f__Corynebacteriaceae	0.02	0.004	0.093

Tumor #	p__Actinobacteria|c__Actinobacteria|o__Actinomycetales|f__Corynebacteriaceae|g__Corynebacterium	0.02	0.004	0.093
Tumor #	p__Bacteroidetes	-0.09	0.004	0.093
Tumor #	p__Bacteroidetes|c__Bacteroidia	-0.09	0.004	0.093
Tumor #	p__Bacteroidetes|c__Bacteroidia|o__Bacteroidales	-0.09	0.004	0.093
Tumor #	p__Actinobacteria|c__Actinobacteria|o__Actinomycetales|f__Micrococcaceae|g__Arthrobacter	0.01	0.004	0.097
Tumor #	p__Actinobacteria|c__Actinobacteria|o__Actinomycetales	0.02	0.005	0.105
Tumor #	p__Firmicutes|c__Bacilli|o__Lactobacillales|f__Aerococcaceae|g__Aerococcus	0.02	0.010	0.163
Tumor #	p__Firmicutes	0.06	0.012	0.163

Model= Apc (Mut or Wt) x DbDb (Mut or Wt) x Diet (LF or HF) x Sex (M or F) x Tumors (number of tumors present). Abbreviations: Mut, mutant; Wt, wildtype; LF, low fat; HF, high fat; p_, phylum; c_, class; o_, order; f_, family; g_, genus; s_, species. N= 41 (includes WtWt mice). Taxa in bold were also identified to be associated with that trait (variable) in the LDA effect size analysis.

Figure S1.

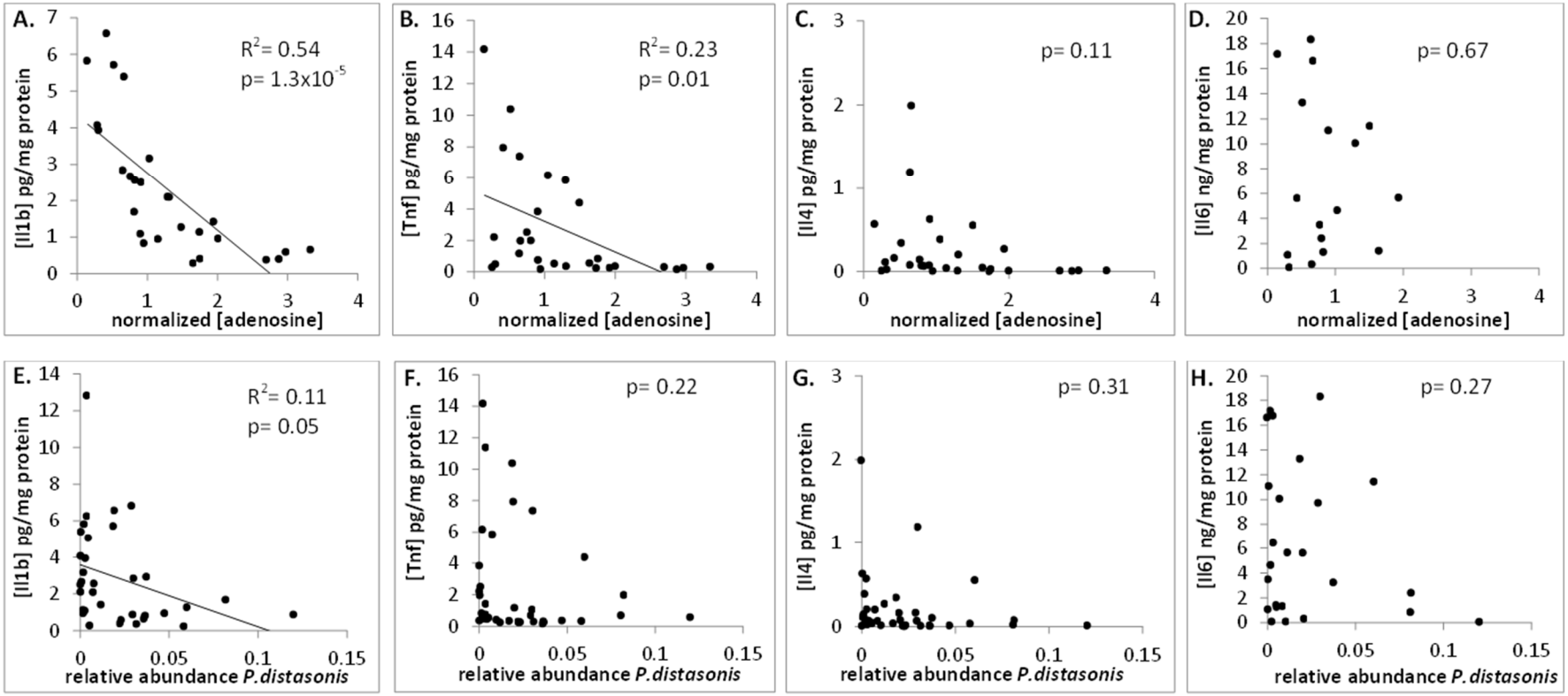
A.
[Il1b] pg/mg protein
normalized [adenosine]
R2= 0.54
p= 1.3x10-5
B.
[Tnf] pg/mg protein
normalized [adenosine]
R2= 0.23
p= 0.01
C.
[Il4] pg/mg protein
normalized [adenosine]
p= 0.11
D.
[Il6] ng/mg protein
normalized [adenosine]
p= 0.67
E.
[Il1b] pg/mg protein
relative abundance P.distasonis
R2= 0.11
p= 0.05
F.
[Tnf] pg/mg protein
relative abundance P.distasonis
p= 0.22
G.
[Il4] pg/mg protein
relative abundance P.distasonis
p= 0.31
H.
[Il6] ng/mg protein
relative abundance P.distasonis
p= 0.27

Figure Legends

Figure 1. Effect of diet and genotype on body weight and tumor burden.
A. Weight of *female* mice by group. * $p<0.05$ vs. LF, # $p<0.05$ vs. LF (all time points), □ $p<0.05$ vs. HF (all time points).
B. Weight of *male* mice by group. * $p<0.05$ vs. LF, # $P<0.05$ vs. LF (all time points), β $p<0.05$ vs. HF
C. Small intestinal tumor burden by group. p_{trend} <0.001 for tumor number and burden. Groups with different number are significantly different by post-test ($p<0.05$).

Figure 2. LDA effect size analysis of between group differences in stool bacterial abundances in Apc^{1638N} mice.
A. Output showing effect size of 29 significantly enriched taxa in each group. Model = group x gender.
B. Significant taxa plotted onto a cladogram. F, Firmicutes; P, Proteobacteria; B, Bacteroidetes; c_, class; o_, order; f_, family; g_genus, s_, species. Asterisks indicate taxa that were also associated with that group in the MaASLin analysis. N= 29.

Figure 3.Impact of obesity and intestinal tumor presence on the fecal metabolome of mice.
Low and high fat fed mice are compared in the first column (A,D,G). Low fat fed and genetically obese mice are compared in the second column (B,E,H). Mice with and without intestinal tumors are compared in the third column (C,F,I). The top row (A-C) shows heat maps of top 25 most significantly different metabolites for each comparison ($p<0.05$); color represents normalized metabolite concentration from low (blue) to high (red). The second row (D-F) shows discrimination of groups using partial least squares discriminate analysis. The third row (G-I) shows the metabolites most strongly influencing discrimination by the partial least squares discriminate analysis. The Variable Importance In Projection (VIP) score is the weighted sum of squares for the partial least-squares loadings with the amount of variance explained by each component taken into account.

Figure S1. Association of fecal adenosine concentration and Parabacteroides distasonis abundance with inflammatory cytokine production by the colonic mucosa.
Normalized adenosine concentration in fecal matter correlates with Il1b (A) and Tnf (B) but not Il4 (C) and Il6 (D) production in *ex vivo* colonic tissue. Relative abundance of *Parabacteroides distasonis* in fecal matter correlates with Il1b (E) but not Tnf (F), Il4 (G) and Il6 (H) production in *ex vivo* colonic tissue.

Table Legends

Table 1. Diet composition. Diets: LF, Low fat . HF, High fat . BioServ (custom) catalog numbers F6654, and F6653 respectively.

Table 2. Physiological characteristics of mice by group. Total lean and fat mass measured by MRI. M, male; F , female. Samples size in parentheses. * $p<0.05$ vs LF (of same sex).

Table 3. Multivariate Association with Linear Models (MaAsLin) output. Model= Apc (Mut or Wt) x DbDb (Mut or Wt) x Diet (LF or HF) x Sex (M or F) x Tumors (number of tumors present).
Abbreviations: Mut, mutant; Wt, wildtype; LF, low fat; HF, high fat; p_, phylum; c_, class; o_, order; f_,

family; g_, genus; s_, species. N= 41 (includes WtWt mice). Taxa in bold were also identified to be associated with that trait (variable) in the LDA effect size analysis.

References

1. Siegel R, Desantis C, Jemal A (2014) Colorectal cancer statistics, 2014. CA Cancer J Clin 64: 104-117.
2. Calle EE, Kaaks R (2004) Overweight, obesity and cancer: epidemiological evidence and proposed mechanisms. Nat Rev Cancer 4: 579-591.
3. Flores MB, Rocha GZ, Damas-Souza DM, Osorio-Costa F, Dias MM, et al. (2012) Obesity-induced increase in tumor necrosis factor-alpha leads to development of colon cancer in mice. Gastroenterology 143: 741-753 e741-744.
4. Gravaghi C, Bo J, Laperle KM, Quimby F, Kucherlapati R, et al. (2008) Obesity enhances gastrointestinal tumorigenesis in Apc-mutant mice. Int J Obes (Lond) 32: 1716-1719.
5. Aleman JO, Eusebi LH, Ricciardiello L, Patidar K, Sanyal AJ, et al. (2014) Mechanisms of obesity-induced gastrointestinal neoplasia. Gastroenterology 146: 357-373.
6. Yehuda-Shnaidman E, Schwartz B (2012) Mechanisms linking obesity, inflammation and altered metabolism to colon carcinogenesis. Obes Rev 13: 1083-1095.
7. McCoy AN, Araujo-Perez F, Azcarate-Peril A, Yeh JJ, Sandler RS, et al. (2013) Fusobacterium is associated with colorectal adenomas. PLoS One 8: e53653.
8. Shen XJ, Rawls JF, Randall T, Burcal L, Mpande CN, et al. (2010) Molecular characterization of mucosal adherent bacteria and associations with colorectal adenomas. Gut Microbes 1: 138-147.
9. Wang T, Cai G, Qiu Y, Fei N, Zhang M, et al. (2012) Structural segregation of gut microbiota between colorectal cancer patients and healthy volunteers. ISME J 6: 320-329.
10. Ahn J, Sinha R, Pei Z, Dominianni C, Wu J, et al. (2013) Human gut microbiome and risk for colorectal cancer. J Natl Cancer Inst 105: 1907-1911.
11. Zackular JP, Baxter NT, Iverson KD, Sadler WD, Petrosino JF, et al. (2013) The gut microbiome modulates colon tumorigenesis. MBio 4: e00692-00613.
12. Baxter NT, Zackular JP, Chen GY, Schloss PD (2014) Structure of the gut microbiome following colonization with human feces determines colonic tumor burden. Microbiome 2: 20.
13. Turnbaugh PJ, Ley RE, Mahowald MA, Magrini V, Mardis ER, et al. (2006) An obesity-associated gut microbiome with increased capacity for energy harvest. Nature 444: 1027-1031.
14. Turnbaugh PJ, Backhed F, Fulton L, Gordon JI (2008) Diet-induced obesity is linked to marked but reversible alterations in the mouse distal gut microbiome. Cell Host Microbe 3: 213-223.
15. Turnbaugh PJ, Gordon JI (2009) The core gut microbiome, energy balance and obesity. J Physiol 587: 4153-4158.
16. Wu GD, Chen J, Hoffmann C, Bittinger K, Chen YY, et al. (2011) Linking long-term dietary patterns with gut microbial enterotypes. Science 334: 105-108.
17. Fodde R, Edelmann W, Yang K, van Leeuwen C, Carlson C, et al. (1994) A targeted chain-termination mutation in the mouse Apc gene results in multiple intestinal tumors. Proc Natl Acad Sci U S A 91: 8969-8973.
18. Liu Z, Ciappio ED, Crott JW, Brooks RS, Nesvet J, et al. (2011) Combined inadequacies of multiple B vitamins amplify colonic Wnt signaling and promote intestinal tumorigenesis in BAT-LacZxApc1638N mice. FASEB J 25: 3136-3145.
19. Huffman DM, Augenlicht LH, Zhang X, Lofrese JJ, Atzmon G, et al. (2013) Abdominal obesity, independent from caloric intake, accounts for the development of intestinal tumors in Apc(1638N/+) female mice. Cancer Prev Res (Phila) 6: 177-187.

20. Hummel KP, Dickie MM, Coleman DL (1966) Diabetes, a new mutation in the mouse. Science 153: 1127-1128.
21. Siegmund B, Lehr HA, Fantuzzi G, Dinarello CA (2001) IL-1 beta-converting enzyme (caspase-1) in intestinal inflammation. Proceedings of the National Academy of Sciences of the United States of America 98: 13249-13254.
22. Ohta T, Masutomi N, Tsutsui N, Sakairi T, Mitchell M, et al. (2009) Untargeted metabolomic profiling as an evaluative tool of fenofibrate-induced toxicology in Fischer 344 male rats. Toxicol Pathol 37: 521-535.
23. Evans AM, DeHaven CD, Barrett T, Mitchell M, Milgram E (2009) Integrated, nontargeted ultrahigh performance liquid chromatography/electrospray ionization tandem mass spectrometry platform for the identification and relative quantification of the small-molecule complement of biological systems. Anal Chem 81: 6656-6667.
24. Dehaven CD, Evans AM, Dai H, Lawton KA (2010) Organization of GC/MS and LC/MS metabolomics data into chemical libraries. J Cheminform 2: 9.
25. Xia J, Mandal R, Sinelnikov IV, Broadhurst D, Wishart DS (2012) MetaboAnalyst 2.0--a comprehensive server for metabolomic data analysis. Nucleic Acids Res 40: W127-133.
26. Caporaso JG, Lauber CL, Walters WA, Berg-Lyons D, Lozupone CA, et al. (2011) Global patterns of 16S rRNA diversity at a depth of millions of sequences per sample. Proc Natl Acad Sci U S A 108 Suppl 1: 4516-4522.
27. Caporaso JG, Kuczynski J, Stombaugh J, Bittinger K, Bushman FD, et al. (2010) QIIME allows analysis of high-throughput community sequencing data. Nat Methods 7: 335-336.
28. DeSantis TZ, Hugenholtz P, Larsen N, Rojas M, Brodie EL, et al. (2006) Greengenes, a chimera-checked 16S rRNA gene database and workbench compatible with ARB. Appl Environ Microbiol 72: 5069-5072.
29. Segata N, Izard J, Waldron L, Gevers D, Miropolsky L, et al. (2011) Metagenomic biomarker discovery and explanation. Genome Biol 12: R60.
30. Ye J, Coulouris G, Zaretskaya I, Cutcutache I, Rozen S, et al. (2012) Primer-BLAST: a tool to design target-specific primers for polymerase chain reaction. BMC Bioinformatics 13: 134.
31. R_Core_Team (2013) R: A Language and Environment for Statistical Computing. R Foundation for Statistical Computing.
32. Genomics and Bioinformatics Group LoMPL, Center for Cancer Research (CCR) National Cancer Institute (NCI). CIMminer.
33. Mane J, Pedrosa E, Loren V, Ojanguren I, Fluvia L, et al. (2009) Partial replacement of dietary (n-6) fatty acids with medium-chain triglycerides decreases the incidence of spontaneous colitis in interleukin-10-deficient mice. J Nutr 139: 603-610.
34. Finucane MM, Sharpton TJ, Laurent TJ, Pollard KS (2014) A taxonomic signature of obesity in the microbiome? Getting to the guts of the matter. PLoS One 9: e84689.
35. Daniel H, Moghaddas Gholami A, Berry D, Desmarchelier C, Hahne H, et al. (2014) High-fat diet alters gut microbiota physiology in mice. ISME J 8: 295-308.
36. Zitomersky NL, Atkinson BJ, Franklin SW, Mitchell PD, Snapper SB, et al. (2013) Characterization of adherent bacteroidales from intestinal biopsies of children and young adults with inflammatory bowel disease. PLoS One 8: e63686.
37. Kverka M, Zakostelska Z, Klimesova K, Sokol D, Hudcovic T, et al. (2011) Oral administration of Parabacteroides distasonis antigens attenuates experimental murine colitis through modulation of immunity and microbiota composition. Clin Exp Immunol 163: 250-259.
38. Antonioli L, Fornai M, Colucci R, Ghisu N, Da Settimo F, et al. (2007) Inhibition of adenosine deaminase attenuates inflammation in experimental colitis. J Pharmacol Exp Ther 322: 435-442.
39. Brown JB, Lee G, Grimm GR, Barrett TA (2008) Therapeutic benefit of pentostatin in severe IL-10-/- colitis. Inflamm Bowel Dis 14: 880-887.

40. Siegmund B, Rieder F, Albrich S, Wolf K, Bidlingmaier C, et al. (2001) Adenosine kinase inhibitor GP515 improves experimental colitis in mice. J Pharmacol Exp Ther 296: 99-105.
41. Odashima M, Bamias G, Rivera-Nieves J, Linden J, Nast CC, et al. (2005) Activation of A2A adenosine receptor attenuates intestinal inflammation in animal models of inflammatory bowel disease. Gastroenterology 129: 26-33.
42. Mabley J, Soriano F, Pacher P, Hasko G, Marton A, et al. (2003) The adenosine A3 receptor agonist, N6-(3-iodobenzyl)-adenosine-5'-N-methyluronamide, is protective in two murine models of colitis. Eur J Pharmacol 466: 323-329.
43. Antonioli L, Fornai M, Colucci R, Awwad O, Ghisu N, et al. (2010) The blockade of adenosine deaminase ameliorates chronic experimental colitis through the recruitment of adenosine A2A and A3 receptors. J Pharmacol Exp Ther 335: 434-442.
44. Friedman DJ, Kunzli BM, YI AR, Sevigny J, Berberat PO, et al. (2009) From the Cover: CD39 deletion exacerbates experimental murine colitis and human polymorphisms increase susceptibility to inflammatory bowel disease. Proc Natl Acad Sci U S A 106: 16788-16793.
45. Frick JS, MacManus CF, Scully M, Glover LE, Eltzschig HK, et al. (2009) Contribution of adenosine A2B receptors to inflammatory parameters of experimental colitis. J Immunol 182: 4957-4964.
46. Muller-Haegele S, Muller L, Whiteside TL (2014) Immunoregulatory activity of adenosine and its role in human cancer progression. Expert Rev Clin Immunol 10: 897-914.
47. Antonioli L, Blandizzi C, Pacher P, Hasko G (2013) Immunity, inflammation and cancer: a leading role for adenosine. Nat Rev Cancer 13: 842-857.
48. Hausler SF, Del Barrio IM, Diessner J, Stein RG, Strohschein J, et al. (2014) Anti-CD39 and anti-CD73 antibodies A1 and 7G2 improve targeted therapy in ovarian cancer by blocking adenosine-dependent immune evasion. Am J Transl Res 6: 129-139.
49. Burghoff S, Flogel U, Bongardt S, Burkart V, Sell H, et al. (2013) Deletion of CD73 promotes dyslipidemia and intramyocellular lipid accumulation in muscle of mice. Arch Physiol Biochem 119: 39-51.
50. Weir TL, Manter DK, Sheflin AM, Barnett BA, Heuberger AL, et al. (2013) Stool microbiome and metabolome differences between colorectal cancer patients and healthy adults. PLoS One 8: e70803.

VI. Manuscript IV- Specific Aim 3

****NOTE: The following manuscript is included in this dissertation because it addresses the transcriptional component (Figures 1, 2 and 3; Table 1 and 2) of Specific Aim 3. The additional analyses comparing the colonic microbiome and metabolome was work done largely done by my co-authors and is outside the scope of the specified endpoints in Specific Aim 3, and is therefore not addressed further in this thesis.**

Interactions between the colonic transcriptome, metabolome and microbiome in mouse models of obesity-induced cancer

Authors

Anna C Pfalzer[1,2,3], Frederick K Kamanu[4], Laurence D Parnell[5], Albert K Tai[6], Zhenhua Liu[1,7], Joel B. Mason[1,2,3], and Jimmy W. Crott[1,2,3*]

[1]Cancer Cluster, USDA Jean Mayer Human Nutrition Research Center on Aging at Tufts University, Boston, Massachusetts; [2]Vitamins and Carcinogenesis Laboratory, USDA Jean Mayer Human Nutrition Research Center on Aging at Tufts University, Boston, Massachusetts; [3]Friedman School of Nutrition Science and Policy, Tufts University, Boston, Massachusetts; [4]Nutrition and Genomics Laboratory, USDA Jean Mayer Human Nutrition Research Center on Aging at Tufts University, Boston, Massachusetts; [5]Agricultural Research Service, USDA, Jean Mayer Human Nutrition Research Center on Aging at Tufts University, Boston, Massachusetts; [6]Genomics Core, Tufts University School of Medicine, Boston, Massachusetts; [7]School of Public Health and Health Sciences, University of Massachusetts, Amherst, Massachusetts

Running head: Obesity-induced changes in the colonic transcriptome

Keywords: obesity, Akt, transcriptome, metabolome, microbiome

*Correspondence:

Jimmy W Crott PhD

USDA HNRCA at Tufts University
711 Washington St, Boston, MA 02111.
Jimmy.crott@tufts.edu

Abstract

Obesity is a significant risk factor for colorectal cancer (CRC); however, the relative contribution of high-fat consumption and excess adiposity remains unclear. It is becoming apparent that obesity perturbs both the intestinal microbiome and gut metabolome, and each has the potential to induce pro-tumorigenic changes in the epithelial transcriptome. The physiologic consequences and the degree to which these different biologic systems interact remain poorly defined. To better understand the mechanisms by which obesity drives colonic tumorigenesis, we profiled the colonic epithelial transcriptome of high fat (HF) diet-induced and genetically-induced (DbDb) obese mice with a genetic predisposition to intestinal tumorigenesis (Apc^{1638N}). 266 and 584 genes were differentially expressed in the colonic mucosa of HF and DbDb mice respectively. These genes mapped to pathways involved in immune function, and cellular proliferation and cancer. Furthermore, Akt was central within the networks of interacting genes identified in both gene sets. Co-expression analysis comparing associations between the colonic transcriptome and microbiome revealed that three bacterial taxa previously correlated with tumor burden were significantly correlated with a gene module enriched for Akt-related genes. Similarly, co-expression analysis of the colonic transcriptome and metabolome found that adenosine, which was negatively associated with inflammatory markers and tumor burden, was also correlated with a gene module enriched with Akt regulators. Our findings provide evidence that high-fat consumption and excess adiposity result in changes in the colonic transcriptome that, although distinct, both appear to converge on Akt signaling. Such changes could be mediated by alterations in the colonic microbiome and metabolome.

Introduction

Colorectal cancer (CRC) is the third most common cancer and third most common cause of cancer deaths in the United States [1], affecting over half a million people annually [1]. Amongst the many risk factors for this disease is obesity: those with a BMI of 25-29.9 have a relative risk of 1.2 and 1.5 for developing CRC, while those with a BMI > 30 have a relative risk of 1.5 and 2.0 for females and males, respectively [2]. Mouse studies corroborate the epidemiological findings and prove causality: both high fat-induced obesity and genetically-promoted obesity having been shown to significantly elevate tumor burden [3]. Among gastrointestinal cancers, CRC is a good candidate for preventive strategies as there is a prolonged phase of development—estimated at ten years—during which normal mucosa evolves into a carcinoma[4]. As the worldwide incidence of obesity remains stable, it is clear that strategies aimed at reducing the risk of CRC in the obese will require more than lifestyle and diet alterations.

Currently there are three prevailing hypotheses for the mechanism underlying the link between obesity and CRC where the central players are insulin resistance, adipokines and chronic inflammation. An apparent unifying characteristic of these three hypotheses is the Akt pathway. Insulin [5], leptin [6], and pro-inflammatory cytokines [7] all have been consistently demonstrated to signal through Protein Kinase B, also known as Akt. Thus, regardless of the particular up-stream events, Akt activation and the various transcriptional consequences are likely to be an important molecular link between obesity and intestinal tumorigenesis. Akt has been studied extensively as a master regulator of critical cellular processes including growth, proliferation and cell cycle control. In this regard, over-activation of Akt signaling has been identified consistently as a critical component of initiation, promotion and progression of human tumors[8]. Furthermore,

PI3K/Akt signaling has been found to be activated in human colorectal tumors and evidence suggests that mutations could be involved in tumorigenesis and metastasis[9]. Several *Akt* inhibitors show promise as chemotherapeutic agents [10], further demonstrating the importance of Akt in tumorigenesis.

It is becoming increasingly apparent that the gut microbiota is a major determinant of various aspects of health and disease, including tumor formation. Indeed, several reports have documented alterations in the gut microbiota in those harboring colonic adenomas and carcinomas [11]. One mechanism by which the gut microbiota might affect tumor formation is by directly affecting cellular signaling. Recent studies estimate that approximately 10% of the colonic epithelial transcriptome may be sensitive to the microbial composition, with many of these genes having roles in immune modulation, proliferation and cell cycle regulation [12]. The ability of the microbiome to interact with the colonic epithelium has substantial implications for understanding the relationship between obesity and elevated CRC risk. Although it is well-recognized that experimental obesity enhances tumorigenesis [13], it remains unclear whether it is the excess adiposity, consumption of high-fat diet, or some other factor associated with obesity that is responsible for the alteration in pro-carcinogenic signaling pathways that drive the process.

Studies have demonstrated that diet-induced obesity elevates intestinal tumorigenesis; however, saturated fats activate pro-carcinogenic signaling pathways, and thus it has been difficult to distinguish the effects of obesity *per se* from elevated saturated fat intake [14]. Saturated fatty acids as well as n-6 polyunsaturated fatty acids are also known to induce an elevation in pro-inflammatory cytokines [15]. This is particularly important in understanding the association

between obesity and CRC, as one of the prevailing hypotheses posits that the chronic, low-grade inflammatory state associated with obesity is responsible for the elevation in cancer risk primarily through the ability of cytokines to stimulate pro-tumorigenic cell signaling pathways such as Toll-like receptor signaling [3]. As such, it is important to gain a better understanding of how different models of obesity differentially alter interactions between the colonic microbiome and the transcriptome and their potential impact on cellular programming and tumorigenesis.

Materials and Methods

Animal Study

All animal procedures were approved by the institutional review board of the Jean Mayer USDA Human Nutrition Research Center on Aging at Tufts University. The Apc^{1638N} (NCI Mouse Repository. Frederick, MD) strain of mice was used in order to study intestinal tumorigenesis. Apc^{1638N} mice were maintained on a low-fat diet (10% calories from fat) or made obese either through the consumption of a high-fat diet (60% calories from fat) or the presence of the leptin receptor mutation (DbDb; Jackson Laboratory, Bar Harbor, Maine). A full description of the animal protocol has previously been reported [16]. Briefly, these three groups of mice were maintained for 16 weeks and then euthanized, at which time tumor burden was documented. In addition, stool was collected for profiling the microbiome and metabolome. Finally, after rinsing the colon with PBS, followed by PBS plus protease inhibitors (Roche, Indianapolis, IN), we collected the colonic mucosa by gentle scraping with glass microscope slides. Mucosa was frozen in liquid N_2 and stored at -80°C for gene expression analyses.

Gene expression profiling

RNA was isolated from the colonic mucosa (n=10 per group) using the Ambion® RiboPure™ Kit (Life Technologies, Grand Island, NY) and quality assessed using the 2100 Bioanalyzer system (Agilent Technologies, Santa Clara, CA) to verify that the RNA Integrity Number was greater than 8. cDNA libraries were prepared with the TruSeq RNA Sample Preparation Kit v2 (Illumina, San Diego, CA), with 1 μg of input RNA per sample. Quality was assessed using the Fragment Analyzer (Advanced Analytical, Ames, IA). Single-end sequencing was performed on the HiSeq 2500 (Illumina, San Diego, CA). The demultiplexed FASTQ files were generated using CASAVA 1.8.2 (Illumina), and the QC reports were generated with FastQC. Samples were considered of acceptable quality if the mean quality score was at least 30 and the percentage of bases with a quality score of ≥ 30 was at least 85%.

TopHat and Cufflinks programs within the Tuxedo Suite programming package were used as the primary method of RNA-Seq analysis. The RNA-Seq reads from the FASTQ files were aligned to the mouse genome (mm10, GRCm38) using TopHat (http://ccb.jhu.edu/software/tophat/index.shtml) version 2.0.11. The output read alignments contained in BAM files were used by Cufflinks (http://cufflinks.cbcb.umd.edu/index.html) version 2.2.1 to assemble transcripts. BAM files from TopHat output were converted to SAM files using Samtools, available from http://www.htslib.org/. HTseq-count, an open-source tool available from http://www-huber.embl.de/HTSeq, was used to count the number of reads mapping to each gene. DESeq2, an open-source Bioconductor package, was then used in R to identify differentially expressed genes[17]. DESeq2 estimates the effect size by calculating the $\log_2$ fold change of the 'treatment' sample compared to control. A False Discovery Rate with a cutoff

of q< 0.10 was used for determining differential expression in the analysis of the colonic transcriptome. Comparisons of gene lists from both obese conditions, LF versus HF and LF versus DbDb, were done using VENNY, an online Venn diagram tool [18] that identified genes common to both data sets.

Ingenuity Pathway Analysis (IPA®; Qiagen, Redwood City, CA) was used to identify functional categories and networks that were enriched in the differentially expressed genes (q < 0.10) obtained from the DESeq2 analysis of two comparisons: LF versus HF and LF versus DbDb. Top diseases and functions were identified based upon a network score generated from a hypergeometric distribution and calculated with the right-tailed Fishers Exact Test. For instance, a network composed of 35 molecules with a Fisher Exact Test of $1x10^{-6}$ has a network score = -log(Fishers Exact Test)= 6. This network score can be interpreted as there being a 1 in a million chance of observing a network containing the same number of molecules by chance when randomly picking 35 molecules [19].

Co-expression analysis

The Weighted Correlation Network Analysis (WGCNA)[20] algorithm, in R/Bioconductor [21], was used to identify gene co-expression modules. In the construction of the weighted gene network, a soft thresholding power was selected based on the approximate free topology described in detail elsewhere [22]. Correlations between gene expression profiles with gut microbiome species abundance and fecal metabolites were determined. For each gene, WGCNA quantifies module membership as the correlation of the module eigengene and its corresponding expression profile.

Validation

Six genes found to be differentially expressed by RNA-seq were selected for validation by RT-PCR. cDNA synthesized using Superscript III reverse transcriptase (Invitrogen, Grand Island, NY) from RNA extracted above. Real-time PCR was performed with Taqman probe-based assays for *Creb3l3*, *Mfge8*, *Fabp5*, and *Rbp1* on a QuantStudio 6 Flex (Applied Biosystems, Foster City, CA). *Gapdh* was used as the control gene. Relative expression was calculated using the $2^{-\Delta\Delta Ct}$ method and statistical analyses were performed on ΔCt values. All data is reported as mean ± SEM. Statistical calculations were performed in Systat (San Jose, CA) and GraphPad Prism (La Jolla,CA). Significance was accepted when $p<0.05$ and Tukey's post-hoc test for multiple comparisons when appropriate.

Results

Physiological, tumor, microbiome and metabolome data have been reported [16]. Briefly, both genetically-induced (DbDb) and diet-induced (HF) mice had significantly greater body weight compared to LF-diet (LF) fed mice. Fat mass was significantly higher in DbDb mice compared to HF- and LF-diet fed mice and HF-diet fed mice had significantly greater body fat than LF-diet fed mice [16]. Tumor incidence was 33%, 67% and 100% in LF, HF and DbDb mice, respectively ($P<0.005$). All tumors were histologically-confirmed to be adenomatous polyps. A similar significant step-wise increase in tumor multiplicity and burden was also observed [16].

Transcriptome

An average of 18,043,084 single-end reads were retrieved per sample (range: $14.2 – 41.2 \times 10^6$). Reads were aligned to 23,338 mouse reference mRNAs using the mouse genome build, mm10.

Compared to the lean group, 266 (157 up-regulated and 109 down-regulated) and 584 (308 up-regulated and 276 down-regulated) differentially expressed genes were detected in HF and DbDb mice, respectively, using DeSeq2 (Q<0.10) (Figure 1 A, B and Supplementary Table S1 and S2). Common to both comparisons were 74 significantly differentially expressed genes, and each was altered in the same direction.

Lists of differentially expressed genes were analyzed with Ingenuity Pathway Analysis (IPA) to identify enrichment of specific canonical pathways, biological functions and networks of interacting genes. For the HF effect, 157 genes were assigned to pathways by IPA and the top 5 canonical pathways identified were related to immune function as well as cell death and survival (Table 1). Among the top 5 cellular functions were cellular growth and proliferation and cell-to-cell signaling and interaction. The most commonly attributed diseases for genes differentially expressed in HF mice were endocrine disorders, gastrointestinal and immunological diseases as well as disorders related to inflammatory response (Table 1). For the DbDb effect, 345 genes were assigned to pathways by IPA and the top 5 pathways were also related to immunity and lipid metabolism was identified as another prominent network. The top cellular functions were associated with cellular function and maintenance, and lipid metabolism. The top diseases identified were cardiovascular disease and disorders associated with inflammatory response (Table 2). Interestingly, although not differentially expressed in our dataset, Protein Kinase B (*Akt*) was a central component of the top network in both comparisons (Figure 2A, B). Moreover, several known regulators of Akt were differentially expressed in both obese comparisons: Retinol binding protein (*Rbp1*), CAMP responsive element binding protein 3 like-3 (*Creb3l3*), Milk fat globule EGF factor 8 (*Mfge8*) and Fatty acid binding protein 5 (*Fabp5*).

Phosphoinositide-3 kinase (PI3K) signaling and forkhead-box O4 identified within the top network for the DbDb comparison were also of interest as they are known Akt regulators. These six genes were chosen for validation using RT-PCR. *Creb3l3* and *Rbp1* were shown to be down-regulated approximately 60% in HF and DbDb by both RNA-sequencing and RT-PCR. *Mfge8* and *Fabp5* also had significantly elevated expression in both HF and DbDb comparisons – consistent with RNA-seq data. *Foxo4* was found to be significantly upregulated by RNA-seq in the both DbDb and HF colon while *Pik3r5* was only significantly elevated in the DbDb colon – a change verified by RT-PCR.

Associations

To identify putative pathways by which the colonic microbiome and metabolome might modulate tumorigenesis, we analyzed their association with gene expression modules via weighted co-expression correlation analysis [23]. For the microbiome analysis, WGCNA identified 15 gene modules that significantly associated with at least one of 16 bacterial taxa (Figure 3A). Among these taxa, *Clostridium* (R=0.58, p<0.01), *Sarcina* (R=0.33, p=0.03) and *Rikenellacea* (R=-0.28, p=0.07) were previously found to be associated with tumor burden in these mice [16]. Interestingly, the 'grey60' gene module was negatively associated with the two genera (*Clostridium* and *Sarcina*) that were positively associated with tumor burden, while it was positively associated with one family (*Rikenellacea*) that is negatively associated with tumor burden [16]. The grey60 module contains 206 genes and pathway analysis revealed that the top disease category associated with this gene set was cancer (151 genes; p= 8.5 x 10^{-3} – 1.25 – x$10^{-4)}$ while the top function category associated with these genes was 'cell-to-cell signaling and interaction' (19 genes; p= 8.5x10^{-3} – 1.8x10^{-5}). Of note, the highest scoring network (score =41)

of genes pertained to 'Cellular Growth and Proliferation, Cellular Development, Hematological System Development and Function' and focused on Akt (Figure 3B).

For the metabolite analysis, WGCNA identified 12 gene modules that significantly associated with at least one of 54 stool metabolites (Figure 4A). Among these metabolites, we previously found adenosine concentrations measured from fecal water to be significantly depleted in obese and tumor bearing mice and also to be inversely associated with colonic Tnfa and Il1b concentrations [16]. In this analysis adenosine was found to be associated with two gene expression modules (Figure 4A: 'royal blue' (948 genes; p=0.001) and 'green' (1907 genes; p=0.001). Pathway analysis of the 'royal blue' gene set found that the top disease category was cancer (702 genes; $p=4.7x10^{-3} – 1.6x10^{-9}$) and the top function associated with these genes is 'Cellular Growth and Proliferation' (295 genes; $p= 4.59 \times 10^{-3} – 3.2 \times 10^{-12}$). Pathway analysis of the 'green' gene set also found the top disease category to be cancer (1418 genes; $p= 1.91 x10^{-3} – 2x10^{-18}$) while the top functional category associated with these genes was lipid metabolism (324 genes; $p =1.9x10^{-3} – 1.5 \times 10^{-19}$). Relevant to tumorigenesis, the second highest scoring network in the 'green' module (score = 37) pertains to 'Cellular Assembly and Organization, Amino Acid Metabolism, Developmental Disorder' and again focused on *Akt* (Figure 4B).

Discussion

In this study we demonstrate that the induction of obesity with both a high-fat diet (HF) and mutation of the leptin receptor (DbDb) promote transcriptional changes in the colonic mucosa which may, in part, be responsible for the observed increase in tumorigenesis [16]. DbDb animals displayed more intestinal tumors and more transcriptional changes in the colon compared to HF-fed animals. The greater body weight and fat mass in the DbDb animals compared to the HF-fed

animals [16] is a more profound perturbation to homeostasis and hence is one explanation for these findings. Additionally, it is possible that the more pronounced tumor formation in DbDb mice perhaps results from direct effects of impaired leptin signaling as leptin is a known transcriptional regulator, primarily through the activation of the STAT transcription factor as well as regulation of AMPK activity [24]. Interestingly, although the transcriptional response to obesity varies significantly by model, the most prominent physiologic consequence for both obese comparisons, as identified by pathway analysis, appears to be related to immune function and inflammatory response. These findings agree with previous reports suggesting that obesity blunts the immune response and often results in low-grade biochemical inflammation in various tissues [25]. Interestingly, our transcriptional analyses did not suggest that pro-inflammatory cytokines were differentially expressed, but changes at the protein level remain possible.

The nature of the observed overlap in differentially expressed genes suggests that the physiologic pathways altered in obesity *per se* are regulated by Akt. Furthermore, co-expression analyses identified several gene modules associated with the colonic microbiome and metabolome, which also focused on *Akt* and several known regulators. Moreover, particular bacterial taxa and metabolites were also associated with tumor burden, suggesting that obesity-induced changes in the microbiome, metabolome and transcriptome all converge upon *Akt* to promote intestinal tumorigenesis.

Protein kinase B, also known as Akt, is a central 'hub' upon which numerous signaling pathways converge [26]. These signaling pathways regulate a variety of biological processes making Akt a central regulator of many cellular functions, including but not limited to cellular proliferation, apoptosis, growth, and differentiation [26] . Consistent with these regulatory functions is the fact

that changes in Akt activity consistently have been associated with several human cancers [10]. Certain genes identified by our transcriptome analysis are known to be both altered in obese models and known *Akt* regulators are potential mechanisms by which obesity may be elevating intestinal tumorigenesis. For instance, fatty-acid binding protein 5 (*Fabp5*) was upregulated 3-fold in HF and 4-fold in DbDb models. FABPs are expressed in various tissues and closely associated with energy metabolism; however, *Fabp5* has been linked specifically to cancer as it has been shown to regulate PPAR transcriptional activity and proliferation[27]. Milk fat globule EGF factor 8 (Mfg8), also known as lactadherin, which is a membrane glycoprotein expressed in many tissues including the intestine [28] was also significantly upregulated in both obese models. Mfge8 facilitates phagocytosis of apoptotic cells and consistently has been demonstrated to be upregulated in various tumors compared to normal tissue [29]. Another differentially expressed gene was retinol binding protein 1 (*Rbp1*), which belongs to the same family of fatty-acid binding proteins as FABP5 [30]. *Rbp1* was down-regulated in both obese models and has been shown to be frequently hypermethylated in tumors and cancer cell lines, which results in suppression of mRNA levels in tumors [30]. This supports our findings that a reduction in Rbp1 may be a component of the molecular mechanism by which obesity promotes pro-tumorigenic alterations the colonic epithelium. Lastly, Creb3l3, also known as Crebh, has been associated with Akt activity and has been shown to directly regulate cell proliferation rates *in vitro* [31]. *Crebh* mRNA was reduced in hepatoma tissues and cells while the elevated expression of *Crebh* suppressed proliferation [32] suggesting that a reduction in Crebh levels may result in uncontrolled proliferation within the gut that would be fertile ground for the development of intestinal tumors. Interestingly, the Forkhead box O4 (Foxo4) transcription factor, although elevated in both HF and DbDb animals, typically has been associated inversely with tumor growth and

proliferation [33]. Foxo4 is also known for its ability to maintain cellular homeostasis in multiple cell types and as such, the over- or under-expression of this protein is hypothesized to have deleterious effects on the cell [33].

Our study also investigated the interaction of obesity-induced changes in the fecal microbiome and metabolome with transcriptional changes in the colon. It has been estimated that approximately 10% of the mouse epithelial transcriptome is regulated by the microbiome [12]. Consistent with the notion that the microbiome can affect the host transcriptome, our co-expression analysis between transcript and microbe abundances identified 16 bacterial taxa significantly associated with at least one gene module. Of interest, the genera *Clostridium* and *Sarcina* (positively associated with tumor burden) were negatively correlated with the gene module 'grey60'. Conversely, the family *Rikenellaceae* (was negatively associated with tumor burden) was positively correlated with this specific gene module. IPA analysis of this module again reveled an enrichment of cancer-related genes and of Akt regulators. Thus we suggest that the differing association these taxa with tumor burden could be due to their opposite effect on a gene set enriched for Akt and cancer related genes.

To further explore the complex relationship between obesity and colon cancer and to provide data on the molecules that could facilitate the interplay between colonic epithelium and the microbiome, we considered associations between the colonic metabolome and transcriptome. Twelve gene modules were significantly associated with at least one of the 54 metabolites. Among these, adenosine is of particular interest as it was negatively associated with pro-inflammatory cytokines Il1b and Tnfa and also with tumor burden [16]. Adenosine was most strongly associated with 'royal blue' and 'green' modules, of which the top disease identified by

pathway analysis was cancer and furthermore, both gene networks focused on Akt. Given that adenosine has been shown to directly regulate the activity of Akt,[34] we posit that obesity-induced reductions in luminal adenosine could promote tumorigenesis by activating Akt signaling.

In this study we have attempted to gain a better understanding of the mechanisms by which obesity promotes CRC by comparing colonic gene expression signatures of diet and genetically-induced obese mice. A modest degree of overlap was observed for these models: 74 genes were altered in both comparisons, comprising 27% and 12% of altered genes in HF and DbDb mice, respectively. Among these common genes, we confirmed expression changes for several regulators of Akt. Moreover, networks focusing on Akt were the most robust found within each gene set. To assess the possible influence of the gut microbiome and metabolome on gene expression, co-expression analyses were performed. Several gene modules were found to associate significantly with numerous taxa and metabolites. Of particular interest were modules that associated with metabolites and taxa that were associated with tumor burden in these mice. Pathway analyses of these modules again highlighted Akt signaling, with the strongest network of genes for each module once more focusing on Akt. These data suggest that although high-fat feeding and genetic obesity have distinct effects on the colonic transcriptome, there is considerable overlap and Akt appears to be a common target for both perturbations. Likewise, we have identified specific metabolites and microbes that could mediate the activation, or de-repression, of Akt in obesity and as such are potential targets for CRC prevention in the obese.

Acknowledgements

We thank Donald Smith and the staff of the Comparative Biology Unit at the HNRCA for their assistance with animal care. We would especially like to thank Dr. Simin Meydani for her

generous support of the Cancer Cluster as well as Drs. Peter and Joan Cohn and the HNRCA Directors Student Innovation Fund for providing additional support for this study. This study was funded in part by the Agricultural Research Service of the United States Department of Agriculture, Cooperative Agreement #58-1950-0-014. Partial support for this work was provided by the Tufts Collaborates Seed Initiative from the Office of the Vice Provost. Opinions and ideas expressed in this publication are not necessarily those of the U.S. Department of Agriculture. Any opinions, findings, conclusion, or recommendations expressed in this publication are those of the author(s) and do not necessarily reflect the view of the U.S Dept. of Agriculture.

References

1. Siegel R, Desantis C, Jemal A. Colorectal cancer statistics, 2014. *CA Cancer J Clin*. 2014;64(2):104-117. doi:10.3322/caac.21220.

2. Moore LL, Bradlee ML, Singer MR, et al. BMI and waist circumference as predictors of lifetime colon cancer risk in Framingham Study adults. *Int J Obes Relat Metab Disord*. 2004;28(4):559-567. doi:10.1038/sj.ijo.0802606.

3. Flores MB, Rocha GZ, Damas-Souza DM, et al. Obesity-induced increase in tumor necrosis factor-alpha leads to development of colon cancer in mice. *Gastroenterology*. 2012;143(3):741-744. doi:10.1053/j.gastro.2012.05.045.

4. Temraz S, Mukherji D, Shamseddine A. Potential targets for colorectal cancer prevention. *Int J Mol Sci*. 2013;14(9):17279-17303. doi:10.3390/ijms140917279.

5. Hermann C, Assmus B, Urbich C, Zeiher AM, Dimmeler S. Insulin-mediated stimulation of protein kinase Akt: A potent survival signaling cascade for endothelial cells. *Arter Thromb Vasc Biol*. 2000;20(2):402-409. http://www.ncbi.nlm.nih.gov/pubmed/10669636.

6. Stattin P, Lukanova A, Biessy C, et al. Obesity and colon cancer: does leptin provide a link? *Int J Cancer*. 2004;109(1):149-152. doi:10.1002/ijc.11668.

7. Huang X-F, Chen J-Z. Obesity, the PI3K/Akt signal pathway and colon cancer. *Obes Rev*. 2009;10(6):610-616. doi:10.1111/j.1467-789X.2009.00607.x.

8. Samuels Y, Wang Z, Bardelli A, et al. High frequency of mutations of the PIK3CA gene in human cancers. *Science*. 2004;304(5670):554. doi:10.1126/science.1096502.

9. Lan Y-T, Jen-Kou L, Lin C-H, et al. Mutations in the RAS and PI3K pathways are associated with metastatic location in colorectal cancers. *J Surg Oncol*. 2015;111(7):905-910. doi:10.1002/jso.23895.

10. Garcia-Echeverria C, Sellers WR. Drug discovery approaches targeting the PI3K/Akt pathway in cancer. *Oncogene*. 2008;27(41):5511-5526. doi:10.1038/onc.2008.246.

11. Zackular JP, Baxter NT, Iverson KD, et al. The gut microbiome modulates colon tumorigenesis. *MBio*. 2013;4(6):e00692-13. doi:10.1128/mBio.00692-13.

12. Sommer F, Nookaew I, Sommer N, Fogelstrand P, Bäckhed F. Site-specific programming of the host epithelial transcriptome by the gut microbiota. *Genome Biol*. 2015;16(1):62. doi:10.1186/s13059-015-0614-4.

13. Gravaghi C, Bo J, Laperle KM, et al. Obesity enhances gastrointestinal tumorigenesis in Apc-mutant mice. *Int J Obes*. 2008;32(11):1716-1719. doi:10.1038/ijo.2008.149.

14. Barden A, Mas E, Croft KD, Phillips M, Mori T a. Short-term n-3 fatty acid supplementation but not aspirin increases plasma proresolving mediators of inflammation. *J Lipid Res*. 2014;55(11):2401-2407. doi:10.1194/jlr.M045583.

15. Teng K-T, Chang C-Y, Chang LF, Nesaretnam K. Modulation of obesity-induced inflammation by dietary fats: mechanisms and clinical evidence. *Nutr J*. 2014;13(1):12. doi:10.1186/1475-2891-13-12.

16. Pfalzer AC, Nesbeth P-DC, Parnell LD, et al. Diet- and Genetically-Induced Obesity Differentially Affect the Fecal Microbiome and Metabolome in Apc1638N Mice. *PLoS One*. 2015;10(8):e0135758. doi:10.1371/journal.pone.0135758.

17. MI L, Huber W, Anders S. Moderated estimation of fold change and dispersion for RNA-Seq data with DESeq2. *bioRxiv*. 2014. doi:http://dx.doi.org/10.1101/002832,http://dx.doi.org/10.1101/002832.

18. Oliveros JC. VENNY. An interactive tool for comparing lists with Venn Diagrams. *BioinfoGP of CNB-CSIC*. 2007:http://bioinfogp.cnnb.csic.es/tools/venny/index.ht. http://bioinfogp.cnnb.csic.es/tools/venny/index.html.

19. Qiagen. No Title. *'http://ingenuity.force.com/ipa/IPATutorials?id=ka250000000TNBZCA4"*.

20. Langfelder P, Horvath S. WGCNA: an R package for weighted correlation network analysis. *BMC Bioinformatics*. 2008;9:559. doi:10.1186/1471-2105-9-559.

21. R Development Core Team. R: A language and environment for statistical computing. R Foundation for Statistical Computing, Vienna, Austria. URL http://www.R-project.org/. *R Found Stat Comput Vienna, Austria*. 2013.

22. Zhang B, Horvath S. A general framework for weighted gene co-expression network analysis. *Stat Appl Genet Mol Biol*. 2005;4:Article17. doi:10.2202/1544-6115.1128.

23. Langfelder P, Horvath S. WGCNA: an R package for weighted gene co-expression network analysis. *BMC Bioinformatics*. 2008;9:559. doi:10.1186/1471-2105-9-559.

24. Morris DL, Rui L. Recent advances in understanding leptin signaling and leptin resistance. *Am J Physiol Endocrinol Metab*. 2009;297:E1247-E1259. doi:10.1152/ajpendo.00274.2009.

25. Milner JJ, Beck MA. The impact of obesity on the immune response to infection. *Proc Nutr Soc*. 2012;71(2):298-306. doi:10.1017/S0029665112000158.

26. Chan CH, Jo U, Kohrman A, et al. Posttranslational regulation of Akt in human cancer. *Cell Biosci*. 2014;4(1):59. doi:10.1186/2045-3701-4-59.

27. Thumser AE, Moore JB, Plant NJ. Fatty acid binding proteins: tissue-specific functions in health and disease. *Curr Opin Clin Nutr Metab Care*. 2014;17(2):124-129. doi:10.1097/MCO.0000000000000031.

28. Li B-Z, Zhang H-Y, Pan H-F, Ye D-Q. Identification of MFG-E8 as a novel therapeutic target for diseases. *Expert Opin Ther Targets*. 2013;17(11):1275-1285. doi:10.1517/14728222.2013.829455.

29. Oba J, Moroi Y, Nakahara T, Abe T, Hagihara a., Furue M. Expression of milk fat globule epidermal growth factor-VIII may be an indicator of poor prognosis in malignant melanoma. *Br J Dermatol*. 2011;165:506-512. doi:10.1111/j.1365-2133.2011.10409.x.

30. Esteller M, Guo M, Moreno V, et al. Hypermethylation-associated inactivation of the cellular retinol-binding-protein 1 gene in human cancer. *Cancer Res*. 2002;62(20):5902-5905.

31. Peltier J, O'Neill A, Schaffer D V. PI3K/Akt and CREB regulate adult neural hippocampal progenitor proliferation and differentiation. *Dev Neurobiol*. 2007;67(10):1348-1361. doi:10.1002/dneu.20506.

32. Chin K-T, Zhou H-J, Wong C-M, et al. The liver-enriched transcription factor CREB-H is a growth suppressor protein underexpressed in hepatocellular carcinoma. *Nucleic Acids Res*. 2005;33(6):1859-1873. doi:10.1093/nar/gki332.

33. Su L, Liu X, Chai N, et al. The transcription factor FOXO4 is down-regulated and inhibits tumor proliferation and metastasis in gastric cancer. *BMC Cancer*. 2014;14:378. doi:10.1186/1471-2407-14-378.

34. Merla R, Ye Y, Lin Y, et al. The central role of adenosine in statin-induced ERK1/2, Akt, and eNOS phosphorylation. *Am J Physiol Heart Circ Physiol*. 2007;293(3):H1918-H1928. doi:10.1152/ajpheart.00416.2007.

Figure Legends

Figure 1. Differential expression analysis of colonic transcriptome. Volcano plots of the log2 fold change for genes differentially expressed in A) HF vs LF mice and B) DbDb vs LF mice. A grey line indicates q-value= 0.10. Differential expression was determined using DESEq2 and significance was set using a q-value< 0.10.

Figure 2. Pathway analysis of genes differentially expressed in diet and genetically induced obese mice. A) Top-scoring IPA network amongst HF-induced changes is associated with 'Humoral Immune Response, Protein Synthesis, Cellular Function and Maintenance' while the top-scoring network for the B) Top-scoring IPA network amongst DbDb-induced changes is associated with 'Cellular Function and Maintenance, Cell-to-Cell Signaling and Interaction, Cellular Movement.' Gene names written in ovals were differentially expressed (q-value < 0.10) in our transcriptional analysis and genes and/or protein complexes in rectangles were not included in transcriptome analysis. Genes in red ovals indicate an upregulation and genes in green ovals indicate a down-regulation in obese mice compared to lean. Shades of color indicate the degree of fold-change.

Figure 3. Validation of gene expression changes. Real-Time PCR validation of genes identified to be differentially expressed in both HF and DbDb mice compared to lean animals and known regulators of Akt. LF, low-fat; HF, high-fat; DbDb, genetically-induced obese mice. Data represents the mean ± SEM. Bars sharing the same superscript letter are not significantly different. An asterisk indicates the p-value=.08 versus LF.

Figure 4. Associations between colonic transcriptome and microbiome. A) Weighted co-expression correlation analysis (WCGCA) identified clusters of genes from the colonic epithelial transcriptome which were associated with microbial communities in obese and lean mice. Each color along the *y*-axis indicates a cluster of genes associated with a particular microbial population. For each comparison, we generated a correlation coefficient and corresponding p-value. An asterisk indicates p-value <0.05. Color indicates the direction and strength of the correlation; deeper shades of red indicate a more positive correlation and deeper shades of green indicate a more negative correlation. The 'grey60' gene module significantly correlated with three bacterial taxa also associated with tumor burden[16]. Abbreviations: c, class; o, order; *f, family; g, genus; s, species*; B) Ingenuity Pathway Analysis (IPA) of the 'grey60' module identified the top network function relating to 'Cellular Growth and Proliferation, Cellular Development, Hematological System Development and Function' and *Akt* was the central target of genes within this network.

Figure 5. Associations between colonic transcriptome and metabolome. A) WCGCA identified clusters of genes from the colonic epithelial transcriptome which were associated with fecal metabolites enriched in in obese and lean mice. Each color along the *y*-axis indicates a cluster of

genes associated with a particular metabolite along the x-axis. The number '10' corresponding to adenosine is in bold and the full name of metabolites are listed below. For each comparison, we generated a correlation coefficient and corresponding p-value. An asterisk indicates p-value <0.05. Color indicates the direction and strength of the correlation; darker shades of red indicate a more positive correlation and darker shades of green indicate a more negative correlation. The 'green' gene module significantly correlated with adenosine. 1, 1-oleoyglycerophosphoglycerol; 2, 1-stearoylglycerophosphoinositol; 3, 13-methylmyristic acid; 4, 2-aminobutyrate; 5, 3-dehydrocarnitine; 6, 3-dehydrocholate; 7, 3-dehydroxypropanoate; 8, 4-hydroxyphenylacetate; 9, 8-hydroxyoctanoate; 10, adenosine; 11, adenosine-2,3-cyclic monophosphate; 12, adrenate; 13, alanine; 14, alanyileucine; 15, alanylphenylalanine; 16, azelate; 17, beta-alanine; 18, carnitine; 19, cholate; 20, cholestanol; 21, cis-vaccenate; 22, citrate; 23, cyclo(leu-phe); 24, cysteine; 25, delta-tocopherol; 26, diaminopilmelate; 27, dodecanedioate; 28, gamma-tocopherol; 29, glutamine; 30, guanosine-2,3-cyclic monophosphate; 31, octadecanoic acid; 32, isoleucylmethionine; 33, isoleucyltyrosine; 34, L-urobilin; 35, lithocholate; 36, N-acetylaspartate; 37, octadecanedioate; 38, prolyltyrosine; 39, serylleucine; 40, serylphenylalanine; 41, spermidine; 42, suberate; 43, taurine; 44, threonylmethionine; 45, undecanedioate; 46, uridine; 47, uridine-2,3-cyclic monophosphate; 48, val-val-val; 49, valylisoleucine; 50, valylleucine; 51, valylmethionine; 52, valylmethionine; 53, valylphenylalanine; 54, valylvaline. B) IPA of the 'green' module identified the top disease category as 'Cancer' and *Akt* was the central target of genes within this network.

Figure 1

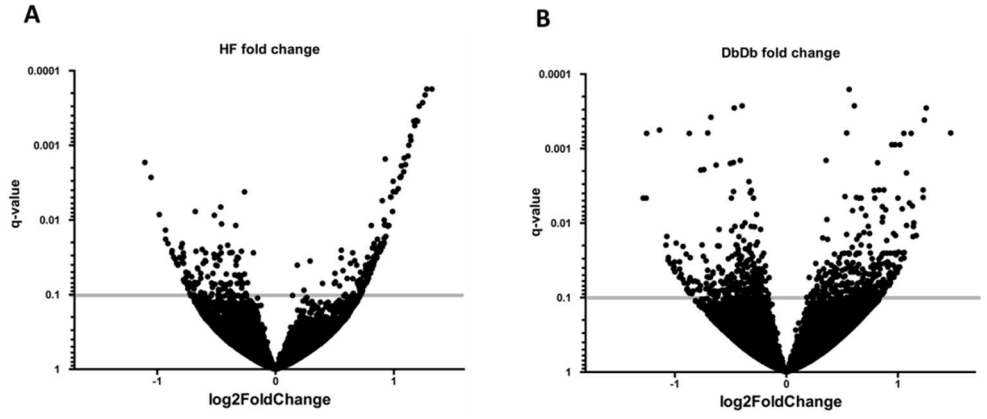

Figure 2

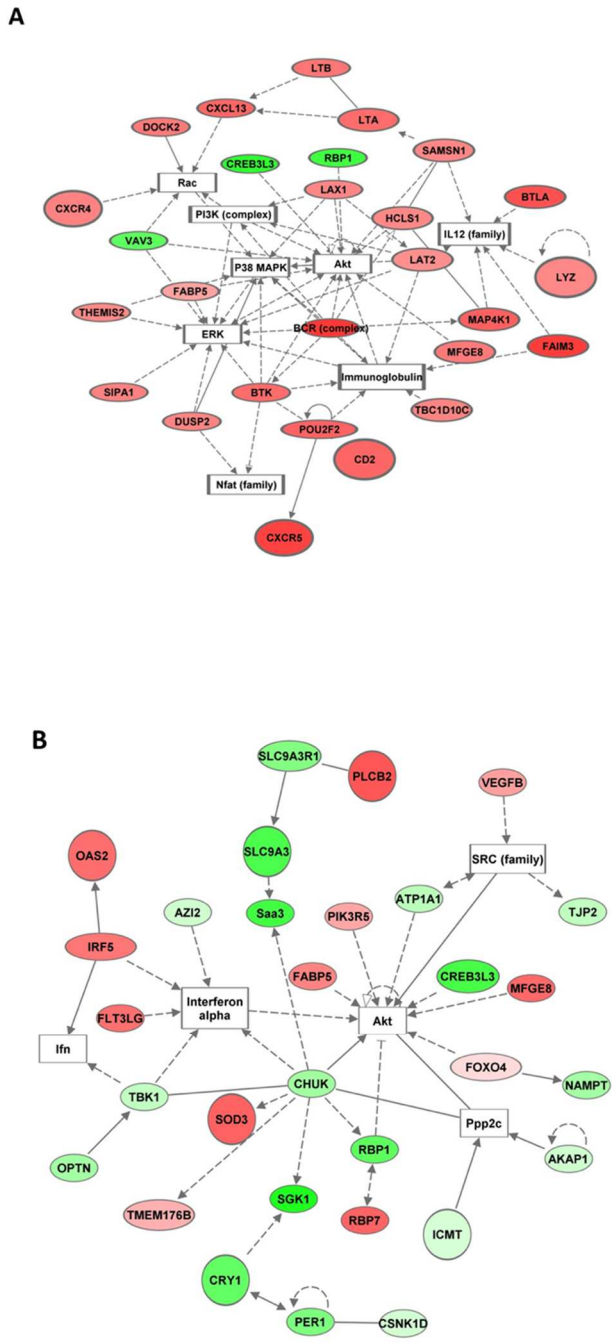
A
LTB
CXCL13
LTA
DOCK2
SAMSN1
CREB3L3
RBP1
Rac
LAX1
BTLA
CXCR4
PI3K (complex)
HCLS1
IL12 (family)
VAV3
P38 MAPK
Akt
LAT2
LYZ
FABP5
THEMIS2
MAP4K1
ERK
BCR (complex)
MFGE8
FAIM3
Immunoglobulin
SIPA1
BTK
TBC1D10C
DUSP2
POU2F2
CD2
Nfat (family)
CXCR5
B
SLC9A3R1
PLCB2
VEGFB
OAS2
SLC9A3
SRC (family)
ATP1A1
AZI2
Saa3
PIK3R5
TJP2
IRF5
FABP5
CREB3L3
MFGE8
FLT3LG
Interferon alpha
Akt
Ifn
FOXO4
NAMPT
TBK1
CHUK
SOD3
Ppp2c
RBP1
AKAP1
OPTN
SGK1
TMEM176B
RBP7
ICMT
CRY1
PER1
CSNK1D

Figure 3

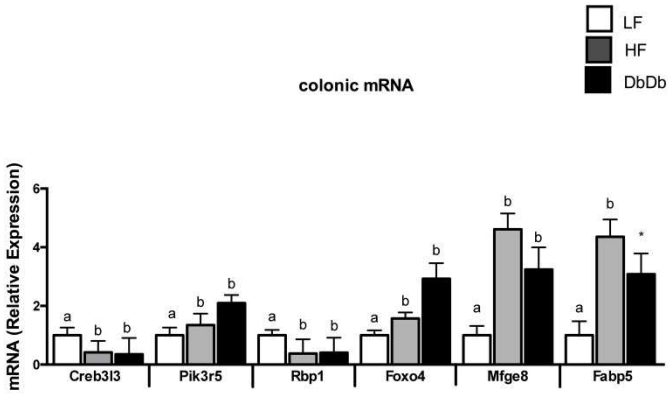

Figure 4

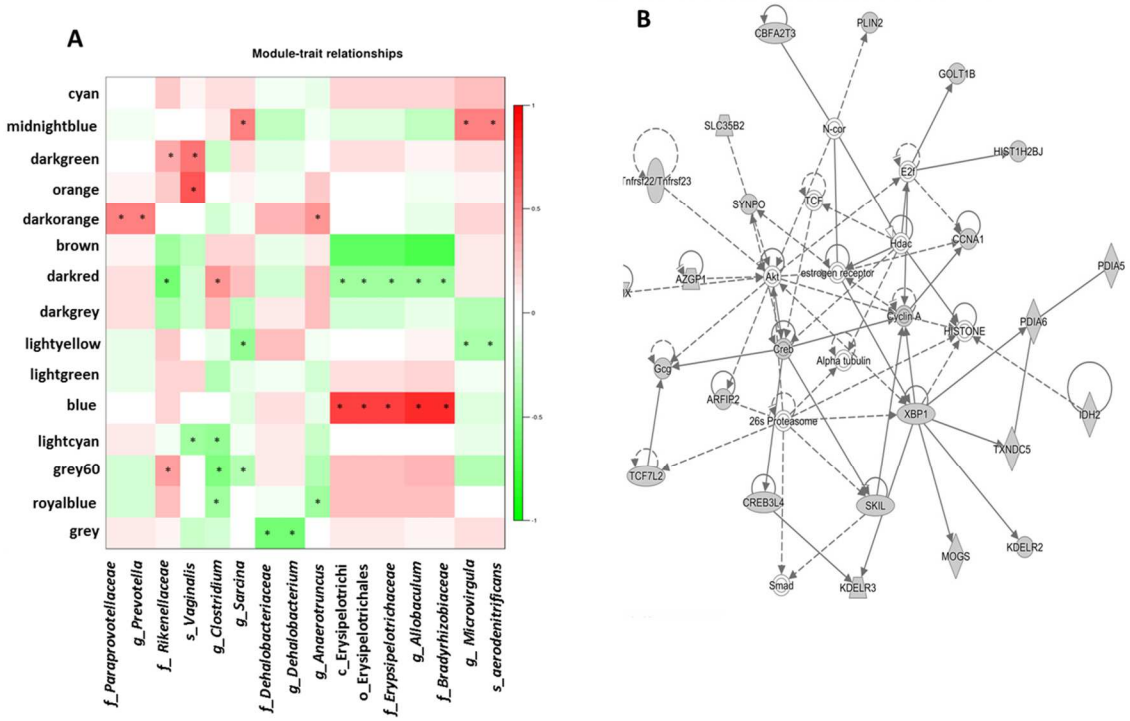

Figure 5

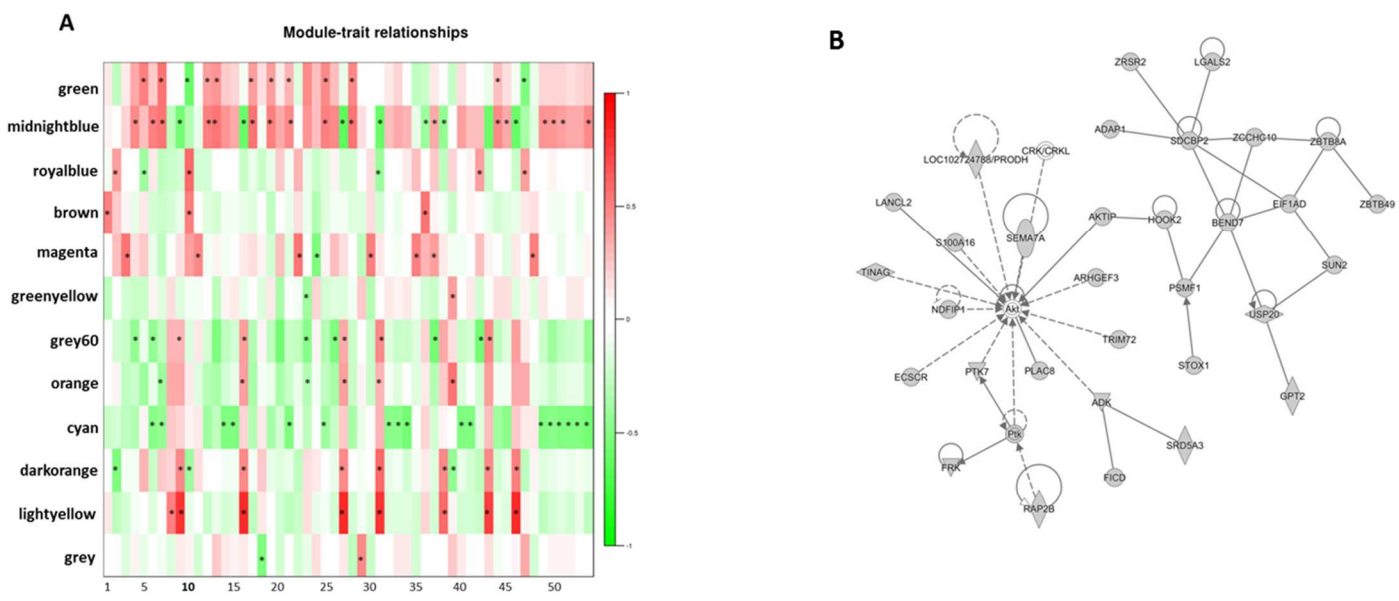
A
Module-trait relationships
green
midnightblue
royalblue
brown
magenta
greenyellow
grey60
orange
cyan
darkorange
lightyellow
grey
1
5
10
15
20
25
30
35
40
45
50
B
ZRSR2
LGALS2
ADAP1
SDCBP2
ZCCHC10
ZBTB8A
LOC102724788/PRODH
CRK/CRKL
LANCL2
AKTIP
HOOK2
BEND7
EIF1AD
ZBTB49
S100A16
SEMA7A
SUN2
TINAG
ARHGEF3
PSMF1
NDFIP1
Akt
USP20
TRIM72
ECSCR
PTK7
PLAC8
STOX1
ADK
GPT2
Ptk
SRD5A3
FRK
FICD
RAP2B

Table 1. Top 5 diseases, functions and networks associated with genes differentially expressed in HF versus LF mice.

Diseases and Disorders	**p-value**	**# Molecules**
Endocrine System Disorders	2.16E-03 – 3.97E-29	46
Gastrointestinal Disease	2.72E-03 –3.97E-29	57
Immunological Disease	1.33E-03 –3.97E-29	71
Metabolic Disease	7.14E-04 – 3.97E-29	52
Inflammatory Response	2.91E-03 – 3.01E-18	92
Molecular and Cellular Functions	**p-value**	**# Molecules**
Cellular Function and Maintenance	2.99E-03 – 2.97E-27	93
Cellular Development	2.91E-03 - 6.95E-25	93
Cellular Growth and Proliferation	2.33E-03 – 6.95E-25	97
Protein Synthesis	8.49E-04 – 2.00E-22	53
Cell-To-Cell Signaling and Interaction	2.91E-03 – 3.01E-18	68
Top Networks		
Network ID	**Network Functions**	**Score**
1	Hematological System Development and Function, Humoral Immune Response, Tissue Morphology	38
2	Humoral Immune Response, Protein Synthesis, Cellular Function and Maintenance	38
3	Endocrine System Disorders, Gastrointestinal Disease, Metabolic Disease	36
4	Cellular Function and Maintenance, Hematological System Development and Function, Cell Death and Survival	31
5	Humoral Immune Response, Protein Synthesis, Hematological System	29

Table 2. Top 5 diseases, functions and networks associated with genes differentially expressed in DbDb versus LF mice.

Diseases and Disorders	**p-value**	**# Molecules**
Cardiovascular Disease	2.99E-02 – 4.95E-04	27
Organismal Injury and Abnormalities	2.99E-02 – 4.95E-04	75
Inflammatory Response	2.99E-02 – 8.22E-04	54
Infectious Disease	2.99E-02 – 1.26E-03	32
Hematological Disease	2.99E-02 – 1.30E-03	14
Molecular and Cellular Functions	**p-value**	**# Molecules**
Cellular Function and Maintenance	2.99E-02 – 7.28E-06	124
Cell Signaling	4.46E-03 – 4.25E-05	26
Lipid Metabolism	2.99E-02 – 5.78E-03	53
Small Molecule Biochemistry	2.99E-02 – 5.78E-03	57
Vitamin and Mineral Metabolism	2.99E-02 – 5.78E-03	20
Top Networks		
Network ID	**Network Functions**	**Score**
1	Cellular Function and Maintenance, Cell-To-Cell Signaling and Interaction, Cellular Movement	39
2	Cell Death and Survival, Carbohydrate Metabolism, Cell Signaling	29
3	Cell Death and Survival, Cellular Development, Cancer	25
4	Cardiovascular Disease, Connective Tissue Disorders, Cancer	20
5	Cellular Development, Growth and Proliferation, Embryonic Development	20

Supplementary Table 1. Genes differentially expressed in the HF colonic epithelium compared to LF. Differential expression was determined using DESEq2 and significance was set using a q-value < 0.10.

Supplementary Table 2. Genes differentially expressed in the DbDb colonic epithelium compared to LF. Differential expression was determined using DESEq2 and significance was set using a q-value < 0.10.

VII. Discussion and Future Directions

Observations from this thesis identify several potential contributions that the establishment of an inflammatory milieu in the colonic mucosa may play in explaining the enhanced risk of colon cancer due to excess adiposity. Our work has demonstrated that adiposity results in an elevation of select pro-inflammatory cytokines in the colon of humans and mice and that this elevation is coupled with cytokinetic and molecular changes that may promote the development of colorectal cancer. Further, my work with the IL-1 receptor knockout mouse suggests that the elevation in colonic cytokines is not just an epiphenomenon of obesity, but rather a factor that is mechanistically responsible for many of the observed precancerous molecular and cytokinetic changes that accompany obesity. Of all the experiments I performed, only one included the actual endpoint of neoplasms, but this study clearly showed that adiposity *per se*—regardless of its cause—increases intestinal tumorigenesis, thereby underscoring the import of the molecular and cytokinetic alterations I found in my other studies. I found it particularly informative that although diet- and genetically-induced obesity induce very distinct changes in the colonic transcriptome, the transcriptional alterations observed in each condition converge on and suggest activation of Akt, which as explained in earlier sections is a kinase that possesses a diverse spectrum of actions including the activation of a number of the pro-cancerous pathways that are of particular relevance to colonic carcinogenesis such as Wnt and NFκB[1].

Therefore, future work intended to block the promotional effects of obesity on cancer risk might rightfully target Akt, although blocking this activation would have to be approached with great caution since it would have a broad diversity of downstream effects, some of which might have detrimental cellular and physiologic consequences.

It is worth emphasizing that my observations in both animals and humans suggest that even modest degrees of adiposity are sufficient to produce the biochemical and molecular changes that were noted in the colon, and this is consistent with the clinical observation that even modest degrees of excess weight carries with it an increased risk of CRC[2]. Further, although obesity only modestly increased colonic cytokine levels in both the animals and humans, it is important to emphasize that obesity produces chronic exposure to this inflammatory environment, which over time would likely magnify its impact on the colonic epithelium.

Although we did not look at the issue in depth in our murine studies, my observations in humans indicated that alterations in systemic inflammation were not good predictors of the inflammatory status of the colon. Not only did plasma and colonic cytokine levels not concur but NSAID use had no apparent effect on systemic levels while their use was associated with significant reductions in colonic cytokines – suggesting that: 1) NSAID use has tissue-specific effects and 2) colonic cytokines are regulated in a different manner than plasma cytokines. Thus, to the extent that pro-inflammatory cytokines mediate CRC risk, they need to be assessed in the colon rather than in the plasma.

Among those cytokines elevated in obese mice, we found evidence that IL-1β in particular is a critical mediator of both cytokine production and proliferation in the colon. Furthermore, we found that IL-1 signaling is necessary for the obesity-mediated alterations in cytokine concentrations and proliferation. This provides evidence that blockade of this particular

molecule could be another effective means of blocking obesity-promoted CRC although, like the blockade of Akt, its effects would be diverse and would have to be monitored for undesirable side effects.

Although we could not prove causality in our human study, our observations certainly were consistent with our mouse data that suggests that obesity is mechanistically linked to an activation of Wnt signaling. It is widely recognized that over-activation of this pathway is one of the earliest steps in the development of colonic tumorigenesis[3,4]. These findings provide evidence that elevations in colonic cytokines are associated with an activation of Wnt signaling and in particular, that IL-1 signaling has a critical role in this relationship. Several inhibitors of Wnt signaling are already available, providing yet another avenue by which obesity-promoted colon cancer might be blocked. However this potential target would also have to be approached very cautiously since, as mentioned above, a certain basal level of Wnt signaling is required in the colon since it is responsible for normal maintainence of the population of colonocyte stem cells in the colonic crypts[4].

Although this project has contributed several important pieces of information towards understanding the relationship between obesity, inflammation, and elevated CRC risk, there are several critical questions which remain unanswered and require additional investigation. First, although our transcriptional work suggested that the Wnt, NFκB, and ERK signaling pathways may be elevated in the colons of obese humans, we were not able to examine the potential functional consequences of these changes in the transcriptome, which would require assessing the gene products of the relevant transcripts and/or performing actual functional assays of the signaling pathways that would directly measure their activation; nor did we have sufficient samples in our human study to assess relevant changes in cytokinetics such as proliferation and

apoptosis. In addition, it remains unclear what particular cell type is responsible for the production of these cytokines. Thus, an appropriate follow-up clinical study to my initial translational study would investigate functional measures of Wnt, NFκB, and ERK activation as well as relevant downstream consequences of their activation in the colonic mucosa of obese and lean individuals. This follow-up study should also identify the particular cell type responsible for the production of the cytokines in the colonic mucosa. Several well-accepted methodologies exist for isolating cell types from intact tissue[5]. One such methodology would be fluorescence activated cell sorting (FACS) using flow cytometry and fluorescently-labeled antibodies to selectively sort for the desired cell type[6]. Cytokines can then be measured on homogeneous cell populations to begin identifying the cellular source of inflammation. Similarly, it will also be important to identify the particular cell type responsible for the elevation in colonic cytokines in obese mice. As mentioned previously, we found that there was no difference in colonic cytokine concentrations in isolated colonocytes from obese and lean mice, however, we did see a significant elevation in the colonic mucosa of obese mice. A follow-up study which collects the colonic mucosa and further isolates individual cell types from this heterogeneous sample would provide greater insight into the specific cells which are secreting the pro-inflammatory cytokines. The same FACS analysis identified above could again be utilized to identify the particular cell type responsible for the elevation in inflammation in the colon[6]. Identifying the exact cells responsible for the inflammatory environment in the obese human and mouse colon is an important piece of information because it would identify specific cell populations to target to prevent the pro-carcinogenic changes which occur as a result of elevated biochemical inflammation. Based upon previous studies examining the impact of obesity on inflammation in mice, macrophages are the most likely source of pro-inflammatory cytokine production. In fact,

it has been demonstrated that macrophages migrate to adipose tissue in response to high-fat feeding[7]. Furthermore, there is a significant increase in macrophage infiltration in mouse models of colitis compared to control animals[8,9].

Lastly, we provide convincing evidence for the connection between elevated colonic cytokines and activation of pro-tumorigenic signaling; however, we have yet to demonstrate a direct connection to the development of intestinal tumorigenesis. In order to begin connecting elevations in colonic cytokines to the development of colonic carcinogenesis, we would need to demonstrate that the absence of select cytokines leads to a reduction in tumorigenesis. In fact, mice lacking functional TNF-signaling do show significant reductions in chemically-induced intestinal tumorigenesis[9]; however, the impact of IL-1 signaling specifically on tumorigenesis is unclear. To do so, we could repeat the study in Specific Aim 2, utilizing mice that lack functional IL-1 signaling and chemically-induce colonic carcinogenesis. We would expect that should IL-1 signaling directly impact tumorigenesis, these mice would have reductions in colonic carcinogenesis compared to control mice.

VIII. Limitations

Specific Aim 1

The study design of my translational study called for a subject enrollment of 60, although we ultimately only recruited 43 subjects, 42 of whom completed the study. It is noteworthy that the original sample size calculation indicated that only 40 subjects were necessary to achieve statistically significant differences between the groups but the desired recruitment was increased by 50% to account for the fact that data from obese animals was used to estimate sample size and we wanted to account for possible differences between human and rodent biology. Regardless of

recruitment success, this human study was of modest size and its results should be confirmed by a larger study.

This study included both males and females in order to achieve the desired sample size. It is well-known that obesity-associated colon cancer risk varies by gender and it is possible that the biochemical and molecular changes occurring within the colon also vary by gender. Unfortunately, due to our small sample size, we were unable to stratify our analyses by gender and are thus unable to differentiate the effect of gender on our endpoints. Similarly, we intentionally only included Caucasians in this study since we did not wish to confound the results with the recognized racial differences in inflammatory response[10,11] and cytokine levels[12]; a larger study would therefore also allow for stratification by race.

Specific Aim 2

The study design that examined the role of IL-1 signaling utilized a mouse model which lacks the IL-1 receptor (IL1RKO), and both IL-1α and IL-1β serve as ligands for this receptor. Thus, we were not able to distinguish the effect of IL-1β specifically. However, IL-1β appears to be the principal form of IL-1 acting upon non-neoplastic colonocytes in humans[13] so the assumption in this study is that most of the IL-1 mediated effects are due to IL-1β.

Additionally, there is evidence that leptin and insulin signaling are both regulated, in part, by IL-1 signaling. Although the exact mechanism remains unclear, it is likely that IL-1 signaling through its receptor alters the downstream signaling events associated with leptin and insulin[14,15]. For instance, both insulin and leptin signal through PI3K: insulin through the activation of insulin receptor substrate 1(IRS1) and leptin through the leptin receptor[14,15]. PI3K is considered the predominant activator of Akt[16], in fact, signaling through this pathway is often referred to as

the 'PI3K/Akt pathway'[16]. As previously mentioned, IL-1β secretion leads to the phosphorylation (activation) of Akt[1]. Although we were interested in the effects of IL-1β in particular, it has also been demonstrated that other pro-inflammatory cytokines can activate Akt[17]. As such, it is difficult to distinguish the effects of IL-1 signaling independent of its' effect on insulin and leptin signaling on our primary endpoints. Nevertheless, the significant degree of cross-talk between IL-1 signaling and these mitogenic pathways further validates the importance of IL-1 signaling in obesity-promoted CRC.

It is feasible that one of the methodologies we used in our IL-1 signaling study may have introduced artifacts. Our protocol for the isolation of colonocytes requires the calcium chelator, EDTA, which is a commonly used technique to isolate particular cell types from intact tissues[18]. However, particularly in colon cancer cell lines, EDTA can alter protein expression and signaling pathways relevant for colonic carcinogenesis such as cell death and oxidative stress[18]. We did attempt to minimize any potential effects of EDTA on our molecular endpoints of interest by conducting the entire protocol at 4˚C in order to arrest metabolism and thereby limit any additional alterations to the inflammatory or molecular programming of the cell due to EDTA treatment.

Lastly, we were compelled to use indirect markers of Akt and NFκB activation as we were unable to detect levels of more direct indicators of activation: phospho-Akt and phospho-p65, even though we had added phosphatase inhibitors to our preparations. Previous investigators have also found it difficult to assay phosphorylated proteins in these pathways in samples derived from *in vivo* experiments (as opposed to measuring them in cell culture experiments), and like myself, found it necessary to use these surrogates to evaluate Akt and

NFκB activation as well[19,20]. Thus, our indirect measures of these pathways may not have been sensitive enough to detect differences in activation.

Specific Aim 3

The study design of the diet- versus genetically-induced obesity experiment utilized a mouse model of colorectal cancer which developed tumors in the small intestine. Although Apc^{1638N} mice are commonly used to study colon cancer, ultimately tumors develop in the small bowel—a limitation common to most genetically-engineered murine models of colon cancer[21]. However, they do develop microscopic precursors of adenomas in the colon such as aberrant crypt foci (ACF), which develop in parallel with the small intestinal neoplasms[22], thereby demonstrating that similar, if not identical, forces are operating in the colon. We did not access ACF in the colons of these mice as it has been previously shown that obesity elevates ACF in the colons of rodents[23] and furthermore, the colon was reserved for the transcriptome analysis. Further, in prior studies by us[22] and others[24] it has been shown that dietary modifications known to alter human CRC risk similarly alter small intestinal tumorigenesis in the Apc1638N mouse, underscoring the clinical relevance of this model.

Colonic mucosal scrapings are a heterogeneous mixture of cells from the epithelium, muscularis mucosa, and lamina propria as opposed to a single isolated cell type. As such, it was difficult to attribute molecular changes observed in the colonic mucosa to an isolated cell type. We did address this issue, in part, in our IL1RKO study [specific aim #2] by comparing results from scraped mucosa and isolated colonocytes but this issue was not of sufficient priority in the cancer cluster study to warrant separate preparations. As such, we cannot attribute the transcriptional changes observed in our RNA-sequencing analysis to a particular cell type.

Furthermore, there is limited information available about the transcriptional impact of obesity on isolated cell types in the mouse colon to provide additional insight regarding which cells are responsible for the observed transcriptional changes.

Additionally, we did not observe a difference in pro-inflammatory cytokine production in these animals in either the colonic or small intestinal mucosa. We speculate that the difference in Apc1638N background of these animals may have attenuated any obesity-induced elevation in cytokine production. Indeed, a previous study in Apc1638N mice found that they also had a suppressed inflammatory response compared to control animals[25]. The authors suggest that the mechanism responsible for this observation relates to the interaction between β-catenin and E-cadherin – which has been associated with immune function[25].

Lastly, this study included males and females due to the difficulty of breeding sufficient animals with aberrant alleles at two separate loci over the course of a practical timeframe. Male and female mice are known to respond differently to high-fat feeding: females are more resistant to diet-induced obesity[26]. Indeed, females in our study in the high-fat diet group achieved more moderate degrees of obesity compared to males in the same group. However, ultimately due to the small sample size, we were unable to stratify our analyses by gender.

IX. Concluding Remarks

I believe that my thesis work has contributed several critical pieces of information towards understanding the mechanism(s) involved in mediating the relationship between obesity and elevated colon cancer risk. Despite some limitations of my studies, I have provided convincing evidence that obesity in fact induces inflammation in the colon and that select inflammatory cytokines may be responsible for alterations in cell signaling pathways thereby promoting cancer

risk in the colon. Aside from contributing to our mechanistic understanding of this cancer risk factor, I am particularly excited about the possibility of using my thesis work to develop means to attenuate the burden of obesity-promoted cancer.

References

1. Kaler P, Godasi BN, Augenlicht L, Klampfer L. The NF-kappaB/AKT-dependent Induction of Wnt Signaling in Colon Cancer Cells by Macrophages and IL-1beta. *Cancer Microenviron*. 2009. doi:10.1007/s12307-009-0030-y.

2. Calle EE, Rodriguez C, Walker-Thurmond K, Thun MJ. Overweight, obesity, and mortality from cancer in a prospectively studied cohort of U.S. adults. *N Engl J Med*. 2003;348(17):1625-1638. doi:10.1056/NEJMoa021423.

3. Taketo MM. Shutting down Wnt signal-activated cancer. *Nat Genet*. 2004;36(4):320-322. doi:10.1038/ng0404-320.

4. de Lau W, Barker N, Clevers H. WNT signaling in the normal intestine and colorectal cancer. *Front Biosci*. 2007;12:471-491. doi:2076 [pii].

5. Alberts B, Johnson A, Lewis J, Raff M, Roberts K, Walter P. Isolating Cells and Growing Them in Culture. 2002. http://www.ncbi.nlm.nih.gov/books/NBK26851/. Accessed February 20, 2016.

6. Basu S, Campbell HM, Dittel BN, Ray A. Purification of specific cell population by fluorescence activated cell sorting (FACS). *J Vis Exp*. 2010;(41). doi:10.3791/1546.

7. Lumeng CN, Bodzin JL, Saltiel AR. Obesity induces a phenotypic switch in adipose tissue macrophage polarization. *J Clin Invest*. 2007;117(1):175-184. doi:10.1172/JCI29881.

8. Platt AM, Bain CC, Bordon Y, Sester DP, Mowat AM. An independent subset of TLR expressing CCR2-dependent macrophages promotes colonic inflammation. *J Immunol*. 2010;184(12):6843-6854. doi:10.4049/jimmunol.0903987.

9. Popivanova BK, Kitamura K, Wu Y, et al. Blocking TNF-alpha in mice reduces colorectal carcinogenesis associated with chronic colitis. *J Clin Invest*. 2008;118(2):560-570. doi:10.1172/JCI32453.

10. Kelley-Hedgepeth A, Lloyd-Jones DM, Colvin A, et al. Ethnic differences in C-reactive protein concentrations. *Clin Chem*. 2008;54(6):1027-1037. doi:10.1373/clinchem.2007.098996.

11. Khera A, McGuire DK, Murphy SA, et al. Race and gender differences in C-reactive protein levels. *J Am Coll Cardiol*. 2005;46(3):464-469. doi:10.1016/j.jacc.2005.04.051.

12. Carroll JF, Fulda KG, Chiapa AL, et al. Impact of race/ethnicity on the relationship between visceral fat and inflammatory biomarkers. *Obesity (Silver Spring)*. 2009;17(7):1420-1427. doi:10.1038/oby.2008.657.

13. Jarry a, Vallette G, Cassagnau E, et al. Interleukin 1 and interleukin 1beta converting enzyme (caspase 1) expression in the human colonic epithelial barrier. Caspase 1 downregulation in colon

cancer. *Gut*. 1999;45(caspase 1):246-251. doi:10.1136/gut.45.2.246.

14. Xu AW, Kaelin CB, Takeda K, Akira S, Schwartz MW, Barsh GS. PI3K integrates the action of insulin and leptin on hypothalamic neurons. *J Clin Invest*. 2005;115(4):951-958. doi:10.1172/JCI200524301.

15. Maya-Monteiro CM, Bozza PT. Leptin and mTOR: Partners in metabolism and inflammation. *Cell Cycle*. 2008;7(12):1713-1717. doi:10.4161/cc.7.12.6157.

16. Fresno Vara JA, Casado E, de Castro J, Cejas P, Belda-Iniesta C, González-Barón M. PI3K/Akt signalling pathway and cancer. *Cancer Treat Rev*. 2004;30(2):193-204. doi:10.1016/j.ctrv.2003.07.007.

17. O'toole A, Moule SK, Lockyer PJ, Halestrap AP. Tumour necrosis factor-alpha activation of protein kinase B in WEHI-164 cells is accompanied by increased phosphorylation of Ser473, but not Thr308. *Biochem J*. 2001;359(Pt 1):119-127. http://www.pubmedcentral.nih.gov/articlerender.fcgi?artid=1222127&tool=pmcentrez&rendertype=abstract. Accessed February 22, 2016.

18. Pajak B, Orzechowski A. Ethylenediaminetetraacetic acid affects subcellular expression of clusterin protein in human colon adenocarcinoma COLO 205 cell line. *Anticancer Drugs*. 2007;18(1):55-63. doi:10.1097/CAD.0b013e32800fee9e.

19. Wehenkel M, Ban J-O, Ho Y-K, Carmony KC, Hong JT, Kim KB. A selective inhibitor of the immunoproteasome subunit LMP2 induces apoptosis in PC-3 cells and suppresses tumour growth in nude mice. *Br J Cancer*. 2012;107(1):53-62. doi:10.1038/bjc.2012.243.

20. Zhao S, Fu J, Liu F, Rastogi R, Zhang J, Zhao Y. Small interfering RNA directed against CTMP reduces acute traumatic brain injury in a mouse model by activating Akt. *Neurol Res*. 2014;36(5):483-490. doi:10.1179/1743132814Y.0000000353.

21. Karim BO, Huso DL. Mouse models for colorectal cancer. *Am J Cancer Res*. 2013;3(3):240-250. doi:10.1038/sj.onc.1203036.

22. Liu Z, Ciappio ED, Crott JW, et al. Combined inadequacies of multiple B vitamins amplify colonic Wnt signaling and promote intestinal tumorigenesis in BAT-LacZxApc1638N mice. *FASEB J*. 2011;25(9):3136-3145. doi:10.1096/fj.11-184143.

23. Weber R V, Stein DE, Scholes J, Kral JG. Obesity potentiates AOM-induced colon cancer. *Dig Dis Sci*. 2000;45(5):890-895. http://www.ncbi.nlm.nih.gov/pubmed/10795750. Accessed February 22, 2016.

24. Yang WC, Mathew J, Velcich A, et al. Targeted Inactivation of the p21WAF1/cip1 Gene Enhances Apc-initiated Tumor Formation and the Tumor-promoting Activity of a Western-Style High-Risk Diet by Altering Cell Maturation in the Intestinal Mucosa. *Cancer Res*. 2001;61(2):565-569. http://cancerres.aacrjournals.org/content/61/2/565.long. Accessed February 22, 2016.

25. Fox JG, Dangler CA, Whary MT, Edelman W, Kucherlapati R, Wang TC. Mice carrying a truncated ABC gene have diminished gastric epithelial proliferation, gastric inflammation, and humoral immunity in response to Helicobacter felis infection. *Cancer Res*. 1997;57(18):3972-3978.

http://www.embase.com/search/results?subaction=viewrecord&from=export&id=L27427685\nhttp://sfx.library.uu.nl/utrecht?sid=EMBASE&issn=00085472&id=doi:&atitle=Mice+carrying+a+truncated+ABC+gene+have+diminished+gastric+epithelial+proliferation,+gastric+infla.

26. Gallou-Kabani C, Vigé A, Gross M-S, et al. C57BL/6J and A/J mice fed a high-fat diet delineate components of metabolic syndrome. *Obesity (Silver Spring)*. 2007;15(8):1996-2005. doi:10.1038/oby.2007.238.

X. Laboratory methods

A. Plasma cytokines

Protocol

1. Spin blood at 1,000g for 10 min. at 4°C.
2. Take off top layer (plasma) and put into a microfuge tube. Store at -80°C until ready for use.
3. Thaw samples on ice
4. Add 50 µl of sample to each well in 96-well multi-plex assay plate (Meso Scale, S600, Rockville, MD)
5. Incubate sample 2 hours at room temperature (RT)
6. Wash with 100 µl wash buffer 3x
7. Incubate sample with 50 µl primary antibody
8. Wash with 100 µl wash buffer 3x
9. Incubate sample with detection antibody
10. Wash with 100 µl wash buffer 3x
11. Add 50 µl read buffer and read plate on MSD instrument
12. Calculate concentrations of cytokines
13. Calculate coefficient of variation (CV) for each analyte: standard deviation of each cytokine/ mean concentration of cytokine – CVs were ≤ 6% for each analyte in humans.

B. Plasma insulin and leptin

Protocol

1. Spin blood at 1,000g for 10 min. at 4°C.
2. Take off top layer (plasma) and put into a microfuge tube. Store at -80°C until ready for use.
3. Thaw samples on ice
4. Add 50 µl of sample to each well in 96-well duplex assay for insulin and leptin (Meso Scale, S600, Rockville, MD)
5. Incubate sample 2 hours at room temperature (RT)
6. Wash with 100 µl wash buffer 3x
7. Incubate sample with 50 µl primary antibody
8. Wash with 100 µl wash buffer 3x
9. Incubate sample with detection antibody

10. Wash with 100 µl wash buffer 3x
11. Add 50 µl read buffer and read plate on MSD instrument
12. Calculate concentrations of insulin/leptin
13. Calculate coefficient of variation (CV) for each analyte: standard deviation of each analyte/ mean concentration of analyte – CVs were ≤ 5% for each analyte in both humans and mice.

C. Colonic Cytokines (*ex vivo*, *lysates*)

Protocol

Ex Vivo

1. Incubate freshly collected colonic biopsy in 200 µl cell culture medium (Dulbecco's Modified Eagle Medium with 1% Glutamine and .1% Anti-biotic, Anti-mycotic cocktail)
2. Incubate at 37˚C with 5% $C0^2$ for 24 hours
3. Collect supernatant and freeze at -80 ˚C until later use.
4. Thaw supernatant on ice.
5. Add 50 µl of sample to each well in 96-well multi-plex assay plate (Meso Scale, S600, Rockville, MD)
6. Incubate sample 2 hours at room temperature (RT)
7. Wash with 100 µl wash buffer 3x
8. Incubate sample with 50 µl primary antibody
9. Wash with 100 µl wash buffer 3x
10. Incubate sample with detection antibody
11. Wash with 100 µl wash buffer 3x
12. Add 50 µl read buffer and read plate on MSD instrument
13. Calculate concentrations of cytokines by adjusting for total protein: picogram of cytokine/milligram of protein
14. Calculate coefficient of variation (CV) for each analyte: standard deviation of each cytokine/ mean concentration of cytokine – CVs were ≤ 8% for each analyte in both humans and mice.

Tissue lysates

15. Add a single colonic biopsy to 200 uL chilled RIPA.
16. Homogenize on ice.
17. Centrifuge at around 15,000 g for 20 min at 4°C.
18. Remove and keep the supernatant.
19. Determine the protein concentration (Bradford assay).
20. Add 50 µl of sample to each well in 96-well multi-plex assay plate (Meso Scale, S600, Rockville, MD)
21. Incubate sample 2 hours at room temperature (RT)
22. Wash with 100 µl wash buffer 3x
23. Incubate sample with 50 µl primary antibody
24. Wash with 100 µl wash buffer 3x
25. Incubate sample with detection antibody

26. Wash with 100 µl wash buffer 3x
27. Add 50 µl read buffer and read plate on MSD instrument
28. Adjust cytokine concentration for milligram of protein.

D. Isolation of RNA from colon and small intestine using Trizol

Materials

• Trizol Reagent
• Chloroform.
• Isopropyl alcohol (aka isopropanol, 2-propanol).
• Ethanol.
• RNase free water.
• Optional: RNase away to swab pipettes and workspace.

Protocol

1. Place liver samples in liquid nitrogen.
2. Add 700 uL Trizol to a microfuge tube for each sample.
3. Quickly remove sample from liquid nitrogen and cut a small piece (approx. 100 mg) with a scalpel and put into tube with Trizol, being careful not to defrost liver.
4. Mash liver with plastic pestle and then add 300 uL more Trizol.
5. Incubate at room temp for 5 min.
6. Add 200 uL chloroform, vortex and let sit at room temp for 5-10 min.
7. Spin at 12,000 g for 10 min at 4°C.
8. Remove upper aqueous layer containing RNA into a new conical tube. Interface contains DNA while lower layer contains protein. These can be extracted from the same preparation (see product insert).
9. Add 0.5 volumes isopropanol and mix by inversion to precipitate RNA. Sit at room temp for 10 min.
10. Spin at 12,000 g for 10 min at 4°C.
11. Decant supernatant and wash RNA pellet with 1 volume 75% ethanol.
12. Spin at 12,000 g for 10 min at 4°C.
13. Decant supernatant and stand tubes upside down on tissue paper to drain for 10 min.
14. Stand tubes to air dry at room temp or use speed-vac.
15. Resuspend RNA in 100 µl RNase free water.
16. Incubate at 60°C for 10 min to dissolve and store at -80°C until ready to use.
17. Run on an electrophoresis gel (1.8% agarose in TAE/TBE buffer with ethidium bromide) to confirm RNA quality. Load 5 uL sample (with 10% loading buffer) and run for 30 min. at 100V. Upon UV visualization, there should be 2 distinct bands representing the 2 ribosomal subunits.
18. Quantify RNA by adding 98 uL of ddH2O + 2 uL of sample, including a blank, to each well of a 96-well plate, in duplicate. Mix by pipetting and read plate at 260 and 280 nm.

Concentration(ng/uL)= (260 corrected abs.)x50x40.
260/280 ratio indicates purity and should be in the range 1.7-2.

E. Isolation of colonocytes

1. Remove colon from mouse and keep on ice.

2. Flush contents of colon with PBS with protease and phosphatase inhibitors (Roche, Indianapolis, IN)
3. Cut entire colon longitudinally and place in chilled colon isolation buffer (PBS +30mM EDTA) in 100mm cell culture dish
4. Incubate cell culture dish at 4°C on shaker for 20 minutes
5. Remove colon tissue and collect all cell culture media in 5ml conical tube.
6. Centrifuge supernatant at 1,000g for 15 min. at 4°C.
7. Aspirate supernatant to leave remaining cell pellet and freeze at -80°C until later use.

F. Western blot of colonic proteins (CTMP and IκBα)

Materials

- Lysis buffer (RIPA buffer, Sigma R0278):
  - 150 mM NaCl
  - 50 mM Tris-Cl, pH 8.0
  - 50 mM EDTA, pH 8
  - 1.0% Igepal CA-630 (NP-40)
  - 0.5% Sodium Deoxycholate
  - 0.1% Sodium Dodecyl Sulfate (SDS)

Just before using, add freshly:

-Add 1mM PMSF (Phenylmethylsulphonylfluoride, Sigma, 78830. Usually 10 mL of 100 mM PMSF in isopropanol to 1 L buffer to make the final concentration of PMSF as 1mM).

-Add proteinase inhibitor cocktail (Sigma, P8340, including aprotinin and leupeptin, adding about 1 uL per 20 mg bovine liver).

- 2x sample buffer (Loading buffer,Sigma S3401):
  - 125 mM Tris-Cl, pH approx. 6.8
  - 20% (v/v) Glycerol
  - 4.0% (w/v) SDS (Sodium Dodecyl Sulphate)
  - 0.004% Bromophenol blue
  - 10% 2-mercaptoethanol
  - Store at -20°C
- *Alternatively, 3x sample buffer recipe of Bio-Rad:*
  - Deionized water 3.55 mL
  - 0.5 M Tris-HCl, pH 6.8 1.25 mL
  - Glycerol 2.5 mL
  - 10% (w/v) SDS 2.0 mL
  - 0.5 % (w/v) bromophenol blue 0.2 mL
  - Store at room temperature. Immediately before using, add 50 uL β-mercaptoethanol to 950 uL sample buffer. Dilute the sample at least 1:2 with sample buffer.
- 10x running buffer (Biorad, 161-0772): 1L
  - 30.3 g Trizma base (= 0.25 M)
  - 144 g Glycine (= 1.92 M)
  - 10 g SDS(1%), add last

    - Dissolve and bring total volume to 1000 mL with dionized water. Do not adjust pH with acid or base. Store at 4°C. If precipitation occurs, warm to room temperature before use. Dilute 10 times with deionized water before use.
- 10x transfer buffer (Biorad, 161-0771): 1 L
    - 30.3 g Trizma base (= 0.25 M)
    - 144 g Glycine (= 1.92 M)
    - pH should be 8.3, do not adjust
    - *Before use, make 2 L of 1x Blotting buffer with methanol added:*
    - 400 mL Methanol
    - 200 mL 10x Blotting buffer
    - 1400 mL water
- Blocking buffer:
    - 3 % powder dry milk in 1X PBS with 0.1% Tween-20 (Sigma, p 5927).
- Washing buffer (PBST):
    - 1X PBS+0.1% Tween20
- Other chemicals:
    - 30% acrylamide/bisacrylamide (29:1 mix), (Bio-Rad)
    - TEMED, N,N,N′,N′-Tetramethylethylenediamine (Sigma, 87689)
    - Ammonium persulfate
    - Kaleidoscope prestained standards (bio-rad, 161-0375)
    - Amersham ECL kit (RPN 2106)

Protocol

<u>Preparation of whole cell lysates</u>

29. Add 200 uL RIPA buffer to isolated colonocytes.
30. Homogenize on ice.
31. Centrifuge at around 15,000 g for 20 min at 4°C.
32. Remove and keep the supernatant.
33. Determine the protein concentration (Bradford assay).
34. Mix 20 uL protein sample with 20 uL 2x sample buffer in PCR tubes and heat-denature at 95°C for 3 min.
35. Aliquot and store at -80°C.

<u>Running the gel</u>

1. Place Criterion precast gel (BioRad) in gel rig and immerse in running buffer.
2. Prior to running the gel, flush the wells out thoroughly with running buffer.
3. After flash spinning the samples, load 60 ug into the wells.
4. Be sure to use markers. *We use 15 µl Bio-Rad Kaleidoscope Prestained Standards #161-0324 directly.*
5. Run with constant current (35 - 37 mA with voltage set at 100 V) for approx. 2 hrs at RT.

<u>Preparation of membrane and transferring the membrane</u>

1. Cut a piece of PVDF membrane which is the same size as the gel (Biorad, 162-0116).
2. Cut bottom right corner and soak in methanol for 3 seconds, then in water or transfer buffer for about 5 min. until it sinks when pressed down carefully. Do not let it try.

3. Wet sponge, filter paper, membrane for about 30 min in transfer buffer at RT.
4. Assemble "sandwich" for Bio-Rad's Transblot:

Sponge - filter paper - gel - membrane - filter paper - sponge

5. For the Mini-Transblot, transfer with prechilled transfer buffer for 1.5 hrs at 90 V at 4°C on a stir plate with an ice pack.
6. Wash with PBST 2 x 10 min (always put membrane protein side up- side that was in contact with gel).
7. When finished, immerse membrane in blocking buffer and block 1 hr or overnight.

Antibody incubation and detection

1. Wash membrane 3 times for 5 min in washing buffer (*or using the alternative washing process, this step is optional*).
2. Incubate with primary antibody diluted in blocking buffer (1:1000 for protein) overnight at 4°C.
3. Wash 3 x 10 min with washing buffer (*or using the alternative washing process*).
4. Incubate with secondary antibody diluted in blocking buffer (1:2,000) for 1 hr at RT.
5. Turn on developing machine in dark room.
6. Wash 3 x 10 min with washing buffer (*or using the alternative washing process*).
7. Detect with Amersham ECL kit. Mix 750 uL of each reagent in a microfuge and pipet over membrane several times to coat thoroughly. Let sit approx. 5 min.
8. Develop film in dark room.
9. Wash 3 x 10 min with washing buffer (or using the alternative washing process), and keep the membrane in PBS+0.1% Tween20 solution at 4°C.
10. If protein sizes are different, stripping the membrane is not necessary. Incubate with GAPDH primary Ab (1:2000 1 hr at RT), wash, and then secondary Ab (1:10,000 1 hr at RT), etc.

G. Immunohistochemistry for intra-nuclear β-catenin and ki-67

1. Deparaffinize and hydrate slides through the following solutions:
2. Quench endogenous peroxidase by placing slides in 3% hydrogen peroxide for 15 mins. Perform Heat Induced Epitope Retrieval using steamer.
    a. **Prepare steamer.** Fill rice steamer (Black & Decker) with distilled water. Turn on the steamer and set the timer about 20 minutes. Cover and bring to a boil.
    b. **Pre- heat citrate buffer.** Heat a coplin jar filled with citrate buffer (10 mM) in a microwave for about 3 minutes. Buffer should be hot but not boiling.
    c. Transfer slides to be retrieved into coplin with hot citrate buffer. Place Coplin into boiling steamer. DO NOT cover soplin jar with a lid, but DO cover steamer with its lid to trap in the steam. **Steam slides for 20 minutes**. Cool for 45 mins.
3. Place the slide in a coplin jar with dd H_2O, and thenplace the slides in the cassette and fill 2 times with dd H_2O.
4. Prepare blocking solution (Normal Horse Serum + AVIDIN): 3 drop (150 ul) of stock serum (Normal Horse Serum) + 2.5 ml PBS + 10 drops of Avidin (500 ul)=3.15 ml for 20 slides. (*Serum for blocking nonspecific receptors which may combine 1st Ab, and avidin for blocking the tissue avidin receptors which may combine avidin-hrp in the labeling*

antibody. The normal blocking serum is prepared from species in which second antibody is made.)

5. Add 2-3 drops blocking solution per sample (100-150 ul).Block 1 h in humidified chamber at RT, or 2 hr in cold room (4°C).
6. Apply primary antibody:
7. Prepare primary antibody at 1:500 dilution (ki-67) and 1:1,000 (β-catenin)
8. Add 4 drops of BIOTIN for every ml.
9. Dispense 100-150 ul per slide, and incubate for 1 hr in humidified chamber at 37 C, 2 hr at RT, or overnight in cold room.
10. Rinse slides 5 times (PBS-T, PBS-T, PBS, PBS, PBS).
11. Apply secondary antibody
    a. Get secondary antibody from Vectastain Kit.
    b. Prepare secondary antibody. Add 3 drops (150 ul) of serum stock (yellow label) to 5 ml PBS buffer in mixing bottle, and then add one drop (50 ul) of biotynilated antibody stock. (*Can be stored 1 week*).
12. Use 100-150 ul per slide, and incubate slides for 20 mins.
13. Rinse slides 5 times (PBS-T, PBS-T, PBS, PBS, PBS).
14. Apply labeled antibody (*Identify the secondary antibody. The labed antibody is conjugated with enzyme):*
    a. Get label antibody from Vectastain Kit (**ABC reagent**).
    b. Add 2 drops of reagent A (Gray label) to 2.5 ml of PBS buffer in the ABC reagent large mixing bottle, mix immediately, and add 2 drops of reagent B and mix well (Vortex), allow the ABC reagent to stand for 5-30 mins before use. (*Prepare daily*).
15. Apply label antibody 100-150 ul per slide, and incubate for 10' at RT.
16. Rinse slides 5 times (PBS-T, PBS-T, PBS, PBS, PBS).
17. Apply Vector DAB Chromagen for 1 mins (*react with the enzyme conjugated on the labeled antibody*):
18. Prepare DAB solution: In 2.5 ml of dd H_2O, add 1 drop buffer solution, 2 drops of DAB and mix well. Then 1 drop of H_2O_2, and mix well. (*Unused working DAB solution is stable for up to 2 weeks if stored at 2-8 C. If precipitate forms, mix well before using.*)
19. Apply DAB solution 100-150 ul per slide, and incubate for 1 min at RT.
20. Rinse with water.
21. Counter stain with Modified Harris Hematoxylin for 30 sec. Transfer slides from cassettes into coplin jar. Rinse with tap water until water is clear.
22. Place slides in automation buffer for 1 mins with gentle agitation to blue slides.
23. Dehydrate through the following solutions.
24. Cover slip with permount.

XI. Appendices

Manuscript I

Table S1.

No.	Gene ID	Entrez Gene Name	log2FC	p-adj
1	SBF1P1	SET binding factor 1 pseudogene 1	2.17	0.056
2	CELF3	CUGBP, Elav-like family member 3	2.13	0.011
3	TAC1	tachykinin, precursor 1	2.12	0.030
4	ASCL2	achaete-scute family bHLH transcription factor 2	2.07	0.002
5	LOC644990	uncharacterized LOC644990	2.02	0.080
6	CYP2W1	cytochrome P450, family 2, subfamily W, polypeptide 1	2.00	0.002
7	CYR61	cysteine-rich, angiogenic inducer, 61	1.83	0.073
8	SLC16A11	solute carrier family 16, member 1	1.82	0.015
9	EPHB3	EPH receptor B3	1.79	0.019
10	NMU	neuromedin U	1.77	0.009
11	NR4A2	nuclear receptor subfamily 4, group A, member 2	1.76	0.086
12	CDT1	chromatin licensing and DNA replication factor 1	1.70	0.032
13	DGAT2	diacylglycerol O-acyltransferase 2	1.68	0.003
14	CHGA	chromogranin A (parathyroid secretory protein 1)	1.68	0.086
15	DES	desmin	1.65	0.093
16	CAMK2B	calcium/calmodulin-dependent protein kinase II beta	1.61	0.063
17	ANKRD18A	ankyrin repeat domain 18A	1.60	0.044
18	C19orf45	chromosome 19 open reading frame 45	1.59	0.083
19	MT3	metallothionein 3	1.59	0.101
20	MYL9	myosin, light chain 9, regulatory	1.59	0.086
21	ALDH1B1	aldehyde dehydrogenase 1 family, member B1	1.59	0.002
22	TERT	telomerase reverse transcriptase	1.56	0.037
23	CCDC85B	coiled-coil domain containing 85B	1.55	0.086
24	SMTN	smoothelin	1.50	0.024
25	CLDN5	claudin 5	1.49	0.062
26	RIMBP2	RIMS binding protein 2	1.49	0.055
27	MSI1	musashi RNA-binding protein 1	1.48	0.077
28	MZT2A	mitotic spindle organizing protein 2A	1.46	0.080
29	NRAP	nebulin-related anchoring protein	1.46	0.072
30	KANK4	KN motif and ankyrin repeat domains 4	1.44	0.011
31	ROBO3	roundabout, axon guidance receptor, homolog 3 (Drosophila)	1.43	0.020
32	IGFBP6	insulin-like growth factor binding protein 6	1.40	0.043
33	ATAD3A	ATPase family, AAA domain containing 3A	1.36	0.059
34	SYN1	synapsin I	1.35	0.098
35	C19orf48	chromosome 19 open reading frame 48	1.34	0.035

36	CELF5	CUGBP, Elav-like family member 5	1.32	0.009
37	RARRES2	retinoic acid receptor responder (tazarotene induced) 2	1.32	0.090
38	SELM	selenoprotein M	1.29	0.089
39	LRP3	low density lipoprotein receptor-related protein 3	1.28	0.059
40	B9D1	B9 protein domain 1	1.28	0.013
41	SPTBN2	spectrin, beta, non-erythrocytic 2	1.26	0.011
42	TEAD4	TEA domain family member 4	1.26	0.083
43	RGMB	repulsive guidance molecule family member b	1.25	0.043
44	RECQL4	RecQ protein-like 4	1.25	0.069
45	NPM3	nucleophosmin/nucleoplasmin 3	1.25	0.078
46	ZNF593	zinc finger protein 593	1.23	0.086
47	POLD2	polymerase (DNA directed), delta 2, accessory subunit	1.23	0.016
48	BCL7C	B-cell CLL/lymphoma 7C	1.22	0.059
49	SLC12A8	solute carrier family 12, member 8	1.19	0.073
50	LRRC45	leucine rich repeat containing 45	1.18	0.086
51	SMOC2	SPARC related modular calcium binding 2	1.18	0.073
52	KIAA1324	KIAA1324	1.17	0.073
53	SCNN1D	sodium channel, non-voltage-gated 1, delta subunit	1.17	0.059
54	BOP1	block of proliferation 1	1.17	0.059
55	MZB1	marginal zone B and B1 cell-specific protein	1.16	0.085
56	LOC100130705	uncharacterized LOC100130705	1.14	0.003
57	SOX4	SRY (sex determining region Y)-box 4	1.13	0.073
58	KHK	ketohexokinase (fructokinase)	1.12	0.075
59	C20orf27	chromosome 20 open reading frame 27	1.12	0.059
60	RAD51	RAD51 recombinase	1.11	0.074
61	WDR18	WD repeat domain 18	1.11	0.077
62	SLC12A2	solute carrier family 12 (sodium/potassium/chloride transporter), member 2	1.10	0.074
63	EPHB4	EPH receptor B4	1.10	0.003
64	SKA1	spindle and kinetochore associated complex subunit 1	1.08	0.086
65	PSRC1	proline/serine-rich coiled-coil 1	1.08	0.086
66	NOC4L	nucleolar complex associated 4 homolog (S. cerevisiae)	1.06	0.088
67	HAUS7	HAUS augmin-like complex, subunit 7	1.05	0.080
68	TMEM201	transmembrane protein 201	1.05	0.043
69	WDR24	WD repeat domain 24	1.04	0.080
70	ZNRF3	zinc and ring finger 3	1.00	0.032
71	SLC43A1	solute carrier family 43 (amino acid system L transporter), member 1	1.00	0.074
72	SFXN2	sideroflexin 2	0.99	0.079
73	POLD1	polymerase (DNA directed), delta 1, catalytic subunit	0.99	0.088
74	TXNRD2	thioredoxin reductase 2	0.97	0.086
75	JAG2	jagged 2	0.97	0.073

76	SNORA70	small nucleolar RNA, H/ACA box 70	0.97	0.079
77	FBL	fibrillarin	0.96	0.066
78	THAP7	THAP domain containing 7	0.94	0.074
79	FGGY	FGGY carbohydrate kinase domain containing	0.93	0.027
80	NFIX	nuclear factor I/X (CCAAT-binding transcription factor)	0.90	0.096
81	ZNF662	zinc finger protein 662	0.90	0.043
82	HMBS	hydroxymethylbilane synthase	0.89	0.086
83	IMPDH2	IMP (inosine 5'-monophosphate) dehydrogenase 2	0.87	0.059
84	MRTO4	mRNA turnover 4 homolog (S. cerevisiae)	0.87	0.099
85	ANKRD36B	ankyrin repeat domain 36B	0.86	0.059
86	CHEK1	checkpoint kinase 1	0.84	0.098
87	SARS2	seryl-tRNA synthetase 2, mitochondrial	0.83	0.080
88	VARS	valyl-tRNA synthetase	0.82	0.098
89	BAIAP2	BAI1-associated protein 2	0.81	0.087
90	ERCC2	excision repair cross-complementation group 2	0.80	0.059
91	ERI3	ERI1 exoribonuclease family member 3	0.79	0.083
92	KDM1A	lysine (K)-specific demethylase 1A	0.76	0.088
93	LZTS2	leucine zipper, putative tumor suppressor 2	0.70	0.075
94	CAMKK1	calcium/calmodulin-dependent protein kinase kinase 1, alpha	0.68	0.079
95	ZMYND19	zinc finger, MYND-type containing 19	0.64	0.085
96	MLLT1	myeloid/lymphoid or mixed-lineage leukemia (trithorax homolog, Drosophila); translocated to, 1	0.61	0.048
97	RPTOR	regulatory associated protein of MTOR, complex 1	0.57	0.086
98	WARS2	tryptophanyl tRNA synthetase 2, mitochondrial	0.55	0.086
99	GTF2H4	general transcription factor IIH, polypeptide 4, 52kDa	0.53	0.080
100	TMEM167B	transmembrane protein 167B	-0.44	0.066
101	USP9X	ubiquitin specific peptidase 9, X-linked	-0.47	0.099
102	TMEM55B	transmembrane protein 55B	-0.47	0.086
103	OSTF1	osteoclast stimulating factor 1	-0.48	0.092
104	C10orf28	R3H domain and coiled-coil containing 1-like	-0.49	0.080
105	SIRT2	sirtuin 2	-0.49	0.073
106	TFE3	transcription factor binding to IGHM enhancer 3	-0.49	0.077
107	EIF1B	eukaryotic translation initiation factor 1B	-0.51	0.086
108	IFT52	intraflagellar transport 52	-0.54	0.059
109	PCGF5	polycomb group ring finger 5	-0.55	0.086
110	MGAT5	mannosyl (alpha-1,6-)-glycoprotein beta-1,6-N-acetyl-glucosaminyltransferase	-0.55	0.073
111	BFAR	bifunctional apoptosis regulator	-0.56	0.080
112	TRIM14	tripartite motif containing 14	-0.61	0.080
113	HECA	headcase homolog (Drosophila)	-0.61	0.055
114	TP53INP1	tumor protein p53 inducible nuclear protein 1	-0.61	0.074
115	TMEM30A	transmembrane protein 30A	-0.63	0.059

116	MFSD1	major facilitator superfamily domain containing 1	-0.63	0.020
117	ANKRD12	ankyrin repeat domain 12	-0.64	0.086
118	ZFYVE26	zinc finger, FYVE domain containing 26	-0.65	0.087
119	KIAA0494	EF-hand calcium binding domain 14	-0.65	0.098
120	SPTLC1	serine palmitoyltransferase, long chain base subunit 1	-0.66	0.086
121	CCNDBP1	cyclin D-type binding-protein 1	-0.67	0.059
122	OSTM1	osteopetrosis associated transmembrane protein 1	-0.68	0.098
123	CDR2	cerebellar degeneration-related protein 2, 62kDa	-0.68	0.086
124	BIRC2	baculoviral IAP repeat containing 2	-0.69	0.092
125	LEPROTL1	leptin receptor overlapping transcript-like 1	-0.69	0.086
126	ITM2B	integral membrane protein 2B	-0.70	0.086
127	C4orf34	small integral membrane protein 14	-0.72	0.076
128	C12orf5	TP53 induced glycolysis regulatory phosphatase	-0.72	0.077
129	FAM102A	family with sequence similarity 102, member A	-0.73	0.079
130	DDX60L	DEAD (Asp-Glu-Ala-Asp) box polypeptide 60-like	-0.75	0.073
131	GXYLT1	glucoside xylosyltransferase 1	-0.75	0.078
132	ARL6IP5	ADP-ribosylation factor-like 6 interacting protein 5	-0.76	0.059
133	TGOLN2	trans-golgi network protein 2	-0.76	0.080
134	CTSO	cathepsin O	-0.77	0.094
135	PROSC	proline synthetase co-transcribed homolog (bacterial)	-0.78	0.079
136	SNAP23	synaptosomal-associated protein, 23kDa	-0.79	0.020
137	SORL1	sortilin-related receptor, L(DLR class) A repeats containing	-0.79	0.080
138	CTBS	chitobiase, di-N-acetyl-	-0.80	0.059
139	TRIM21	tripartite motif containing 21	-0.83	0.059
140	GNA13	guanine nucleotide binding protein (G protein), alpha 13	-0.85	0.059
141	PSD3	pleckstrin and Sec7 domain containing 3	-0.88	0.096
142	TMEM2	transmembrane protein 2	-0.88	0.094
143	TMEM106B	transmembrane protein 106B	-0.88	0.077
144	IL6R	interleukin 6 receptor	-0.90	0.020
145	TRANK1	tetratricopeptide repeat and ankyrin repeat containing 1	-0.93	0.074
146	KIAA1737	CLOCK-interacting pacemaker	-0.93	0.080
147	NEDD9	neural precursor cell expressed, developmentally down-regulated 9	-0.93	0.073
148	YPEL2	yippee-like 2 (Drosophila)	-0.94	0.059
149	LMBRD1	LMBR1 domain containing 1	-0.94	0.031
150	SLC31A2	solute carrier family 31 (monocarboxylic acid transporter), member 1	-0.96	0.099
151	PUS10	pseudouridylate synthase 10	-0.97	0.048
152	LPIN2	lipin 2	-0.99	0.058
153	KIAA0247	KIAA0247	-1.00	0.080
154	PAG1	phosphoprotein membrane anchor with glycosphingolipid microdomains 1	-1.01	0.092
155	CD68	CD68 molecule	-1.01	0.073

156	NPC1	Niemann-Pick disease, type C1	-1.02	0.059
157	TAP2	transporter 2, ATP-binding cassette, sub-family B (MDR/TAP)	-1.02	0.002
158	RAB9A	RAB9A, member RAS oncogene family	-1.04	0.090
159	B2M	beta-2-microglobulin	-1.04	0.085
160	MYD88	myeloid differentiation primary response 88	-1.09	0.059
161	RP2	retinitis pigmentosa 2 (X-linked recessive)	-1.13	0.094
162	LOC729852	UBAP1-MVB12-associated (UMA) domain containing 1	-1.15	0.032
163	FGD6	FYVE, RhoGEF and PH domain containing 6	-1.17	0.079
164	CTSS	cathepsin S	-1.19	0.062
165	NCEH1	neutral cholesterol ester hydrolase 1	-1.29	0.043
166	NETO2	neuropilin (NRP) and tolloid (TLL)-like 2	-1.34	0.048
167	SLC40A1	solute carrier family 40 (iron-regulated transporter), member 1	-1.35	0.080
168	IFIT2	interferon-induced protein with tetratricopeptide repeats 2	-1.46	0.018
169	DDX60	DEAD (Asp-Glu-Ala-Asp) box polypeptide 60	-1.49	0.007
170	ACOT4	acyl-CoA thioesterase 4	-1.53	0.008
171	CTNND1	catenin (cadherin-associated protein), delta 1	-1.65	0.086
172	CYP4F2	cytochrome P450, family 4, subfamily F, polypeptide 2	-1.68	0.005
173	VNN1	vanin 1	-1.74	0.001
174	PTPLB	protein tyrosine phosphatase-like member b	-1.76	0.003
175	LOC158376	long intergenic non-protein coding RNA 961	-1.79	0.070
176	SEPP1	selenoprotein P, plasma, 1	-1.84	0.009
177	HSD3B2	hydroxy-delta-5-steroid dehydrogenase, 3 beta- and steroid delta-isomerase 2	-1.89	0.006
178	FER1L6	fer-1-like family member 6	-1.97	0.055
179	FLJ35424	long intergenic non-protein coding RNA 955	-2.00	0.083
180	EGFL6	EGF-like-domain, multiple 6	-2.02	0.006
181	UGT1A1	UDP glucuronosyltransferase 1 family, polypeptide A1	-2.12	0.040
182	FLJ42393	uncharacterized LOC401105	-2.17	0.055

Table S1. Differentially expressed genes in the colonic epithelium of obese compared to lean individuals. Differential expression was calculated using DESeq2*(75)* and significance was set at q<0.10. Gene ID, NCBI Entrez Gene ID; Log2FC, $\log_2$ fold change; p-adj, adjusted p-value; A negative (-) Log2FC indicates an upregulation in obese individuals and a (+) positive Log2FC indicates a downregulation in obese individuals.

Manuscript III

Supplementary Table 1.

No.	Log Ratio	ID	Entrez Gene Name	P-adj
1	-1.104	Clca6	chloride channel accessory 4	0.0002
2	-1.053	AI747448	chloride channel accessory 4	0.0002
3	-0.983	Anpep	alanyl (membrane) aminopeptidase	0.0002
4	-0.931	Slc11a2	solute carrier family 11, member 2	0.0003
5	-0.929	Npc1l1	NPC1-like 1	0.0003
6	-0.910	Creb3l3	cAMP responsive element binding protein 3-like 3	0.0005
7	-0.876	Bmp8b	bone morphogenetic protein 8b	0.0005
8	-0.874	Tgm7	transglutaminase 7	0.0005
9	-0.860	Slc6a19	solute carrier family 6 (neutral amino acid transporter)	0.0005
10	-0.847	Mpp6	membrane protein, palmitoylated 6	0.0005
11	-0.835	Rbp1	retinol binding protein 1, cellular	0.0008
12	-0.824	Mal	mal, T-cell differentiation protein	0.0009
13	-0.811	A730036I17Rik	RIKEN cDNA A730036I17 gene	0.0010
14	-0.797	Apoa1	apolipoprotein A-I	0.0014
15	-0.790	Slc26a1	solute carrier family 26 (anion exchanger), member 1	0.0015
16	-0.788	2010109I03Rik	RIKEN cDNA 2010109I03 gene	0.0015
17	-0.779	Gsdmc2	gasdermin C	0.0017
18	-0.778	Reg4	regenerating islet-derived family, member 4	0.0018
19	-0.777	Mpp1	membrane protein, palmitoylated 1, 55kDa	0.0019
20	-0.776	Mttp	microsomal triglyceride transfer protein	0.0023
21	-0.774	Ly6g6c	lymphocyte antigen 6 complex, locus G6C	0.0026
22	-0.771	Adh6a	alcohol dehydrogenase 6A (class V)	0.0027
23	-0.757	Stard5	StAR-related lipid transfer (START) domain containing 5	0.0027
24	-0.757	Vat1l	vesicle amine transport 1-like	0.0027
25	-0.752	Slc30a10	solute carrier family 30, member 10	0.0030
26	-0.748	Saa3	serum amyloid A 3	0.0038
27	-0.742	Svil	supervillin	0.0042
28	-0.738	Calb2	calbindin 2	0.0042
29	-0.733	Ccdc87	coiled-coil domain containing 87	0.0042
30	-0.731	Iqsec3	IQ motif and Sec7 domain 3	0.0049
31	-0.730	Papss2	3'-phosphoadenosine 5'-phosphosulfate synthase 2	0.0049
32	-0.723	Mcpt1	mast cell protease 1	0.0055
33	-0.709	Vav3	vav 3 guanine nucleotide exchange factor	0.0067
34	-0.706	9630028B13Rik	RIKEN cDNA 9630028B13 gene	0.0077
35	-0.693	9130221F21Rik	RIKEN cDNA 9130221F21 gene	0.0077
36	-0.689	Rnf152	ring finger protein 152	0.0085
37	-0.684	Ace2	angiotensin I converting enzyme 2	0.0086
38	-0.679	Plek2	pleckstrin 2	0.0100
39	-0.673	Krt20	keratin 20	0.0113
40	-0.671	Fam118a	family with sequence similarity 118, member A	0.0116
41	-0.670	Pls3	plastin 3	0.0116

42	-0.666	Tfrc	transferrin receptor	0.0118
43	-0.657	Slc39a4	solute carrier family 39 (zinc transporter), member 4	0.0119
44	-0.654	Fa2h	fatty acid 2-hydroxylase	0.0119
45	-0.632	Cast	calpastatin	0.0119
46	-0.632	Mettl7a1	methyltransferase like 7A	0.0119
47	-0.630	Pdlim2	PDZ and LIM domain 2 (mystique)	0.0121
48	-0.620	Me2	malic enzyme 2, NAD(+)-dependent, mitochondrial	0.0137
49	-0.600	Cyp2j6	cytochrome P450, family 2, subfamily J, polypeptide 2	0.0166
50	-0.595	Pls1	plastin 1	0.0176
51	-0.591	Lipa	lipase A, lysosomal acid, cholesterol esterase	0.0181
52	-0.590	Pfkl	phosphofructokinase, liver	0.0181
53	-0.573	Slc9a3r1	solute carrier family 9, subfamily A, member 3 regulator 1	0.0202
54	-0.540	Cyp3a13	cytochrome P450, family 3, subfamily A, polypeptide 7	0.0202
55	-0.533	Slc9a2	solute carrier family 9, subfamily A, member 2	0.0207
56	-0.530	Dsc2	desmocollin 2	0.0207
57	-0.520	Vil1	villin 1	0.0207
58	-0.517	Ptprh	protein tyrosine phosphatase, receptor type, H	0.0207
59	-0.515	Cdh17	cadherin 17, LI cadherin (liver-intestine)	0.0207
60	-0.511	Mtmr11	myotubularin related protein 11	0.0207
61	-0.504	Heph	hephaestin	0.0207
62	-0.494	Car9	carbonic anhydrase IX	0.0218
63	-0.485	Anks4b	ankyrin repeat and sterile alpha motif domain containing 4B	0.0222
64	-0.482	Xk	X-linked Kx blood group	0.0229
65	-0.480	Coro2a	coronin, actin binding protein, 2A	0.0232
66	-0.479	Sectm1b	secreted and transmembrane 1B	0.0232
67	-0.470	Tbc1d1	TBC1 (tre-2/USP6, BUB2, cdc16) domain family, member 1	0.0237
68	-0.467	Tmem150b	transmembrane protein 150B	0.0242
69	-0.463	Clrn3	clarin 3	0.0242
70	-0.463	Hsd17b7	hydroxysteroid (17-beta) dehydrogenase 7	0.0245
71	-0.459	Pgm1	phosphoglucomutase 2	0.0247
72	-0.459	Rxra	retinoid X receptor, alpha	0.0254
73	-0.456	Glt28d2	glycosyltransferase 28 domain containing 2	0.0254
74	-0.449	Coq10b	coenzyme Q10 homolog B (S. cerevisiae)	0.0258
75	-0.440	Tnfsf13b	tumor necrosis factor (ligand) superfamily, member 13b	0.0258
76	-0.427	Pld1	phospholipase D1, phosphatidylcholine-specific	0.0258
77	-0.416	Rgp1	RGP1 retrograde golgi transport homolog (S. cerevisiae)	0.0262
78	-0.405	Otud7b	OTU deubiquitinase 7B	0.0262
79	-0.404	Pacsin2	protein kinase C and casein kinase substrate in neurons 2	0.0262
80	-0.400	Pcyt1a	phosphate cytidylyltransferase 1, choline, alpha	0.0262
81	-0.386	Acad11	acyl-CoA dehydrogenase family, member 11	0.0269
82	-0.386	Sc5d	sterol-C5-desaturase	0.0272
83	-0.384	Ccdc68	coiled-coil domain containing 68	0.0276
84	-0.381	Aco2	aconitase 2, mitochondrial	0.0276
85	-0.376	Ankrd50	ankyrin repeat domain 50	0.0276
86	-0.367	Nab1	NGFI-A binding protein 1 (EGR1 binding protein 1)	0.0276
87	-0.357	Bak1	BCL2-antagonist/killer 1	0.0276

88	-0.346	Pex19	peroxisomal biogenesis factor 19	0.0276
89	-0.336	Stx3	syntaxin 3	0.0276
90	-0.333	Clcn2	chloride channel, voltage-sensitive 2	0.0288
91	-0.333	Osbpl10	oxysterol binding protein-like 10	0.0300
92	-0.324	Klc4	kinesin light chain 4	0.0300
93	-0.324	Ugcg	UDP-glucose ceramide glucosyltransferase	0.0312
94	-0.323	Aph1a	APH1A gamma secretase subunit	0.0312
95	-0.314	Ldha	lactate dehydrogenase A	0.0315
96	-0.310	Ctnnb1	catenin (cadherin-associated protein), beta 1, 88kDa	0.0315
97	-0.304	Arf6	ADP-ribosylation factor 6	0.0315
98	-0.298	Impa1	inositol(myo)-1(or 4)-monophosphatase 1	0.0315
99	-0.291	Arhgef5	Rho guanine nucleotide exchange factor (GEF) 5	0.0318
100	-0.291	Polr3c	polymerase (RNA) III (DNA directed) polypeptide C (62kD)	0.0318
101	-0.288	Psmb10	proteasome (prosome, macropain) subunit, beta type, 10	0.0323
102	-0.287	Tbk1	TANK-binding kinase 1	0.0323
103	-0.284	Psme2	proteasome (prosome, macropain) activator subunit 2 (PA28 beta)	0.0323
104	-0.273	Siah1a	siah E3 ubiquitin protein ligase 1	0.0323
105	-0.262	Ifrd1	interferon-related developmental regulator 1	0.0323
106	-0.253	Cap1	CAP, adenylate cyclase-associated protein 1 (yeast)	0.0323
107	-0.247	Cyb5r4	cytochrome b5 reductase 4	0.0327
108	-0.237	Cyb561d1	cytochrome b561 family, member D1	0.0328
109	-0.188	Vamp3	vesicle-associated membrane protein 3	0.0337
110	0.240	Srebf1	sterol regulatory element binding transcription factor 1	0.0346
111	0.292	Tcf3	transcription factor 3	0.0349
112	0.397	Ctsh	cathepsin H	0.0349
113	0.497	Mbd4	methyl-CpG binding domain protein 4	0.0350
114	0.502	Arhgap33	Rho GTPase activating protein 33	0.0351
115	0.506	Lpcat2	lysophosphatidylcholine acyltransferase 2	0.0354
116	0.541	Lsr	lipolysis stimulated lipoprotein receptor	0.0358
117	0.554	Apbb1ip	amyloid beta protein-binding, family B, member 1 protein	0.0358
118	0.571	Fabp5	fatty acid binding protein 5 (psoriasis-associated)	0.0358
119	0.590	Rgs14	regulator of G-protein signaling 14	0.0359
120	0.605	Hoxd11	homeobox D11	0.0359
121	0.633	Ptp4a3	protein tyrosine phosphatase type IVA, member 3	0.0381
122	0.651	Itgb7	integrin, beta 7	0.0382
123	0.652	Cnr2	cannabinoid receptor 2 (macrophage)	0.0382
124	0.653	Bin1	bridging integrator 1	0.0382
125	0.657	Tgfb1	transforming growth factor, beta 1	0.0382
126	0.669	Fermt3	fermitin family member 3	0.0382
127	0.687	Bach2	BTB and CNC homology 1, basic leucine zipper transcription factor 2	0.0382
128	0.692	Lat2	linker for activation of T cells family, member 2	0.0389
129	0.692	Lrmp	lymphoid-restricted membrane protein	0.0403
130	0.694	Fam65b	family with sequence similarity 65, member B	0.0403
131	0.698	Nkx2-2	NK2 homeobox 2	0.0403
132	0.707	Cd6	CD6 molecule	0.0403
133	0.710	Ms4a7	membrane-spanning 4-domains, subfamily A, member 7	0.0403

134	0.711	S1pr4	sphingosine-1-phosphate receptor 4	0.0403
135	0.712	Msln	mesothelin	0.0403
136	0.713	Slamf6	SLAM family member 6	0.0410
137	0.714	Arhgap4	Rho GTPase activating protein 4	0.0411
138	0.716	Pcsk1n	proprotein convertase subtilisin/kexin type 1 inhibitor	0.0439
139	0.717	Cd83	CD83 molecule	0.0451
140	0.719	Hoxd10	homeobox D10	0.0451
141	0.720	Rnase6	ribonuclease, RNase A family, k6	0.0451
142	0.721	Sp140	SP140 nuclear body protein	0.0451
143	0.725	Plxnc1	plexin C1	0.0457
144	0.726	Il22ra2	interleukin 22 receptor, alpha 2	0.0477
145	0.729	Traf3ip3	TRAF3 interacting protein 3	0.0480
146	0.731	BC013712	thymocyte selection associated family member 2	0.0484
147	0.735	Cybb	cytochrome b-245, beta polypeptide	0.0489
148	0.742	Lyz2	lysozyme	0.0491
149	0.743	Tlr9	toll-like receptor 9	0.0501
150	0.744	Hcls1	hematopoietic cell-specific Lyn substrate 1	0.0501
151	0.744	Parvg	parvin, gamma	0.0515
152	0.745	Evi2b	ecotropic viral integration site 2B	0.0515
153	0.747	Pla2g2d	phospholipase A2, group IID	0.0519
154	0.748	Rgs19	regulator of G-protein signaling 19	0.0519
155	0.749	Tspan32	tetraspanin 32	0.0519
156	0.750	Lyl1	lymphoblastic leukemia associated hematopoiesis regulator 1	0.0519
157	0.750	Samsn1	SAM domain, SH3 domain and nuclear localization signals 1	0.0521
158	0.754	42064	serine/threonine protein kinase 26	0.0526
159	0.756	Lax1	lymphocyte transmembrane adaptor 1	0.0531
160	0.756	Stra6	stimulated by retinoic acid 6	0.0531
161	0.759	Hmha1	histocompatibility (minor) HA-1	0.0531
162	0.760	Dusp2	dual specificity phosphatase 2	0.0544
163	0.761	AB124611	chromosome 19 open reading frame 38	0.0544
164	0.761	Rasal3	RAS protein activator like 3	0.0558
165	0.762	Il16	interleukin 16	0.0558
166	0.764	Rasgrp3	RAS guanyl releasing protein 3 (calcium and DAG-regulated)	0.0558
167	0.764	Slc9a7	solute carrier family 9, subfamily A, member 7	0.0558
168	0.765	Hhex	hematopoietically expressed homeobox	0.0576
169	0.766	Acap1	ArfGAP with coiled-coil, ankyrin repeat and PH domains 1	0.0576
170	0.766	Ccr7	chemokine (C-C motif) receptor 7	0.0576
171	0.766	Tbc1d10c	TBC1 domain family, member 10C	0.0585
172	0.769	Pappa	pregnancy-associated plasma protein A, pappalysin 1	0.0596
173	0.770	Myo1g	myosin IG	0.0598
174	0.773	Ncf4	neutrophil cytosolic factor 4, 40kDa	0.0605
175	0.774	H2-Eb2	histocompatibility 2, class II antigen E beta2	0.0605
176	0.774	Irf4	interferon regulatory factor 4	0.0605
177	0.775	Rhoh	ras homolog family member H	0.0605
178	0.776	Cxcr4	chemokine (C-X-C motif) receptor 4	0.0608
179	0.778	Sipa1	signal-induced proliferation-associated 1	0.0610

180	0.780	A630001G21Rik	RIKEN cDNA A630001G21 gene	0.0620
181	0.781	Car5b	carbonic anhydrase VB, mitochondrial	0.0626
182	0.782	Trf	transferrin	0.0635
183	0.785	Fam169b	family with sequence similarity 169, member B	0.0635
184	0.788	Irf5	interferon regulatory factor 5	0.0646
185	0.792	Fmnl1	formin-like 1	0.0650
186	0.794	Sash3	SAM and SH3 domain containing 3	0.0654
187	0.801	Ms4a4c	membrane-spanning 4-domains, subfamily A, member 4B	0.0654
188	0.802	Cldn8	claudin 8	0.0660
189	0.803	5031414D18Rik	KIAA0226-like	0.0660
190	0.803	Lmo2	LIM domain only 2 (rhombotin-like 1)	0.0660
191	0.809	Fgd2	FYVE, RhoGEF and PH domain containing 2	0.0673
192	0.817	Grap	GRB2-related adaptor protein	0.0673
193	0.819	H2-Eb1	major histocompatibility complex, class II, DR beta 5	0.0684
194	0.819	Plek	pleckstrin	0.0685
195	0.820	H2-Ab1	major histocompatibility complex, class II, DQ beta 1	0.0685
196	0.825	Arhgap25	Rho GTPase activating protein 25	0.0694
197	0.825	Dock2	dedicator of cytokinesis 2	0.0694
198	0.825	Ptpn7	protein tyrosine phosphatase, non-receptor type 7	0.0694
199	0.827	Nckap1l	NCK-associated protein 1-like	0.0694
200	0.829	Ciita	class II, major histocompatibility complex, transactivator	0.0694
201	0.829	Mfge8	milk fat globule-EGF factor 8 protein	0.0694
202	0.832	Il2rg	interleukin 2 receptor, gamma	0.0694
203	0.836	P2ry10	purinergic receptor P2Y, G-protein coupled, 10	0.0694
204	0.837	Cyp4f18	cytochrome P450, family 4, subfamily F, polypeptide 2	0.0694
205	0.839	Ly9	lymphocyte antigen 9	0.0694
206	0.843	Arhgap30	Rho GTPase activating protein 30	0.0694
207	0.844	Gpr18	G protein-coupled receptor 18	0.0694
208	0.849	Scd1	stearoyl-CoA desaturase (delta-9-desaturase)	0.0696
209	0.853	Ltb	lymphotoxin beta (TNF superfamily, member 3)	0.0696
210	0.856	Cd72	CD72 molecule	0.0696
211	0.857	Snn	stannin	0.0696
212	0.862	Cacna1i	calcium channel, voltage-dependent, T type, alpha 1I subunit	0.0699
213	0.868	Cd53	CD53 molecule	0.0701
214	0.873	Itgal	integrin, alpha lymphocyte function-associated antigen 1	0.0701
215	0.878	H2-Aa	major histocompatibility complex, class II, DQ alpha 1	0.0710
216	0.878	Klhl6	kelch-like family member 6	0.0710
217	0.879	Wdfy4	WDFY family member 4	0.0710
218	0.881	Gpr174	G protein-coupled receptor 174	0.0710
219	0.883	Ly6d	lymphocyte antigen 6 complex, locus D	0.0710
220	0.889	Cd180	CD180 molecule	0.0710
221	0.891	Ikzf1	IKAROS family zinc finger 1 (Ikaros)	0.0710
222	0.902	Pax5	paired box 5	0.0710
223	0.903	Pyhin1	interferon, gamma-inducible protein 16	0.0724
224	0.904	Ikzf3	IKAROS family zinc finger 3 (Aiolos)	0.0727
225	0.914	Lta	lymphotoxin alpha	0.0727

226	0.916	Napsa	napsin A aspartic peptidase	0.0727
227	0.917	Clu	clusterin	0.0727
228	0.918	Btk	Bruton agammaglobulinemia tyrosine kinase	0.0728
229	0.918	Dok3	docking protein 3	0.0728
230	0.919	Il21r	interleukin 21 receptor	0.0728
231	0.921	Arhgdib	Rho GDP dissociation inhibitor (GDI) beta	0.0728
232	0.927	Hvcn1	hydrogen voltage-gated channel 1	0.0728
233	0.932	Cd52	CD52 antigen	0.0728
234	0.934	Cd74	CD74 molecule, major histocompatibility complex, class II invariant chain	0.0729
235	0.950	Cd2	CD2 molecule	0.0729
236	0.957	Cxcl13	chemokine (C-X-C motif) ligand 13	0.0739
237	0.957	H2-DMb2	major histocompatibility complex, class II, DM beta	0.0764
238	0.957	Stap1	signal transducing adaptor family member 1	0.0764
239	0.973	Coro1a	coronin, actin binding protein, 1A	0.0765
240	0.976	Pou2f2	POU class 2 homeobox 2	0.0797
241	0.990	Siglecg	sialic acid binding Ig-like lectin 10	0.0798
242	0.995	Map4k1	mitogen-activated protein kinase kinase kinase kinase 1	0.0798
243	0.995	Thrsp	thyroid hormone responsive	0.0800
244	1.015	Fcrl1	Fc receptor-like 1	0.0817
245	1.037	Ptprcap	protein tyrosine phosphatase, receptor type, C-associated protein	0.0827
246	1.052	H2-Oa	major histocompatibility complex, class II, DO alpha	0.0829
247	1.056	Sell	selectin L	0.0839
248	1.060	Fcrla	Fc receptor-like A	0.0842
249	1.064	Cd19	CD19 molecule	0.0854
250	1.083	Btla	B and T lymphocyte associated	0.0873
251	1.088	Chst3	carbohydrate (chondroitin 6) sulfotransferase 3	0.0876
252	1.098	Cd37	CD37 molecule	0.0876
253	1.120	Pou2af1	POU class 2 associating factor 1	0.0881
254	1.126	Ms4a1	membrane-spanning 4-domains, subfamily A, member 1	0.0889
255	1.141	Tnfrsf13c	tumor necrosis factor receptor superfamily, member 13C	0.0920
256	1.144	H2-Ob	major histocompatibility complex, class II, DO beta	0.0920
257	1.168	Fcer2a	Fc fragment of IgE, low affinity II, receptor for (CD23)	0.0927
258	1.177	Blk	BLK proto-oncogene, Src family tyrosine kinase	0.0927
259	1.177	Cxcr5	chemokine (C-X-C motif) receptor 5	0.0933
260	1.189	Cd22	CD22 molecule	0.0957
261	1.200	Treml2	triggering receptor expressed on myeloid cells-like 2	0.0960
262	1.214	Faim3	Fas apoptotic inhibitory molecule 3	0.0960
263	1.243	Cd79b	CD79b molecule, immunoglobulin-associated beta	0.0963
264	1.264	Bank1	B-cell scaffold protein with ankyrin repeats 1	0.0963
265	1.279	Cr2	complement component (3d/Epstein Barr virus) receptor 2	0.0971
266	1.322	Cd79a	CD79a molecule, immunoglobulin-associated alpha	0.0986

Supplementary Table 1. Genes differentially expressed in the HF colonic epithelium compared to LF. Differential expression was determined using DESEq2 and significance was set using a q-value < 0.10. Log Ratio corresponds to the log2 fold change, ID is the PubMed Gene ID, P-adj is the adjusted p-value.

Supplementary Table 2

No.	Log Ratio	ID	Entrez Gene Name	P-adj
1	-1.786	Npc1l1	NPC1-like 1 (cholesterol transporter)	0.0000
2	-1.284	Pla2g4c	phospholipase A2, group IVC	0.0000
3	-1.257	Apoa1	apolipoprotein A-I	0.0002
4	-1.252	Sgk1	serum/glucocorticoid regulated kinase 1	0.0003
5	-1.173	Ak4	adenylate kinase 4	0.0003
6	-1.137	Hoga1	4-hydroxy-2-oxoglutarate aldolase 1	0.0003
7	-1.078	Cyp2c69	cytochrome P450, family 2, subfamily c, polypeptide 40	0.0003
8	-1.072	Mboat2	membrane bound O-acyltransferase domain containing 2	0.0004
9	-1.059	Saa3	serum amyloid A 3	0.0004
10	-1.057	2010109I03Rik	RIKEN cDNA 2010109I03 gene	0.0006
11	-1.039	Creb3l3	cAMP responsive element binding protein 3-like 3	0.0006
12	-1.012	Mal	mal, T-cell differentiation protein	0.0006
13	-1.007	Clca6	chloride channel accessory 4	0.0006
14	-1.001	Slc9a3	solute carrier family 9, subfamily A, member 3	0.0006
15	-0.999	Alas2	aminolevulinate, delta-, synthase 2	0.0006
16	-0.987	Slc6a19	solute carrier family 6, member 19	0.0006
17	-0.959	BB123696	expressed sequence BB123696	0.0006
18	-0.957	Slc11a2	solute carrier family 11 (proton-coupled divalent metal ion transporter), member 2	0.0009
19	-0.956	Prrg4	proline rich Gla (G-carboxyglutamic acid) 4	0.0009
20	-0.943	Krt84	keratin 84	0.0009
21	-0.928	Mpp6	membrane protein, palmitoylated 6	0.0014
22	-0.926	Pde9a	phosphodiesterase 9A	0.0014
23	-0.915	Ttc39c	tetratricopeptide repeat domain 39C	0.0015
24	-0.898	Cyp2d9	cytochrome P450, family 2, subfamily d, polypeptide 9	0.0015
25	-0.892	Rbp1	retinol binding protein 1, cellular	0.0016
26	-0.889	Slc26a1	solute carrier family 26 (anion exchanger), member 1	0.0017
27	-0.886	Sstr1	somatostatin receptor 1	0.0019
28	-0.884	E130307A14Rik	RIKEN cDNA E130307A14 gene	0.0019
29	-0.883	Vip	vasoactive intestinal peptide	0.0019
30	-0.880	Mmp12	matrix metallopeptidase 12 (macrophage elastase)	0.0021
31	-0.875	Igf2bp1	insulin-like growth factor 2 mRNA binding protein 1	0.0028
32	-0.870	Cry1	cryptochrome circadian clock 1	0.0036
33	-0.869	Gzmb	granzyme B	0.0036
34	-0.866	Ace2	angiotensin I converting enzyme 2	0.0036
35	-0.863	Mpp1	membrane protein, palmitoylated 1, 55kDa	0.0036
36	-0.862	Fkbp5	FK506 binding protein 5	0.0036
37	-0.847	Calb2	calbindin 2	0.0038
38	-0.844	Sis	sucrase-isomaltase (alpha-glucosidase)	0.0039
39	-0.835	4931440F15Rik	RIKEN cDNA 4931440F15 gene	0.0044
40	-0.835	Hp	haptoglobin	0.0045
41	-0.818	Gm6329	predicted gene 6329	0.0045
42	-0.796	Papss2	3'-phosphoadenosine 5'-phosphosulfate synthase 2	0.0046

43	-0.793	Usp2	ubiquitin specific peptidase 2	0.0046
44	-0.775	Slc7a9	solute carrier family 7, member 9	0.0046
45	-0.769	Slc30a1	solute carrier family 30 (zinc transporter), member 1	0.0046
46	-0.767	Slc5a1	solute carrier family 5, member 1	0.0046
47	-0.755	Slc6a6	solute carrier family 6, member 6	0.0046
48	-0.744	Ppp2r3a	protein phosphatase 2, regulatory subunit B'', alpha	0.0046
49	-0.741	Akr1c14	aldo-keto reductase family 1, member C14	0.0046
50	-0.740	Fbxo34	F-box protein 34	0.0054
51	-0.722	Lpar2	lysophosphatidic acid receptor 2	0.0059
52	-0.719	Tfrc	transferrin receptor	0.0060
53	-0.717	Per1	period circadian clock 1	0.0064
54	-0.710	Rorc	RAR-related orphan receptor C	0.0064
55	-0.705	Glt28d2	glycosyltransferase 28 domain containing 2	0.0066
56	-0.705	Plek2	pleckstrin 2	0.0068
57	-0.696	Cast	calpastatin	0.0076
58	-0.693	Slc4a4	solute carrier family 4, member 4	0.0079
59	-0.693	Slc9a3r1	solute carrier family 9, subfamily A, member 3 regulator 1	0.0083
60	-0.686	Trpm6	transient receptor potential cation channel, subfamily M, member 6	0.0089
61	-0.685	Npc1	Niemann-Pick disease, type C1	0.0096
62	-0.680	Klf10	Kruppel-like factor 10	0.0099
63	-0.667	Slc2a9	solute carrier family 2, member 9	0.0099
64	-0.662	Pex11a	peroxisomal biogenesis factor 11 alpha	0.0107
65	-0.661	B3gnt3	UDP-GlcNAc:betaGal beta-1,3-N-acetylglucosaminyltransferase 3	0.0110
66	-0.658	Mapk6	mitogen-activated protein kinase 6	0.0111
67	-0.657	Fa2h	fatty acid 2-hydroxylase	0.0111
68	-0.657	Fam102a	family with sequence similarity 102, member A	0.0111
69	-0.655	Ppap2a	phosphatidic acid phosphatase type 2A	0.0111
70	-0.648	P2ry2	purinergic receptor P2Y, G-protein coupled, 2	0.0112
71	-0.642	Rsad1	radical S-adenosyl methionine domain containing 1	0.0121
72	-0.640	Apobec1	apolipoprotein B mRNA editing enzyme, catalytic polypeptide 1	0.0121
73	-0.637	Tgfa	transforming growth factor, alpha	0.0126
74	-0.618	Hsd17b2	hydroxysteroid (17-beta) dehydrogenase 2	0.0134
75	-0.616	Pfkl	phosphofructokinase, liver	0.0138
76	-0.611	Fhdc1	FH2 domain containing 1	0.0138
77	-0.606	Il20rb	interleukin 20 receptor beta	0.0142
78	-0.603	Apob	apolipoprotein B	0.0146
79	-0.603	Coq10b	coenzyme Q10 homolog B (S. cerevisiae)	0.0147
80	-0.603	Lamb3	laminin, beta 3	0.0147
81	-0.603	Tmem150b	transmembrane protein 150B	0.0151
82	-0.587	Coro2a	coronin, actin binding protein, 2A	0.0152
83	-0.578	Sowahb	sosondowah ankyrin repeat domain family member B	0.0152
84	-0.573	Als2cl	ALS2 C-terminal like	0.0158
85	-0.572	Tmcc3	transmembrane and coiled-coil domain family 3	0.0165

86	-0.568	Tesk2	testis-specific kinase 2	0.0165
87	-0.549	Slc9a2	solute carrier family 9, subfamily A, member 2	0.0171
88	-0.543	Secisbp2l	SECIS binding protein 2-like	0.0171
89	-0.542	Dhcr24	24-dehydrocholesterol reductase	0.0180
90	-0.541	Alas1	aminolevulinate, delta-, synthase 1	0.0186
91	-0.541	Slc25a24	solute carrier family 25, member 24	0.0196
92	-0.538	Sema6d	sema domain, transmembrane domain (TM), and cytoplasmic domain, 6D	0.0196
93	-0.534	Arhgap27	Rho GTPase activating protein 27	0.0196
94	-0.534	Ifrd1	interferon-related developmental regulator 1	0.0196
95	-0.525	Chuk	conserved helix-loop-helix ubiquitous kinase	0.0197
96	-0.524	Tmem189	transmembrane protein 189	0.0198
97	-0.519	Unc5b	unc-5 homolog B (C. elegans)	0.0198
98	-0.515	Nipa2	non imprinted in Prader-Willi/Angelman syndrome 2	0.0198
99	-0.514	Bach1	BTB and CNC homology 1, basic leucine zipper transcription factor 1	0.0202
100	-0.514	Nus1	nuclear undecaprenyl pyrophosphate synthase 1 homolog	0.0203
101	-0.512	Pik3c2a	phosphatidylinositol-4-phosphate 3-kinase, catalytic subunit type 2 alpha	0.0203
102	-0.506	Optn	optineurin	0.0205
103	-0.505	Hsd17b7	hydroxysteroid (17-beta) dehydrogenase 7	0.0211
104	-0.502	Nampt	nicotinamide phosphoribosyltransferase	0.0221
105	-0.498	Chmp4c	charged multivesicular body protein 4C	0.0221
106	-0.494	Urgcp	upregulator of cell proliferation	0.0221
107	-0.492	Fastkd3	FAST kinase domains 3	0.0222
108	-0.492	Sdc1	syndecan 1	0.0222
109	-0.492	Tfcp2l1	transcription factor CP2-like 1	0.0237
110	-0.491	Lin7c	lin-7 homolog C (C. elegans)	0.0244
111	-0.489	Lrrc8e	leucine rich repeat containing 8 family, member E	0.0245
112	-0.486	Atrnl1	attractin-like 1	0.0248
113	-0.474	D5Ertd579e	KIAA0232	0.0252
114	-0.474	Pgk1	phosphoglycerate kinase 1	0.0252
115	-0.464	Dock1	dedicator of cytokinesis 1	0.0252
116	-0.461	Efhd2	EF-hand domain family, member D2	0.0252
117	-0.458	Gnai3	guanine nucleotide binding protein (G protein), alpha inhibiting activity polypeptide 3	0.0252
118	-0.454	Dclre1b	DNA cross-link repair 1B	0.0253
119	-0.453	Aim1	absent in melanoma 1	0.0253
120	-0.451	Ldha	lactate dehydrogenase A	0.0253
121	-0.449	Cobl	cordon-bleu WH2 repeat protein	0.0253
122	-0.444	Car9	carbonic anhydrase IX	0.0253
123	-0.442	Exoc5	exocyst complex component 5	0.0253
124	-0.441	Otud7b	OTU deubiquitinase 7B	0.0253
125	-0.440	Cdc25a	cell division cycle 25A	0.0253
126	-0.439	Atl2	atlastin GTPase 2	0.0253
127	-0.433	Txnip	thioredoxin interacting protein	0.0253

128	-0.432	Fuca2	fucosidase, alpha-L- 2, plasma	0.0253
129	-0.432	Vipr1	vasoactive intestinal peptide receptor 1	0.0256
130	-0.432	Zdhhc13	zinc finger, DHHC-type containing 13	0.0261
131	-0.430	Ccdc120	coiled-coil domain containing 120	0.0261
132	-0.428	Herpud1	homocysteine-inducible, endoplasmic reticulum stress-inducible, ubiquitin-like domain member 1	0.0261
133	-0.425	Tnfaip1	tumor necrosis factor, alpha-induced protein 1 (endothelial)	0.0261
134	-0.423	Baz1a	bromodomain adjacent to zinc finger domain, 1A	0.0261
135	-0.422	Twf1	twinfilin actin-binding protein 1	0.0261
136	-0.421	Ddx3x	DEAD (Asp-Glu-Ala-Asp) box helicase 3, X-linked	0.0265
137	-0.420	Cab39	calcium binding protein 39	0.0265
138	-0.419	Ppp1r15b	protein phosphatase 1, regulatory subunit 15B	0.0278
139	-0.419	Rgp1	RGP1 retrograde golgi transport homolog (S. cerevisiae)	0.0279
140	-0.417	Mtmr6	myotubularin related protein 6	0.0279
141	-0.413	Arih2	ariadne RBR E3 ubiquitin protein ligase 2	0.0279
142	-0.410	Ube2e2	ubiquitin-conjugating enzyme E2E 2	0.0279
143	-0.407	Arhgef5	Rho guanine nucleotide exchange factor (GEF) 5	0.0285
144	-0.405	Nek6	NIMA-related kinase 6	0.0289
145	-0.404	Bcar1	breast cancer anti-estrogen resistance 1	0.0290
146	-0.403	Clcn3	chloride channel, voltage-sensitive 3	0.0291
147	-0.401	Xpnpep1	X-prolyl aminopeptidase (aminopeptidase P) 1, soluble	0.0295
148	-0.396	Mtmr7	myotubularin related protein 7	0.0301
149	-0.396	Ssx2ip	synovial sarcoma, X breakpoint 2 interacting protein	0.0301
150	-0.395	Stk40	serine/threonine kinase 40	0.0303
151	-0.394	Mecom	MDS1 and EVI1 complex locus	0.0303
152	-0.392	Micu1	mitochondrial calcium uptake 1	0.0303
153	-0.392	Snx4	sorting nexin 4	0.0303
154	-0.388	Ccdc25	coiled-coil domain containing 25	0.0303
155	-0.388	Gna13	guanine nucleotide binding protein (G protein), alpha 13	0.0315
156	-0.388	Ndfip2	Nedd4 family interacting protein 2	0.0315
157	-0.385	Rbm3	RNA binding motif (RNP1, RRM) protein 3	0.0320
158	-0.384	Ddx10	DEAD (Asp-Glu-Ala-Asp) box polypeptide 10	0.0320
159	-0.384	Nlrc4	NLR family, CARD domain containing 4	0.0327
160	-0.382	Mapk8	mitogen-activated protein kinase 8	0.0331
161	-0.382	Vps54	vacuolar protein sorting 54 homolog (S. cerevisiae)	0.0331
162	-0.380	Kpna1	karyopherin alpha 1 (importin alpha 5)	0.0332
163	-0.379	Snx15	sorting nexin 15	0.0335
164	-0.377	Btbd10	BTB (POZ) domain containing 10	0.0338
165	-0.377	Map2k3	mitogen-activated protein kinase kinase 3	0.0338
166	-0.376	Gmfb	glia maturation factor, beta	0.0338
167	-0.372	Atp1a1	ATPase, Na+/K+ transporting, alpha 1 polypeptide	0.0346
168	-0.371	Usp12	ubiquitin specific peptidase 12	0.0348
169	-0.370	Pvr	poliovirus receptor	0.0348
170	-0.368	Traf6	TNF receptor-associated factor 6, E3 ubiquitin protein ligase	0.0348
171	-0.368	Txnrd1	thioredoxin reductase 1	0.0348

172	-0.363	Picalm	phosphatidylinositol binding clathrin assembly protein	0.0348
173	-0.363	Samd8	sterile alpha motif domain containing 8	0.0348
174	-0.360	Cgn	cingulin	0.0352
175	-0.359	Ube2q1	ubiquitin-conjugating enzyme E2Q family member 1	0.0355
176	-0.359	Usp37	ubiquitin specific peptidase 37	0.0358
177	-0.358	Kras	Kirsten rat sarcoma viral oncogene homolog	0.0358
178	-0.357	Fam76a	family with sequence similarity 76, member A	0.0358
179	-0.356	Man1a2	mannosidase, alpha, class 1A, member 2	0.0358
180	-0.353	Gak	cyclin G associated kinase	0.0366
181	-0.352	Gatad2a	GATA zinc finger domain containing 2A	0.0367
182	-0.347	Ascc2	activating signal cointegrator 1 complex subunit 2	0.0367
183	-0.347	5730559C18Rik	chromosome 1 open reading frame 106	0.0367
184	-0.346	Stx3	syntaxin 3	0.0367
185	-0.344	Tjp2	tight junction protein 2	0.0367
186	-0.343	Agfg1	ArfGAP with FG repeats 1	0.0367
187	-0.342	Ell2	elongation factor, RNA polymerase II, 2	0.0368
188	-0.341	Ppp4r1	protein phosphatase 4, regulatory subunit 1	0.0374
189	-0.340	Tbk1	TANK-binding kinase 1	0.0374
190	-0.339	Tab2	TGF-beta activated kinase 1/MAP3K7 binding protein 2	0.0378
191	-0.336	Gdap2	ganglioside induced differentiation associated protein 2	0.0386
192	-0.335	Tatdn2	TatD DNase domain containing 2	0.0389
193	-0.327	2010315B03Rik	RIKEN cDNA 2010315B03 gene	0.0389
194	-0.327	Cirh1a	cirrhosis, autosomal recessive 1A (cirhin)	0.0389
195	-0.324	Larp4	La ribonucleoprotein domain family, member 4	0.0389
196	-0.322	Ankrd13a	ankyrin repeat domain 13A	0.0389
197	-0.318	Ykt6	YKT6 v-SNARE homolog (S. cerevisiae)	0.0389
198	-0.316	Iars2	isoleucyl-tRNA synthetase 2, mitochondrial	0.0389
199	-0.316	Slc38a2	solute carrier family 38, member 2	0.0389
200	-0.316	Tbcd	tubulin folding cofactor D	0.0389
201	-0.313	Nploc4	nuclear protein localization 4 homolog (S. cerevisiae)	0.0391
202	-0.313	Pcsk7	proprotein convertase subtilisin/kexin type 7	0.0391
203	-0.307	Lin54	lin-54 DREAM MuvB core complex component	0.0391
204	-0.307	Stx12	syntaxin 12	0.0404
205	-0.306	Usp38	ubiquitin specific peptidase 38	0.0409
206	-0.305	Nom1	nucleolar protein with MIF4G domain 1	0.0409
207	-0.304	Ubap1	ubiquitin associated protein 1	0.0412
208	-0.303	Itga3	integrin, alpha 3 (antigen CD49C, alpha 3 subunit of VLA-3 receptor)	0.0412
209	-0.302	Aph1a	APH1A gamma secretase subunit	0.0412
210	-0.302	Ccnyl1	cyclin Y-like 1	0.0412
211	-0.302	Polr3c	polymerase (RNA) III (DNA directed) polypeptide C (62kD)	0.0412
212	-0.298	Strbp	spermatid perinuclear RNA binding protein	0.0412
213	-0.295	Axin1	axin 1	0.0412
214	-0.295	Rab11fip1	RAB11 family interacting protein 1 (class I)	0.0414
215	-0.294	Gosr2	golgi SNAP receptor complex member 2	0.0414

216	-0.292	Hs6st1	heparan sulfate 6-O-sulfotransferase 1	0.0414
217	-0.292	Osbpl10	oxysterol binding protein-like 10	0.0414
218	-0.290	Usp15	ubiquitin specific peptidase 15	0.0427
219	-0.289	Lmbr1	limb development membrane protein 1	0.0430
220	-0.287	Esco1	establishment of sister chromatid cohesion N-acetyltransferase 1	0.0430
221	-0.285	Cdc42se1	CDC42 small effector 1	0.0430
222	-0.285	Reep3	receptor accessory protein 3	0.0432
223	-0.285	Xrn2	5'-3' exoribonuclease 2	0.0436
224	-0.284	Aars	alanyl-tRNA synthetase	0.0436
225	-0.284	Plaa	phospholipase A2-activating protein	0.0436
226	-0.284	Traf4	TNF receptor-associated factor 4	0.0444
227	-0.282	Abcf2	ATP-binding cassette, sub-family F (GCN20), member 2	0.0447
228	-0.279	Pkp2	plakophilin 2	0.0449
229	-0.278	Sumo3	small ubiquitin-like modifier 3	0.0451
230	-0.277	Actr1b	ARP1 actin-related protein 1 homolog B, centractin beta (yeast)	0.0452
231	-0.275	Eif4g1	eukaryotic translation initiation factor 4 gamma, 1	0.0452
232	-0.275	Tex261	testis expressed 261	0.0452
233	-0.272	Hira	histone cell cycle regulator	0.0452
234	-0.271	Dcaf5	DDB1 and CUL4 associated factor 5	0.0452
235	-0.267	Ercc3	excision repair cross-complementation group 3	0.0452
236	-0.266	Cask	calcium/calmodulin-dependent serine protein kinase (MAGUK family)	0.0452
237	-0.265	Akap1	A kinase (PRKA) anchor protein 1	0.0452
238	-0.265	Tomm70a	translocase of outer mitochondrial membrane 70 homolog A (S. cerevisiae)	0.0453
239	-0.260	Azi2	5-azacytidine induced 2	0.0458
240	-0.259	Fbxo38	F-box protein 38	0.0463
241	-0.259	Nemf	nuclear export mediator factor	0.0463
242	-0.259	Ptk2	protein tyrosine kinase 2	0.0464
243	-0.258	Trip12	thyroid hormone receptor interactor 12	0.0469
244	-0.248	Mlx	MLX, MAX dimerization protein	0.0470
245	-0.248	Pptc7	PTC7 protein phosphatase homolog (S. cerevisiae)	0.0470
246	-0.247	Rnf185	ring finger protein 185	0.0471
247	-0.246	Csnk1d	casein kinase 1, delta	0.0472
248	-0.245	AI661453	expressed sequence AI661453	0.0476
249	-0.245	Taf5l	TAF5-like RNA polymerase II, p300/CBP-associated factor (PCAF)-associated factor, 65kDa	0.0481
250	-0.243	Ctdp1	CTD (carboxy-terminal domain, RNA polymerase II, polypeptide A) phosphatase, subunit 1	0.0483
251	-0.243	Ngly1	N-glycanase 1	0.0485
252	-0.241	Ripk1	receptor (TNFRSF)-interacting serine-threonine kinase 1	0.0485
253	-0.237	Papd4	PAP associated domain containing 4	0.0485
254	-0.235	Tbc1d10b	TBC1 domain family, member 10B	0.0485
255	-0.232	Sbds	Shwachman-Bodian-Diamond syndrome	0.0485

256	-0.232	Zfp410	zinc finger protein 410	0.0485
257	-0.231	Ddx50	DEAD (Asp-Glu-Ala-Asp) box polypeptide 50	0.0485
258	-0.231	Icmt	isoprenylcysteine carboxyl methyltransferase	0.0485
259	-0.230	Map3k11	mitogen-activated protein kinase kinase kinase 11	0.0485
260	-0.227	Alkbh5	AlkB family member 5, RNA demethylase	0.0485
261	-0.227	Metap1	methionyl aminopeptidase 1	0.0485
262	-0.226	Ppm1g	protein phosphatase, Mg2+/Mn2+ dependent, 1G	0.0485
263	-0.221	Sec24c	SEC24 family member C	0.0485
264	-0.215	Ppp6r3	protein phosphatase 6, regulatory subunit 3	0.0485
265	-0.214	Rnf170	ring finger protein 170	0.0485
266	-0.206	Ccny	cyclin Y	0.0485
267	-0.204	Smek1	SMEK homolog 1, suppressor of mek1 (Dictyostelium)	0.0498
268	-0.201	Hexim1	hexamethylene bis-acetamide inducible 1	0.0498
269	-0.195	Prdm4	PR domain containing 4	0.0500
270	-0.194	Eif4g3	eukaryotic translation initiation factor 4 gamma, 3	0.0512
271	-0.190	Rragc	Ras-related GTP binding C	0.0514
272	-0.187	Sars	seryl-tRNA synthetase	0.0514
273	-0.186	Gtf2h1	general transcription factor IIH, polypeptide 1, 62kDa	0.0514
274	-0.183	Ahcyl1	adenosylhomocysteinase-like 1	0.0514
275	-0.161	Med17	mediator complex subunit 17	0.0517
276	-0.154	Sec63	SEC63 homolog (S. cerevisiae)	0.0526
277	0.216	Foxo4	forkhead box O4	0.0526
278	0.222	Ift172	intraflagellar transport 172	0.0526
279	0.245	Tpra1	transmembrane protein, adipocyte asscociated 1	0.0526
280	0.259	Wdyhv1	WDYHV motif containing 1	0.0526
281	0.269	Cnnm3	cyclin and CBS domain divalent metal cation transport mediator 3	0.0526
282	0.271	Ncbp2	nuclear cap binding protein subunit 2, 20kDa	0.0526
283	0.273	Srsf7	serine/arginine-rich splicing factor 7	0.0529
284	0.274	Acsl4	acyl-CoA synthetase long-chain family member 4	0.0529
285	0.274	Rpusd4	RNA pseudouridylate synthase domain containing 4	0.0529
286	0.276	Tmem175	transmembrane protein 175	0.0532
287	0.280	Sugp2	SURP and G patch domain containing 2	0.0532
288	0.295	Eif4a2	eukaryotic translation initiation factor 4A2	0.0532
289	0.313	Hdac6	histone deacetylase 6	0.0533
290	0.319	Hdac10	histone deacetylase 10	0.0533
291	0.319	Trub1	TruB pseudouridine (psi) synthase family member 1	0.0537
292	0.321	Snx21	sorting nexin family member 21	0.0537
293	0.324	2310045N01Rik	MEF2B neighbor	0.0537
294	0.326	Mipep	mitochondrial intermediate peptidase	0.0539
295	0.326	Ttc4	tetratricopeptide repeat domain 4	0.0539
296	0.331	Dalrd3	DALR anticodon binding domain containing 3	0.0539
297	0.333	Gm14326	zinc finger protein 442	0.0539
298	0.334	Pomt1	protein-O-mannosyltransferase 1	0.0539
299	0.339	Bri3bp	BRI3 binding protein	0.0539

300	0.348	Sdc4	syndecan 4	0.0539
301	0.350	Sms	spermine synthase	0.0539
302	0.352	Zfp825	expressed sequence AI987944	0.0541
303	0.357	Mmgt2	membrane magnesium transporter 2	0.0548
304	0.360	Twsg1	twisted gastrulation BMP signaling modulator 1	0.0567
305	0.363	Ano8	anoctamin 8	0.0567
306	0.364	Ivd	isovaleryl-CoA dehydrogenase	0.0567
307	0.366	Hibadh	3-hydroxyisobutyrate dehydrogenase	0.0567
308	0.368	Lancl1	LanC lantibiotic synthetase component C-like 1 (bacterial)	0.0567
309	0.370	3830406C13Rik	chromosome 3 open reading frame 14	0.0568
310	0.373	Maz	MYC-associated zinc finger protein (purine-binding transcription factor)	0.0568
311	0.376	D3Ertd751e	chromosome 4 open reading frame 33	0.0569
312	0.390	Mdc1	mediator of DNA-damage checkpoint 1	0.0570
313	0.394	Dguok	deoxyguanosine kinase	0.0578
314	0.397	Kdelc2	KDEL (Lys-Asp-Glu-Leu) containing 2	0.0581
315	0.402	Gm12942	ZMYM6 neighbor	0.0585
316	0.404	Bcl7a	B-cell CLL/lymphoma 7A	0.0586
317	0.404	Csf2ra	colony stimulating factor 2 receptor, alpha, low-affinity (granulocyte-macrophage)	0.0591
318	0.408	Gas8	growth arrest-specific 8	0.0598
319	0.414	Cdc25b	cell division cycle 25B	0.0598
320	0.420	Trim59	tripartite motif containing 59	0.0598
321	0.421	Tmem159	transmembrane protein 159	0.0598
322	0.422	Ifi30	interferon, gamma-inducible protein 30	0.0598
323	0.424	Zfp932	zinc finger protein 932	0.0606
324	0.429	2810006K23Rik	chromosome 12 open reading frame 65	0.0606
325	0.429	Irf2bp2	interferon regulatory factor 2 binding protein 2	0.0606
326	0.431	Nap1l1	nucleosome assembly protein 1-like 1	0.0607
327	0.431	Uros	uroporphyrinogen III synthase	0.0609
328	0.436	Athl1	ATH1, acid trehalase-like 1 (yeast)	0.0609
329	0.441	Tmco6	transmembrane and coiled-coil domains 6	0.0613
330	0.442	Eid1	EP300 interacting inhibitor of differentiation 1	0.0615
331	0.445	C030034I22Rik	RIKEN cDNA C030034I22 gene	0.0615
332	0.447	Smad6	SMAD family member 6	0.0619
333	0.449	Parp1	poly (ADP-ribose) polymerase 1	0.0619
334	0.451	Trim34a	TRIM6-TRIM34 readthrough	0.0619
335	0.463	Trmt1	tRNA methyltransferase 1 homolog (S. cerevisiae)	0.0623
336	0.466	Ggcx	gamma-glutamyl carboxylase	0.0623
337	0.468	Pck2	phosphoenolpyruvate carboxykinase 2 (mitochondrial)	0.0623
338	0.470	2610015P09Rik	KIAA1407	0.0623
339	0.475	Dhx34	DEAH (Asp-Glu-Ala-His) box polypeptide 34	0.0623
340	0.475	Pla2g4b	phospholipase A2, group IVB (cytosolic)	0.0623
341	0.475	Tmem176b	transmembrane protein 176B	0.0627
342	0.487	1190007I07Rik	chromosome 12 open reading frame 73	0.0628
343	0.487	Plod1	procollagen-lysine, 2-oxoglutarate 5-dioxygenase 1	0.0628

344	0.488	Ccdc77	coiled-coil domain containing 77	0.0628
345	0.489	Zfp36l1	ZFP36 ring finger protein-like 1	0.0635
346	0.498	Bbc3	BCL2 binding component 3	0.0637
347	0.501	Crtap	cartilage associated protein	0.0637
348	0.502	Tlcd1	TLC domain containing 1	0.0638
349	0.504	Pkn3	protein kinase N3	0.0639
350	0.513	Ankrd24	ankyrin repeat domain 24	0.0639
351	0.522	Tmem176a	transmembrane protein 176A	0.0639
352	0.526	Spice1	spindle and centriole associated protein 1	0.0639
353	0.526	Ypel2	yippee-like 2 (Drosophila)	0.0639
354	0.528	Ptp4a3	protein tyrosine phosphatase type IVA, member 3	0.0639
355	0.537	Il17rb	interleukin 17 receptor B	0.0641
356	0.537	Pik3r5	phosphoinositide-3-kinase, regulatory subunit 5	0.0645
357	0.540	Anxa13	annexin A13	0.0645
358	0.541	2610020H08Rik	exonuclease NEF-sp	0.0645
359	0.541	Zmym1	zinc finger, MYM-type 1	0.0645
360	0.542	Rbm43	RNA binding motif protein 43	0.0645
361	0.550	Vav1	vav 1 guanine nucleotide exchange factor	0.0645
362	0.553	Dock11	dedicator of cytokinesis 11	0.0652
363	0.555	St6galnac2	ST6 (alpha-N-acetyl-neuraminyl-2,3-beta-galactosyl-1,3)-N-acetylgalactosaminide alpha-2,6-sialyltransferase 2	0.0652
364	0.556	Chid1	chitinase domain containing 1	0.0652
365	0.558	Tmem132a	transmembrane protein 132A	0.0652
366	0.559	Gramd1a	GRAM domain containing 1A	0.0656
367	0.559	Rin3	Ras and Rab interactor 3	0.0657
368	0.560	Oxct1	3-oxoacid CoA transferase 1	0.0669
369	0.563	1810014B01Rik	RIKEN cDNA 1810014B01 gene	0.0677
370	0.563	Ppm1k	protein phosphatase, Mg2+/Mn2+ dependent, 1K	0.0677
371	0.564	Glt8d1	glycosyltransferase 8 domain containing 1	0.0683
372	0.564	Pea15a	phosphoprotein enriched in astrocytes 15	0.0683
373	0.565	Gpr157	G protein-coupled receptor 157	0.0684
374	0.573	Stmn1	stathmin 1	0.0684
375	0.575	Pcyox1l	prenylcysteine oxidase 1 like	0.0684
376	0.575	Vegfb	vascular endothelial growth factor B	0.0684
377	0.579	Hs3st3b1	heparan sulfate (glucosamine) 3-O-sulfotransferase 3B1	0.0684
378	0.582	Ccdc163	coiled-coil domain containing 163	0.0684
379	0.588	Spef1	sperm flagellar 1	0.0684
380	0.589	Trim45	tripartite motif containing 45	0.0684
381	0.591	Echdc3	enoyl CoA hydratase domain containing 3	0.0684
382	0.594	Camk4	calcium/calmodulin-dependent protein kinase IV	0.0686
383	0.594	Plek	pleckstrin	0.0690
384	0.599	Ift80	intraflagellar transport 80	0.0692
385	0.599	Shisa7	shisa family member 7	0.0692
386	0.601	Avil	advillin	0.0697
387	0.601	Itprip	inositol 1,4,5-trisphosphate receptor interacting protein	0.0697

388	0.604	Echdc2	enoyl CoA hydratase domain containing 2	0.0697
389	0.608	4933439C10Rik	RIKEN cDNA 4933439C10 gene	0.0697
390	0.610	Dpp7	dipeptidyl-peptidase 7	0.0697
391	0.612	1700029J07Rik	chromosome 4 open reading frame 47	0.0699
392	0.618	Vkorc1	vitamin K epoxide reductase complex, subunit 1	0.0699
393	0.620	Ccdc28b	coiled-coil domain containing 28B	0.0699
394	0.623	Fzd7	frizzled class receptor 7	0.0699
395	0.624	Slc16a11	solute carrier family 16, member 11	0.0699
396	0.629	Atxn10	ataxin 10	0.0700
397	0.629	Tmem107	transmembrane protein 107	0.0703
398	0.630	Dennd4b	DENN/MADD domain containing 4B	0.0705
399	0.632	Gabbr1	gamma-aminobutyric acid (GABA) B receptor, 1	0.0707
400	0.632	Slc2a4rg-ps	Slc2a4 regulator, pseudogene	0.0715
401	0.633	Adrbk2	adrenergic, beta, receptor kinase 2	0.0715
402	0.633	Mrgpre	MAS-related GPR, member E	0.0730
403	0.638	Slc29a4	solute carrier family 29 (equilibrative nucleoside transporter), member 4	0.0733
404	0.639	Bmyc	brain expressed myelocytomatosis oncogene	0.0742
405	0.640	Fam167a	family with sequence similarity 167, member A	0.0745
406	0.648	Pde1b	phosphodiesterase 1B, calmodulin-dependent	0.0748
407	0.649	Accs	1-aminocyclopropane-1-carboxylate synthase homolog (Arabidopsis)(non-functional)	0.0754
408	0.651	Hist2h2be	histone cluster 1, H2bj	0.0754
409	0.653	Mbd4	methyl-CpG binding domain protein 4	0.0754
410	0.655	Lpin1	lipin 1	0.0754
411	0.662	4930523C07Rik	KIAA0040	0.0756
412	0.665	Cplx2	complexin 2	0.0757
413	0.670	Plcg2	phospholipase C, gamma 2 (phosphatidylinositol-specific)	0.0764
414	0.671	Anxa5	annexin A5	0.0764
415	0.674	Cd97	CD97 molecule	0.0764
416	0.677	Mapk12	mitogen-activated protein kinase 12	0.0764
417	0.680	Rgs13	regulator of G-protein signaling 13	0.0767
418	0.684	S1pr2	sphingosine-1-phosphate receptor 2	0.0767
419	0.685	Arhgef4	Rho guanine nucleotide exchange factor (GEF) 4	0.0770
420	0.686	A230056P14Rik	RIKEN cDNA A230056P14 gene	0.0775
421	0.686	Vmn2r29	vomeronasal 2, receptor 32	0.0775
422	0.687	Rhobtb1	Rho-related BTB domain containing 1	0.0775
423	0.695	Abhd14a	abhydrolase domain containing 14A	0.0775
424	0.695	Card11	caspase recruitment domain family, member 11	0.0775
425	0.695	Limd2	LIM domain containing 2	0.0775
426	0.697	Spata6	spermatogenesis associated 6	0.0775
427	0.702	Ska1	spindle and kinetochore associated complex subunit 1	0.0775
428	0.704	Mdfic	MyoD family inhibitor domain containing	0.0775
429	0.706	Dusp22	dual specificity phosphatase 22	0.0775
430	0.706	Tmod4	tropomodulin 4 (muscle)	0.0775
431	0.708	Fgd2	FYVE, RhoGEF and PH domain containing 2	0.0775

432	0.710	Olfr78	olfactory receptor, family 51, subfamily E, member 2	0.0775
433	0.710	Psrc1	proline/serine-rich coiled-coil 1	0.0775
434	0.711	Cdo1	cysteine dioxygenase type 1	0.0775
435	0.711	Tnfrsf25	tumor necrosis factor receptor superfamily, member 25	0.0775
436	0.713	Sipa1	signal-induced proliferation-associated 1	0.0775
437	0.720	Gm12504	prothymosin alpha pseudogene	0.0775
438	0.722	Ocel1	occludin/ELL domain containing 1	0.0775
439	0.722	Vipr2	vasoactive intestinal peptide receptor 2	0.0775
440	0.725	Tnfrsf19	tumor necrosis factor receptor superfamily, member 19	0.0775
441	0.727	Lca5	Leber congenital amaurosis 5	0.0775
442	0.727	Prr18	proline rich 18	0.0777
443	0.728	Smarcd3	SWI/SNF related, matrix associated, actin dependent regulator of chromatin, subfamily d, member 3	0.0779
444	0.732	4930481A15Rik	RIKEN cDNA 4930481A15 gene	0.0779
445	0.735	Bbs1	Bardet-Biedl syndrome 1	0.0779
446	0.739	Il17d	interleukin 17D	0.0790
447	0.739	Spib	Spi-B transcription factor (Spi-1/PU.1 related)	0.0792
448	0.740	A330023F24Rik	RIKEN cDNA A330023F24 gene	0.0793
449	0.741	Rgs19	regulator of G-protein signaling 19	0.0793
450	0.742	Tbc1d19	TBC1 domain family, member 19	0.0793
451	0.745	Fabp5	fatty acid binding protein 5 (psoriasis-associated)	0.0794
452	0.746	P2rx7	purinergic receptor P2X, ligand-gated ion channel, 7	0.0794
453	0.750	Morn2	MORN repeat containing 2	0.0794
454	0.754	Rgl3	ral guanine nucleotide dissociation stimulator-like 3	0.0795
455	0.758	Fxyd5	FXYD domain containing ion transport regulator 5	0.0795
456	0.759	Cacnb1	calcium channel, voltage-dependent, beta 1 subunit	0.0795
457	0.759	Trpm5	transient receptor potential cation channel, subfamily M, member 5	0.0795
458	0.760	Srpx2	sushi-repeat containing protein, X-linked 2	0.0795
459	0.763	Capsl	calcyphosine-like	0.0795
460	0.765	Ogdhl	oxoglutarate dehydrogenase-like	0.0795
461	0.766	Alox5ap	arachidonate 5-lipoxygenase-activating protein	0.0795
462	0.766	9230110C19Rik	chromosome 11 open reading frame 70	0.0795
463	0.766	Nab2	NGFI-A binding protein 2 (EGR1 binding protein 2)	0.0795
464	0.769	Ptpn14	protein tyrosine phosphatase, non-receptor type 14	0.0797
465	0.770	Kcnn1	potassium intermediate/small conductance calcium-activated channel, subfamily N, member 1	0.0797
466	0.777	1810046K07Rik	chromosome 11 open reading frame 53	0.0807
467	0.779	Tm4sf1	transmembrane 4 L six family member 1	0.0809
468	0.781	Fev	FEV (ETS oncogene family)	0.0809
469	0.782	Calhm2	calcium homeostasis modulator 2	0.0809
470	0.782	Cbx6	chromobox homolog 6	0.0809
471	0.782	Matk	megakaryocyte-associated tyrosine kinase	0.0809
472	0.782	Nat14	N-acetyltransferase 14 (GCN5-related, putative)	0.0809
473	0.788	Gm14322	expressed sequence AI987944	0.0813
474	0.788	Pex5l	peroxisomal biogenesis factor 5-like	0.0815

475	0.789	Csf2rb	colony stimulating factor 2 receptor, beta, low-affinity (granulocyte-macrophage)	0.0815
476	0.790	Plekho1	pleckstrin homology domain containing, family O member 1	0.0815
477	0.793	Rasal1	RAS protein activator like 1 (GAP1 like)	0.0815
478	0.793	Samd14	sterile alpha motif domain containing 14	0.0815
479	0.794	Lyl1	lymphoblastic leukemia associated hematopoiesis regulator 1	0.0815
480	0.795	Wnt4	wingless-type MMTV integration site family, member 4	0.0815
481	0.799	Chst2	carbohydrate (N-acetylglucosamine-6-O) sulfotransferase 2	0.0815
482	0.803	Hvcn1	hydrogen voltage-gated channel 1	0.0815
483	0.805	Amz1	archaelysin family metallopeptidase 1	0.0815
484	0.805	Cmtm7	CKLF-like MARVEL transmembrane domain containing 7	0.0815
485	0.805	Gng11	guanine nucleotide binding protein (G protein), gamma 11	0.0815
486	0.806	Sepn1	selenoprotein N, 1	0.0815
487	0.819	Cox6b2	cytochrome c oxidase subunit VIb polypeptide 2 (testis)	0.0815
488	0.819	Mycbpap	MYCBP associated protein	0.0815
489	0.822	Tmem231	transmembrane protein 231	0.0815
490	0.826	Irf5	interferon regulatory factor 5	0.0815
491	0.829	Armcx6	armadillo repeat containing, X-linked 6	0.0815
492	0.829	Tppp3	tubulin polymerization-promoting protein family member 3	0.0815
493	0.830	Dclk1	doublecortin-like kinase 1	0.0815
494	0.830	Usp11	ubiquitin specific peptidase 11	0.0815
495	0.832	Tuba1a	tubulin, alpha 1a	0.0815
496	0.833	Sirpa	signal-regulatory protein alpha	0.0815
497	0.835	Arhgdib	Rho GDP dissociation inhibitor (GDI) beta	0.0815
498	0.838	Lmo2	LIM domain only 2 (rhombotin-like 1)	0.0819
499	0.839	5330426P16Rik	RIKEN cDNA 5330426P16 gene	0.0819
500	0.840	Il22ra2	interleukin 22 receptor, alpha 2	0.0819
501	0.841	Guca1b	guanylate cyclase activator 1B (retina)	0.0819
502	0.843	Ms4a7	membrane-spanning 4-domains, subfamily A, member 7	0.0819
503	0.845	Tifab	TRAF-interacting protein with forkhead-associated domain, family member B	0.0819
504	0.848	Prkar2b	protein kinase, cAMP-dependent, regulatory, type II, beta	0.0826
505	0.849	Col8a1	collagen, type VIII, alpha 1	0.0826
506	0.851	Lepr	leptin receptor	0.0831
507	0.857	Col6a3	collagen, type VI, alpha 3	0.0838
508	0.859	Mmp11	matrix metallopeptidase 11 (stromelysin 3)	0.0838
509	0.860	Leprel2	leprecan-like 2	0.0838
510	0.860	Nkx2-2	NK2 homeobox 2	0.0841
511	0.861	Flt3l	fms-related tyrosine kinase 3 ligand	0.0844
512	0.861	Traf1	TNF receptor-associated factor 1	0.0844
513	0.864	Rcn3	reticulocalbin 3, EF-hand calcium binding domain	0.0844
514	0.865	Clca2	chloride channel calcium activated 1	0.0844
515	0.865	Tceal1	transcription elongation factor A (SII)-like 1	0.0844
516	0.866	Ifi27l2a	interferon, alpha-inducible protein 27 like 2A	0.0844
517	0.868	Col1a1	collagen, type I, alpha 1	0.0844

518	0.870	P2rx6	purinergic receptor P2X, ligand-gated ion channel, 6	0.0844
519	0.870	Plxnd1	plexin D1	0.0844
520	0.874	Arhgap33	Rho GTPase activating protein 33	0.0844
521	0.874	Col3a1	collagen, type III, alpha 1	0.0844
522	0.876	Fcrla	Fc receptor-like A	0.0844
523	0.876	Stra6	stimulated by retinoic acid 6	0.0844
524	0.878	Oas2	2'-5'-oligoadenylate synthetase 2, 69/71kDa	0.0844
525	0.888	Ppp1r1a	protein phosphatase 1, regulatory (inhibitor) subunit 1A	0.0844
526	0.891	Cfp	complement factor properdin	0.0845
527	0.892	Prelp	proline/arginine-rich end leucine-rich repeat protein	0.0853
528	0.895	Hoxd10	homeobox D10	0.0853
529	0.897	Cd52	CD52 antigen	0.0867
530	0.900	Dleu2	deleted in lymphocytic leukemia, 2	0.0867
531	0.900	Il3ra	interleukin 3 receptor, alpha (low affinity)	0.0869
532	0.900	Sulf1	sulfatase 1	0.0869
533	0.907	Mfge8	milk fat globule-EGF factor 8 protein	0.0869
534	0.908	Ly6g6f	lymphocyte antigen 6 complex, locus G6F	0.0869
535	0.911	1190002F15Rik	RIKEN cDNA 1190002F15 gene	0.0869
536	0.919	Il2rg	interleukin 2 receptor, gamma	0.0871
537	0.920	Lst1	leukocyte specific transcript 1	0.0872
538	0.922	Klf8	Kruppel-like factor 8	0.0876
539	0.923	Cr2	complement component (3d/Epstein Barr virus) receptor 2	0.0876
540	0.932	Rnf144a	ring finger protein 144A	0.0877
541	0.933	Ccl27a	chemokine (C-C motif) ligand 27A	0.0877
542	0.933	Rbp7	retinol binding protein 7, cellular	0.0879
543	0.934	Faim3	Fas apoptotic inhibitory molecule 3	0.0882
544	0.935	Cxcr5	chemokine (C-X-C motif) receptor 5	0.0885
545	0.946	Cdkn1c	cyclin-dependent kinase inhibitor 1C (P57)	0.0885
546	0.947	Dio3os	deiodinase, iodothyronine type III, opposite strand	0.0885
547	0.948	Sod3	superoxide dismutase 3, extracellular	0.0888
548	0.959	Amotl1	angiomotin like 1	0.0888
549	0.962	Spon2	spondin 2, extracellular matrix protein	0.0893
550	0.965	Cib3	calcium and integrin binding family member 3	0.0893
551	0.967	Lyz2	lysozyme	0.0893
552	0.974	Slc22a17	solute carrier family 22, member 17	0.0894
553	0.975	Cd83	CD83 molecule	0.0899
554	0.979	Tesc	tescalcin	0.0899
555	0.980	Slc1a3	solute carrier family 1 (glial high affinity glutamate transporter), member 3	0.0899
556	0.984	Dnase1l3	deoxyribonuclease I-like 3	0.0899
557	0.984	Ppic	peptidylprolyl isomerase C (cyclophilin C)	0.0899
558	0.989	Pcsk1n	proprotein convertase subtilisin/kexin type 1 inhibitor	0.0899
559	0.992	Trf	transferrin	0.0900
560	0.998	Scd1	stearoyl-CoA desaturase (delta-9-desaturase)	0.0901
561	1.001	Fam64a	family with sequence similarity 64, member A	0.0901

562	1.005	Colq	collagen-like tail subunit (single strand of homotrimer) of asymmetric acetylcholinesterase	0.0901
563	1.007	Ubxn11	UBX domain protein 11	0.0901
564	1.017	Adig	adipogenin	0.0902
565	1.019	Plcb2	phospholipase C, beta 2	0.0907
566	1.029	Esm1	endothelial cell-specific molecule 1	0.0911
567	1.039	Rcn1	reticulocalbin 1, EF-hand calcium binding domain	0.0911
568	1.046	Car5b	carbonic anhydrase VB, mitochondrial	0.0911
569	1.054	Agt	angiotensinogen (serpin peptidase inhibitor, clade A, member 8)	0.0911
570	1.056	Car3	carbonic anhydrase III, muscle specific	0.0913
571	1.058	Clu	clusterin	0.0913
572	1.077	Gm684	colorectal cancer associated 2	0.0913
573	1.078	Dync2li1	dynein, cytoplasmic 2, light intermediate chain 1	0.0913
574	1.104	Pde4c	phosphodiesterase 4C, cAMP-specific	0.0915
575	1.120	Pygl	phosphorylase, glycogen, liver	0.0915
576	1.131	C330021F23Rik	RIKEN cDNA C330021F23 gene	0.0915
577	1.136	Ahrr	aryl-hydrocarbon receptor repressor	0.0930
578	1.139	Cfd	complement factor D (adipsin)	0.0930
579	1.143	Aplnr	apelin receptor	0.0938
580	1.165	Cyp2e1	cytochrome P450, family 2, subfamily E, polypeptide 1	0.0940
581	1.227	Pla2g2d	phospholipase A2, group IID	0.0956
582	1.237	Neurl1a	neuralized E3 ubiquitin protein ligase 1	0.0971
583	1.254	Fam129c	family with sequence similarity 129, member C	0.0985
584	1.473	Thrsp	thyroid hormone responsive	0.0996

Supplementary Table 2. Genes differentially expressed in the DbDb colonic epithelium compared to LF. Log Ratio corresponds to the log2 fold change, ID is the PubMed Gene ID, P-adj is the adjusted p-value.